MURDOCH UNIVERSITY
PERTH, WESTERN AUSTRALIA

ENG470 ENGINEERING HONOURS THESIS FINAL REPORT

BIOFOULING ON FORWARD OSMOSIS SYSTEM

Author

Monthat Suwannakarn

Bachelor of Environmental Engineering Honours (BE(Hons))
School of Engineering and Information Technology

SUPERVISORS

Dr. Linda Li

Emeritus Professor Goen Ho

For the partial fulfilment of requirements for the unit ENG470 – Engineering Honours Thesis, at Murdoch University, Western Australia. Completion of report in Semester 1, 2016.

DISCLAIMER

The student confirms that this submission is his own work unless stated otherwise and excluding references, and appendices.

Executive Summary

Fouling is an inevitable issue that all membrane systems have to face. The presence of membrane fouling causes membrane systems (such as reverse osmosis and forward osmosis) to suffer the increase of resistance thus reducing the efficiency of the systems. This raises concerns about the osmosis technology as it also reduces the system and membrane lifetime while increasing the maintenance costs.

From previous papers and literature review, polysaccharides were found to be the main contributor to membrane fouling. The literature explains the polysaccharides that caused the membrane fouling were alginate, BSA, AHA, xanthan and others however, only alginate and xanthan were tested in this research project. The mixing interaction of other cations such as Ca^{2+} with some of the aforementioned polysaccharides (salt in the form of $CaCl_2$ and NaCl were also tested to see the changes in fouling effects when both are combined. Throughout the experiments, a fixed amount of NaCl and $CaCl_2$ and the polysaccharide were kept constant. The draw solution (NaCl mixed with DI water) was always retained to be saturated. These experiments were designed in this way to examine the differences between each polysaccharide and its combination towards fouling behaviour, since alginate and xanthan have different chemical characteristics.

The results show that xanthan causes a higher resistance compared to alginate. In the case where NaCl and $CaCl_2$ were present in the feed solution, the resistance of both polysaccharides greatly increases thus resulting in lowering the flux and ultimately decreasing the system efficiency. Out of all the experiments, the xanthan with salt resulted in highest flux decrease while the alginate only had the least flux decline (excluding the baseline experiment).

Further analysis was done using the total organic carbon (TOC) and confocal laser scanning microscopy (CLSM). These examinations demonstrated the characteristics and properties of the polysaccharide layers that were formed on the membrane surface. The CLSM result was compared with the flux and resistance movement and it was found that they supported each other (and the findings were closely related). Since CLSM analysis is able to show the x, y and z dimension, the thickness can be found within each CLSM images. Therefore the thickness of the polysaccharide (fouling) layer (from CLSM images) was thick and/or dense, the (a higher resistance was achieved) higher the resistance would be and vice versa.

Acknowledgment

I would like to express my special thanks and gratitude to my supervisors, Dr. Linda Li and Emeritus Professor Goen Ho who provided expertise that enabled me to achieve such great results and findings.

I am also thankful to Ph.D. student Zhangwang Xie (John) for his assistance with the experiments and professional criticism on the project.

I am also grateful for the technical assistance Dr. Lucy Skillman has provided, particularly during the confocal laser scanning microscopy analysis.

Finally, I would like to thank Murdoch University Institution for allowing me the opportunity to undertake this project. By providing a high standard of education, world class equipment and with the help of expert staff members, I was able to complete this project successfully.

List of Abbreviations and Acronyms

DI: Deionised

CLSM: Confocal laser scanning microscopy

NaCl: Sodium chloride

$CaCl_2$: Calcium chloride

FO: Forward osmosis

RO: Reverse osmosis

CP: Concentration polarisation

ICP: Internal concentration polarisation

ECP: External concentration polarisation

LMH: Litres per minute per hour

TOC: Total organic carbon

BSA: Bovine serum albumin

AHA: Aldrich humic acid

Table of Contents

Table of Figures

1. Introduction

Since the year 2000, environmental issues have become more severe on a global scale. Apart from the heavy damage caused by environmental disasters such as droughts and floods, lack of resources such as water is affecting arid countries at a massive level, especially in Australia. With Australia being the second driest continent (Australia.gov.au 2016) (first being Antarctica) in the world where harvesting water in those area is becoming a bigger issue. As the pollution and scarcity of fresh water resources are increasing, technologies have been developed to harvest water from other sources, such as from the ocean or sea via desalination or reverse/forward osmosis practice.

Desalination is the process which separates brine into two streams: one being with a low concentration of salt (fresh water stream) while the other is the brine, containing a high concentration of salt dissolved in the stream (Australian Government, Department of the Environment 2006). Reverse osmosis (RO) is a system that is commonly used at desalination-plants in Australia which is connected to houses thus providing high quality drinking water, where the water is met to international standards of drinking water (Water Filters Australia 2016, ESP Water Products 2016). The second type of osmosis system is called forward osmosis (FO) system. It could be used on a larger scale (such as on mining site) but since this technology is at an inferior stage of development, hence its full potential is yet to be discovered (Cath, Childress and Emilech 2006).

One of the challenges that prevents forward osmosis systems from achieving greater efficiency is membrane biofouling. To break it down, biofouling is caused by a microorganism (particularly bacteria) sticking onto the membrane creating a gel film reducing the membrane efficiency and functionality (TES 2016). According to Brink *et al* 2009, the formation of the gel is potentially caused by the combination of cations and polysaccharide. Therefore, a choice of two polysaccharides (alginate and xanthan) with the mixture of salt (sodium chloride and calcium chloride) were studied. Due to the limit of time other polysaccharide such as pullulan cannot be examined. Furthermore, the result was closely compared with an experiment that contains the

only polysaccharide to contrast the effect gel on the forward osmosis system. In addition, the result will also be compared against each polysaccharide to identify the different effects it has on the FO system and biofouling. To investigate this matter, a bench-scale forward osmosis system has been set up in a laboratory to conduct all the designed experiments to obtain a meaningful result.

1.1.Objectives

In order to investigate and study the effect of biofouling on a forward osmosis system, the following set of objectives were established with the recommendation of the assigned supervisors.

i. To investigate and compare the fouling behaviours of alginate and xanthan (two kinds of foulant) followed by the addition of sodium chloride and/or calcium chloride (i.e. salt). All possible combinations of the chemical mixture will be tested (refer to methods & experimental design chapter for more information).
ii. To identify the characteristics of diffusion, cake layer and concentration polarisation, with the addition of generating a model that will aid the understanding of these concepts. CLSM (Confocal Laser Scanning Microscopy) will be used to assist in identifying the cake layers on the membrane.
iii. To analyse the polysaccharide distribution by utilising the TOC result, CLSM images and mass differences calculation.
iv. To compare and contrast the result of flux and fouling behaviour between RO and FO system.

1.2.Management system

To enhance the efficiency of this project's progression, supervisors specialising in forward osmosis systems were assigned to provide guidance, feedback, and technical knowledge. In addition, a weekly meeting was appointed every Wednesday to update the supervisors of the current progression, along with bringing up any issues or problems that may have arisen during the week.

A Gantt chart (Appendix A) was constructed at the beginning of the project and was updated fortnightly to plan for enough time for each task as well as alerting for upcoming deadlines. Moreover, the assessment was assigned by the university which will contribute towards the final mark. This allows the supervisor to receive a formal and full report of the work that was done.

During the first few weeks, Mr. John Zhangwang (a Ph.D. student provided assistance for this thesis project) provided 4 lab sessions where he introduced the forward osmosis system. Within the 4 sessions, a preliminary experiment was conducted using DI water, salt, and alginate. The aim of these 4 sessions was for the thesis candidate to familiarize himself with the system and data manipulation.

2. Background Information

2.1.Forward Osmosis

Hydration Technology Innovations (HTI) describes forward osmosis as 'A Green Technology' where they further elaborate that it is a remarkable young technology that turns contaminated water into clean drinkable water by removing toxic waste and pollutants. (HTI 2010). The International Forward Osmosis Association (IFOA) explained that FO osmotic process utilises a semi-permeable membrane which filters the water from its dissolved solutes (International Forward Osmosis Association 2016). Furthermore, the driving force of the filtration process is caused by the difference in osmotic pressure between a concentrated (draw/permeate) saline solution and lower concentration solution where it has other impurities, such as organics or carbon in particular. In Figure 1, the diagram breakdowns the forward osmosis system where the flux flows from the feed side towards the draw side (permeate).

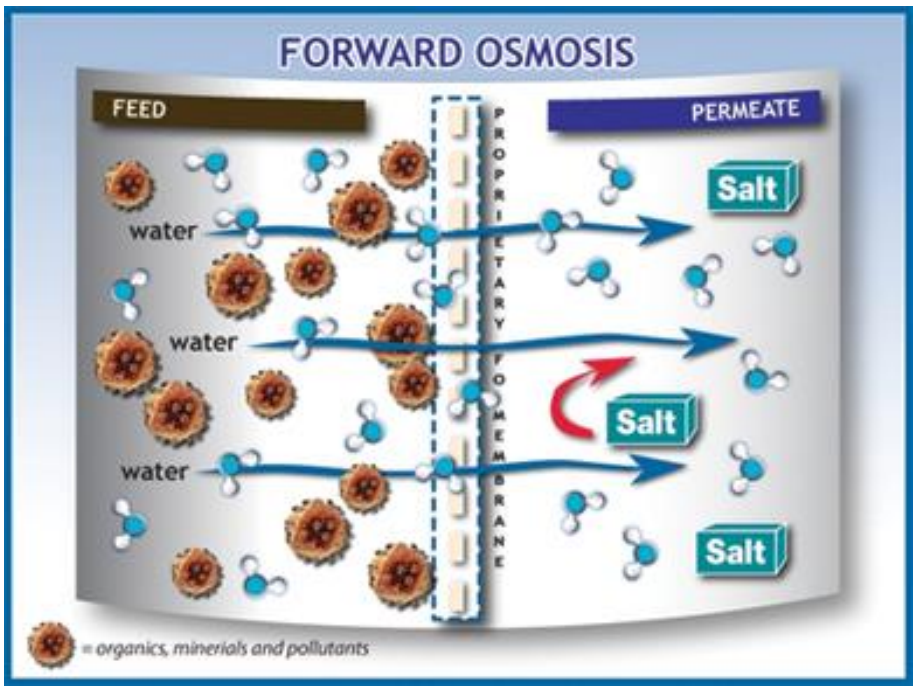

Figure 1: Diagram representation of feed and permeate side of a forward osmosis with the salt and pollutant as part of the system, courtesy of HTI (HTI 2010).

Forward osmosis caught scientists' attention in the 1960s whereby research and multiple studies were conducted throughout the next decade investigating the mechanism. At that period of time, some scientists were curious and believed that the synthetic materials had a great potential to the system hence, special consideration was given to it (Cath, Childress and Elimelech 2006). Even though the reverse osmosis system is the dominating osmosis technology, having a lot more publications and papers supporting it, forward osmosis has been integrated into factories for industrial use. Examples of forward osmosis applications are to concentrate landfill leachate, treating industrial wastewaters (via filtration method), treating liquid food waste, treating wastewaters to a potable reuse quality (Australian Government, Department of the Environment 2006). Recently, the technology of forward osmosis has improved extensively to even provide power generation. Figure 2 is a summary diagram of forward osmosis applications constructed by Zhao *et al* 2012.

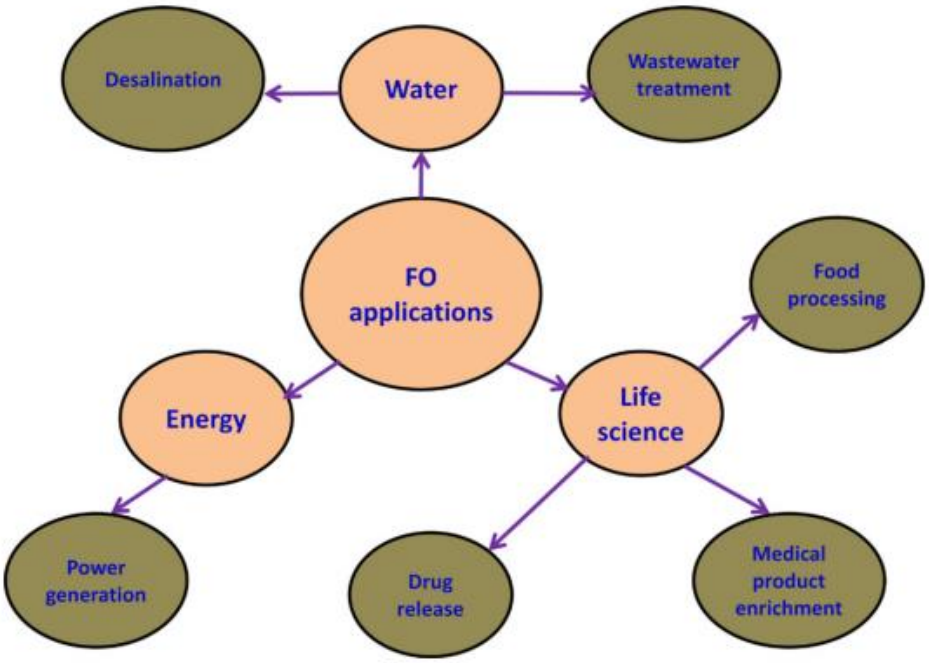

Figure 2: Web diagram of FO application splitting into three categories (water, energy, and life science), courtesy of Zhao et al. (Zhao et al. 2012)

FO system when compared to RO system, it is a premature technology that still has many challenges to overcome in order to increase its potential (Zhao *et al*. 2012). However, scientists are constantly researching new methods to improve on it such as membrane improvement, pressure retarded osmotic system or even increasing the application of FO system hence diversifying its market

In an osmotic system that uses pressure to drive the membrane process, concentration polarisation is a common and inevitable phenomenon. An explanation of concentration polarisation was given by separationprocesses.com as in the following quote,

> *"A layer is formed near the surface of the membrane, whereby the solution immediately adjacent to the membrane surface becomes depleted in the permeating solute on the feed side of the membrane, and its concentration is lower than that in the bulk fluid. On the other hand, the concentration of the non-permeating component increases at the membrane surface. A concentration gradient is formed in the fluid adjacent to the membrane surface. This phenomenon is known as concentration polarisation and it serves to reduce the permeating component's concentration difference across the membrane, thereby lowering its flux and the membrane selectivity."*

To put it in simple terms, when a layer is formed on the membrane as part of the system operation, the concentration of the layer is less than the bulk solution resulting in the differences of concentration. This results in a concentration gradient. This gradient acts as a non-permeating layer hence reducing the driving force, increasing the total resistance of the membrane and ultimately lowering the flux. Figure 3 is a diagram that was constructed by Alvisk and Hägg to illustrate this concept. Note that they denote ICP as internal concentration polarisation.

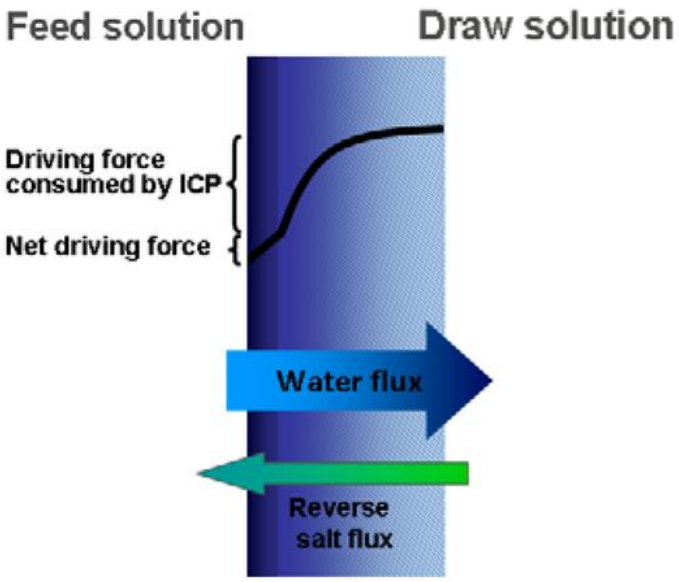

Figure 3: A closer description of flux and diffusion with the ICP between the feed and draw solution, courtesy of Alsvik and Hägg, (Alsvik and Hägg 2013).

Membrane fouling is another inevitable effect for all membrane processes. Zhao *et al* explains that by lowering the fouling effect, the product water would increase, less cleaning is required and the membrane would last longer (Zhao *et al*. 2012). All of this would lead to a lower capital, maintenance and operational cost.

2.2. Polysaccharide

Polysaccharide is mono-saccharide bonded together and where the term 'saccharide' is known as carbohydrates (so it is the linkages of many carbohydrates). Polysaccharide is derived from Greek which literally means many-sugar (poly-sacchar) but exists in the form of complex carbohydrates (NutrientsReview 2016). A typical polysaccharide would consist of 200 to 2500 monosaccharides (Study.com 2016). Alan Imeson stated that when a small amount of calcium ions (Ca^{2+}) is mixed with polysaccharide solution, it causes a drastic increase of viscosity due to

partial and non-permanent cross-linking (Imeson 2010), (Dumitriu 2016). The cross-linking connects between the molecules hence creating a bond which results in the increase of thickness of solution and triggering the gel formation. This increases the resistance and ultimately reduces the flux.

Biofilm formation is triggered by a substance called extracellular polymeric substances (EPS) which is produced by microorganisms that is largely made out of polysaccharides as well as proteins, nucleic acids, lipids and humic substances (Vu *et al*. 2009, Ryderm Byrd and Wozniak 2007).

In the human body system, the polysaccharide is known for storing energy and rationing that energy to be used over a period of time rather than a sudden burst of energy. The energy is stored in two forms: (i) starch and (ii) glycogen; where starch releases the energy in the short term (a mixture of amylose and amylopectin) whereas glycogen is more of a long-term energy storage type (Group 2016) (Stephen, Phillips and Williams 2006).

Another application of polysaccharide is for pharmaceutical purposes such as producing Gaviscon (gastric reflux relief), hydrophilic matrix table, gelatine replacement for hard capsules and hydroxyl-propycellulose (a form of thermoplastic often used for breast implants) (Mitchell 2016).

Two polysaccharide (alginate and xanthan) are chosen because these two has been the spotlight of polysaccharide in regards to both reverse and forward osmosis system. The two polysaccharide are explained further below.

2.2.1. (Sodium) Alginate

This chemical is named as the sodium salt of alginic acid. Sodium alginate is a type of polysaccharide that can be harvested from the cell wall of brown seaweed in cold water regions (off the coast of North Atlantic, South America and Asia) hence making alginate a natural polysaccharide (molecularrecipe.com 2014, Imeson 2010). Sodium alginate's original function in seaweed is to allow its flexible and wave-like motion. On the other hand, it is used artificially as a

food additive to stabilise ice-cream, yogurt, cream and cheese (dairy products) as well as thickening liquid food such as salad dressing, pudding, jam, syrup, tomato juice and canned products (modernist pantry 2015). A paper was published regarding sodium alginate potentially being used for medical purposes such as 'cell encapsulation materials and as wound dressings' (Wang *et al*. 2003). A paper written by Lee *et al* 2010, with the objective of illustrating the differences of fouling behaviour in forward osmosis and reverse osmosis, uses alginate at a concentration of 200mg/L or 0.2g/L as part of their experiment (Wang *et al*. 2003) which is in a similar condition to this report. Other combinations of alginate are ammonium and potassium alginate.

In a website named 'Gourmet Goldmine' sodium alginate was mentioned as a thickening substance that, when mixed with calcium chloride, will trigger a gel-like product which ultimately is the basis for a food called 'caviar' (Gourmet Goldmine 2016). Another source stated that in the presence of calcium and an acid, some alginates can form resilient gels (WillPowder 2012).

Figure 4 is a structural formula developed by Phillips, Wedlock and Williams (under the title of Gums and Stabilisers for the Food Industry 5, 1990) (FAO Corporate Document Repository 1995).

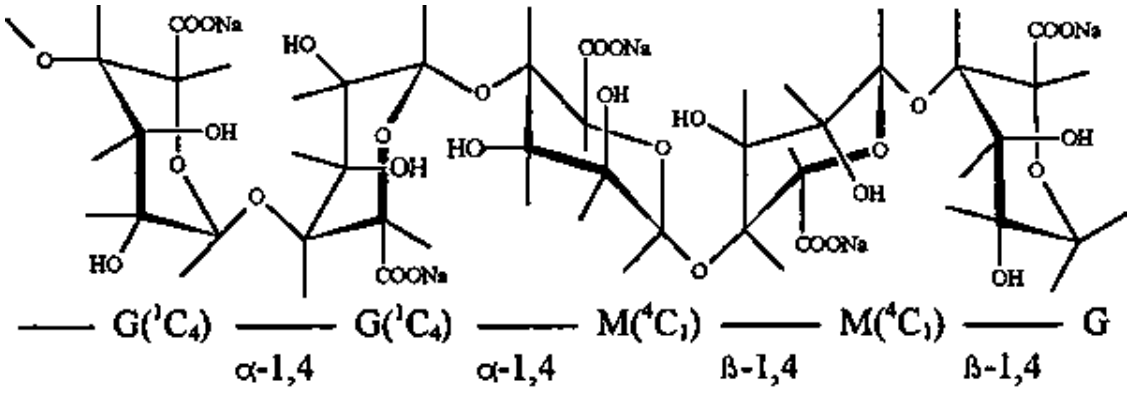

Figure 4: Chemical structure of alginate with it linkages developed by Philips, Wedlock and Williams (1990).

2.2.2. Xanthan

Xanthan, also known as xanthan gum, is produced by the fermentation process of *Xanthomonas campestris,* a bacteria that causes plants to rot (Boulanger *et al*. 2014). This natural

polysaccharide was discovered in the 1950s, from then research began to extend the bacteria's potential. The uses of xanthan range from food to cosmetic, pharmaceutical and even agricultural purposes (Boulanger *et al*. 2014).

Katzbauer published a paper on the properties and application of xanthan gum in 1997 where in one of the paper's section, she describes the wide range of applications of xanthan (Katzbauer 1998). She stated that xanthan acts as a stabiliser in soup and gravy which prevents its thickness. In other words, it is an agent that controls the viscosity. In another source, they added that xanthan gum is also used as an emulsifier and foaming agent as well as being a bulking agent for drugs with and without the use of polymers (Chaplin 2016). Other significant properties of xanthan is its very high low-shear viscosity coupled with its strongly shear-thinning character.

Figure 5 is the structure unit of xanthan gum (Chaplin 2016).

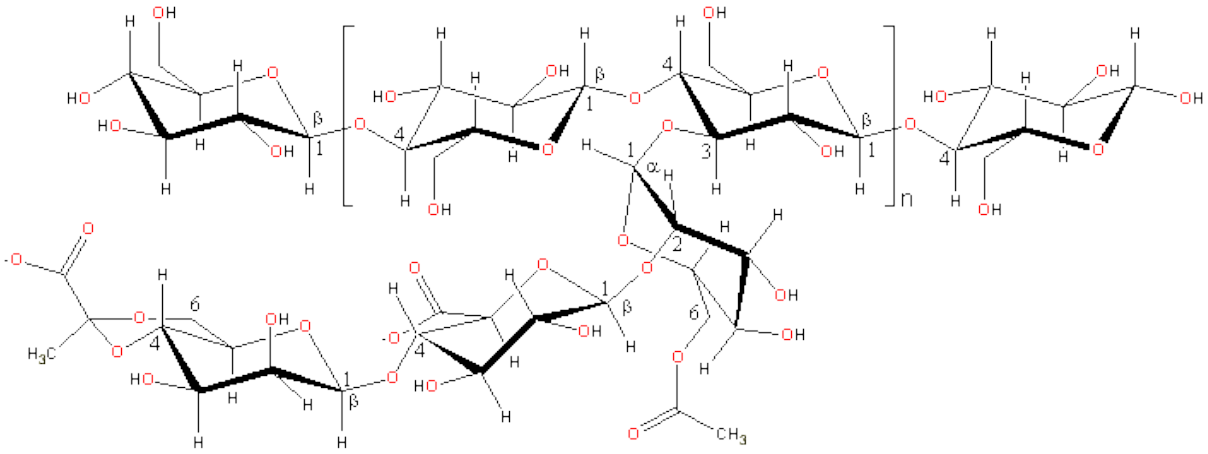

Figure 5: Chemical structure of xanthan gum developed by Chaplin (2016).

2.3.Membrane fouling

Membrane fouling is an inevitable problem that will occur in most filtration processes that involves a membrane. This includes reverse and forward osmosis (Lenntech 2016). The fouling issue often leads to an irreversible effect on osmosis systems. The fouling on membrane includes fouling/scaling, organic fouling, particulate/colloidal fouling and biofouling (or microbial/biological fouling also known as biological contamination) which is shown in figure 6 as a diagram showing how each fouling looks like (Nguyen, Roddick and Fan 2012).

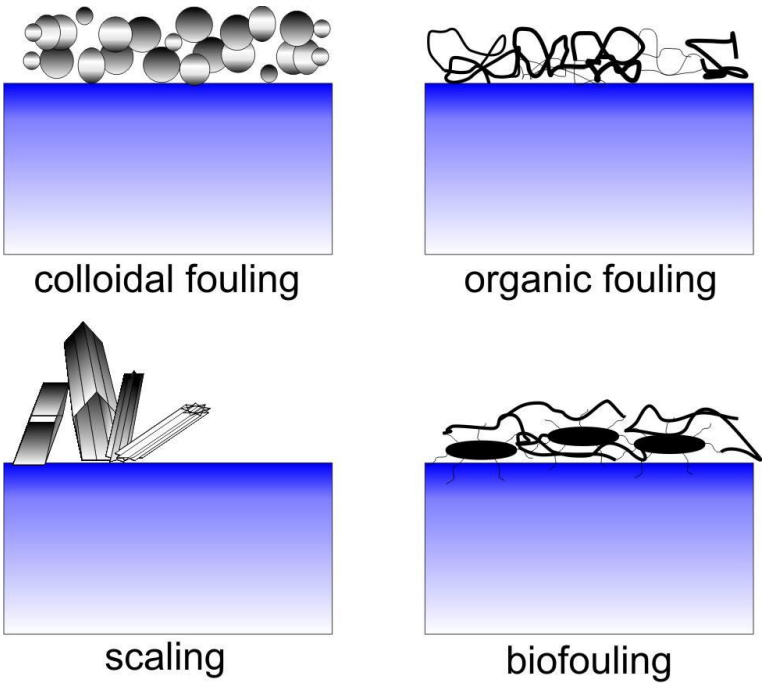

Figure 6: Diagram illustrating the 4 type of fouling, that is; colloidal, organic, scaling and biofouling made by Borkovec (2016).

Biofouling poses several negative effects onto the membrane system which can be illustrated as follows (Nguyen, Roddick and Fan 2012):

- When the biofouling takes effect on membrane, they form a biofilm that increases the resistance of the membrane hence reducing the flux.
- The biofilm will also increase the pressure difference (increase in external concertation polarisation) causing the system to operate at a higher power level
- While the biofilm is formed, salt particles are also deposited on those films as it tries to permeate through the membrane which in turn accumulates the dissolved ions onto the biofilm over time. Therefore, ultimately increasing the internal and external concentration polarisation (a form of resistance) thus decreasing the flux.

With all of these problems causing the resistance to increase and flux to drop, if the system was to be maintained at a levelled production volume, the energy consumption will have to increase thus increasing the operational cost. In the long term, this could potentially damage the machine since the system may not have been designed to operate at such high pressure and causing maintenance to be done at shorter intervals. This would also increase the maintenance cost.

As mentioned earlier, fouling is an irreversible and inevitable issue that all membrane systems will face. The diagram figure 7 shows the process of how the membrane fouling occurs. It's split into 5 stages: first is where the fresh membrane is introduced to the system; secondly it is after the filtration has begun, when the pollutants and solutes are passing through the membrane pores while some are stuck in between the pore causing a blockage; thirdly, after the membrane has been used for a long period, sludge and larger particles are starting to build up on top of the membrane and the pores which will increase the blockage a lot more; fourthly it is when the physical maintenance is conducted, most of the larger particle sludge that were located on top are washed away; the final stage is where the chemical cleaning occurs and this is where most of the solutes are pushed out of the pores. Even though the chemical cleaning is done, there will still be some solutes and colloids in the pores, unable to be removed hence causing an irreversible fouling effect.

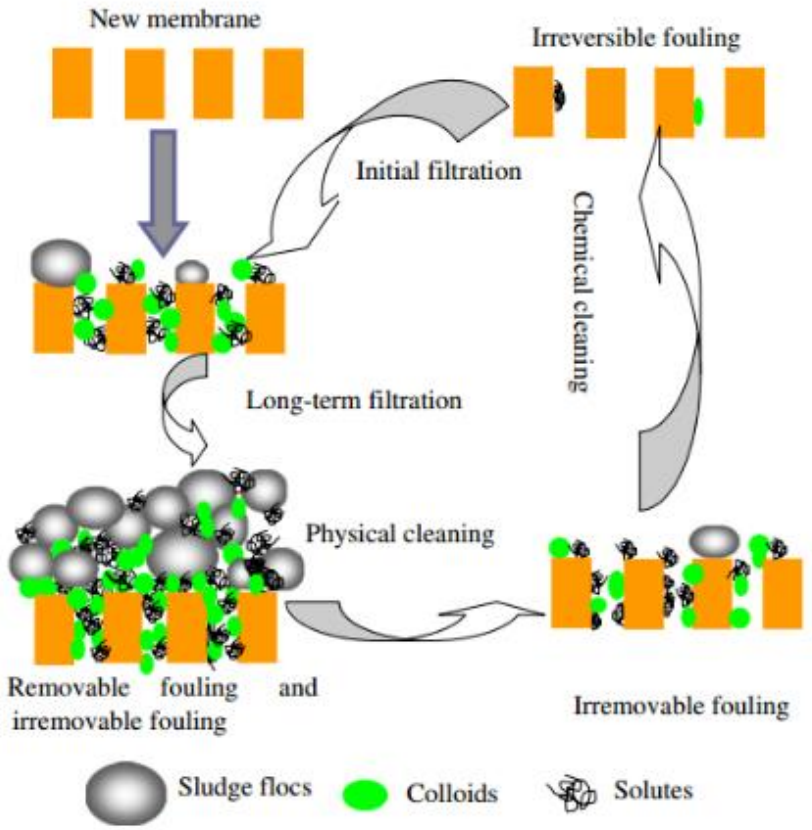

Figure 7: Life cycle of a membrane after fouling into an irreversible fouling stage illustrated by Meng et al. (2009).

2.3.1. Concentration polarisation

Concentration polarisation described by Mark Perry as 'the build-up of concentration gradients both inside and on the surface of forward osmosis membrane during operation. These concentration gradients reduce the effective osmotic pressure difference across the membrane active layer and this limits the attainable water flux' (Perry 2013).

There are two main types of concentration polarisation, namely internal concentration polarisation (ICP) and external concentration polarisation (ECP) where it is further broken down into two sub-categories of concentrative and dilutive (Perry 2013). Figure 8 shows the AL-FS (active layer to feed solution) configuration of concentration polarisation in forward osmosis system. In this AL-FS case, the CECP (concentrative ECP), DICP (dilutive ICP) and DECP (dilutive ECP) exists. Therefore, the main concentration polarisation that occurs here is DICP.

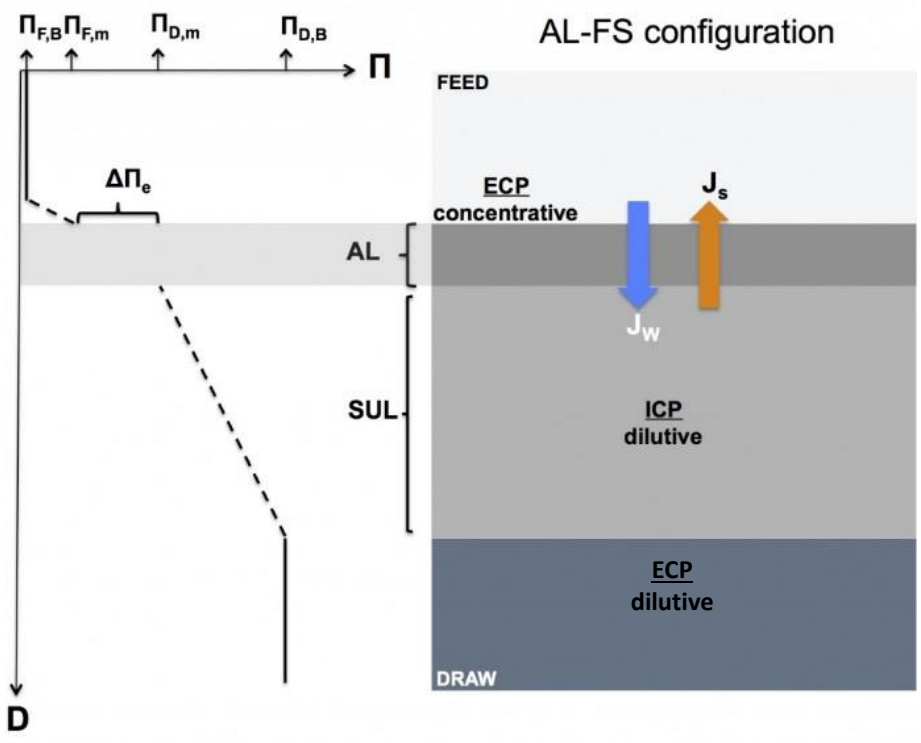

Figure 8: A diagram representing a configuration of forward osmosis system where the active layer of the membrane is faced against the feed side while showing the location of ECPs and ICP (Perry 2013).

Another diagram was constructed by G.T. Gray *et al* in 2006 which elaborates the differences when the membrane's active side is switched between facing the feed and draw solution. Dilutive ICP occurs in forward osmosis mode whereas the concentrative ICP occurs only in pressure retarded osmosis due to the direction of the flux. The reason it is dilutive ICP is because

salt is harder to permeate through the active layer causing the dilutive ICP in the support layer to contain a low concentration of salt in it. On the other hand, when the water flux flows from the feed side to the draw side, the salt solution is able to permeate through the support layer at a faster rate compared to the dilutive ICP case. This causes the salt to deposit on top of the active layer (in the support layer) while more salt solution is constantly flowing in with the water flux, therefore, becoming more concentrated on the active layer hence the name concentrative ICP.

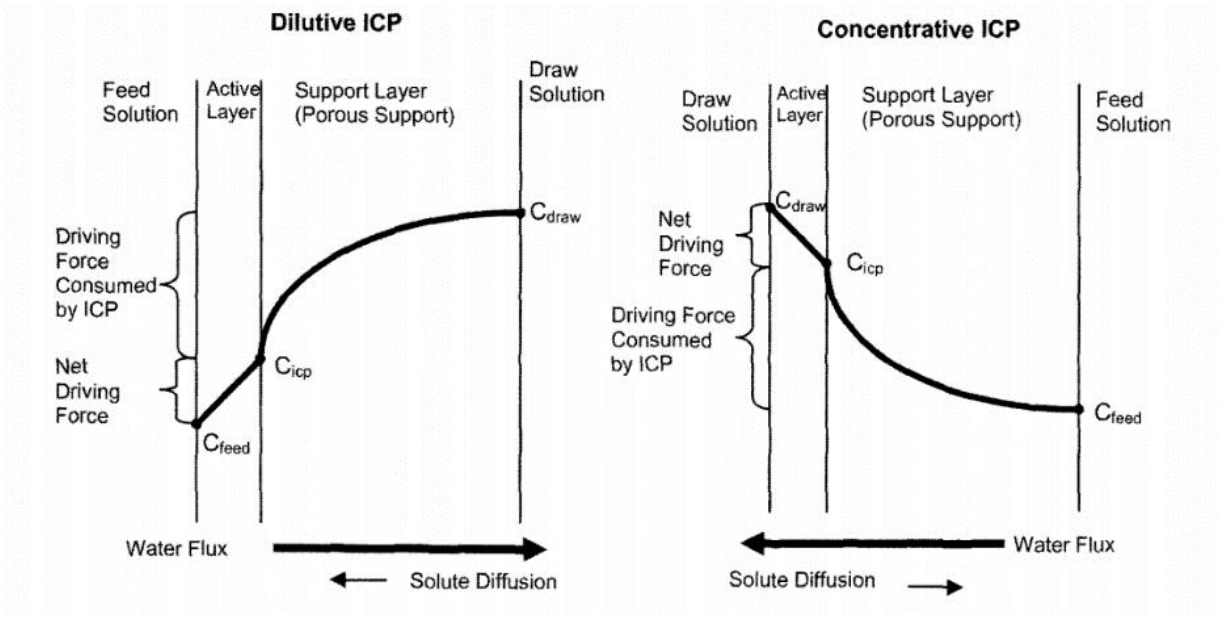

Figure 9: Two graph showing the different type of forward osmosis setup hence having two type of ICPs along with flux and diffusion location (Gray, McCutcheon and Elimelech 2006).

2.3.2. Back diffusion

Diffusion itself is the movement of a solution or air from an area of higher concentration to lower concentration. This is influenced by the kinetic properties of particles of matter and will keep diffusing until the particle concentration are evenly distributed, that is both sides concentration are relatively equal (Marie Helmenstine 2016). A common example of diffusion is spraying perfume in an enclosed room, as the smell diffuses through the air and into your nose while also diffusing into the entire room which eventually, the whole room will have the perfume scent. The perfume particle will stop diffusing once the entire room is equally distributed with the perfume scent.

Back diffusion occurs when the solute permeates in opposite direction of the primary movement of solution or fluid. In a particular case of salt back diffusion of a membrane in FO system, when the permeate flows from low concentration (feed side) towards the higher concentration of salt (draw side), the salt back diffuse against the flux. To put in simple terms, the salt flows from high draw side to a feed side even though the flux is to opposite (feed to draw side). The back diffusion of salt is often hindered by the cake layer resulting in an elevation of osmotic pressure upon the membrane surface (Marie Helmenstine 2016, Boo *et al*. 2012). It was discovered in a paper written by Boo *et al* (Boo *et al* 2016) that the decrease in FO permeate flux will result in an increase in cake-enhanced osmotic pressure. This is due to the reverse diffusion (or back diffusion) of salt from the draw to feed side rather than the fouling behaviour of creating resistance.

2.3.3. Biofilm layer (cake layer)

A literature paper that was written by Jacob, McCutcheon and Shor explained that bacteria produce biofilm naturally as a preventive measure, the generated film increases the tolerance level against desiccation and antimicrobial exposure, to aid in nutrient sequestration and to promote cell-cell coordination (Jacob, McCutcheon and Shor 2014). Another literature described biofilm as aggregates of bacteria attached to a surface (Armstrong , Galleo and Chester) In addition, the authors explain that the biofilm can potentially grow up to several hundred micrometres and become the source of hydraulic resistance (Ahmad *et al*. 2000), in some cases, the flux reduction can be as great as 20% of the original flux.

The biofilm contains 3 different types of forces that promote their bond causing difficulties when the bond is required to be removed. The 3 forces are (i) electrostatic, (ii) hydrogen bonds and (iii) London dispersion forces (Armstrong, Gallego and Chesters 2011). One of the methods that are used to remove the biofilm is chemical treatment such as biocides which shows to be effective to a certain extent but not fully functional for long term purposes.

2.4.Total organic carbon

Total organic carbon (TOC) is used to assess the contamination of water via the synthesis of organic compound and material; identifying chemical characterisation; estimating the carbon content of a soil sample as well as determining the carbon cycling of soil and carbon fluxes in aquatic systems (Bisutti, Hilke and Raessler 2004).

TOC has several application to it rather than just measuring the carbon content, it can be used to differentiate water type. C. Batiot *et al* 2003 state that TOC was a relevant parameter for characterising the behaviour of aquifers, allowing them to differentiate between water types that participate in karstic flow (a type of topography; fast infiltration, located in both saturated and unsaturated zone) (Batiot *et al*. 2003).

3. Methods & Experimental Design

The methods and experimental design will explain in detail how each experiment was conducted, it's experimental setup, the chemical that was used, the length of each experiment and any other information that are vital as part of the experiment to obtain a meaningful result.

3.1.Experimental setup

As part of this thesis, a bench-scale forward osmosis system was set up and used as part of the experiment. Figure 11 shows a photo of how the actual system looks like while figure 10 represents a diagram of how the system is setup. The flow diagram mentions a total of 7 components in order to complete the system. The following are explanations of each component of the system to reason why it is needed:

i. Computer: connected to the system where it is installed with a data logging software that is specially designed for this purpose, the software will log the number on the balance (weight) every minute with the respective time and the record number;
ii. Scale: is weighing the draw solution constantly to measure the increase of weight which ultimately is the permeate solution, this is connected to the computer;

iii. Pump: to maintain the system so that it runs at a fixed pressure flow and keeping the solution constantly flowing

iv. Water bath: is present to control the temperature of the solution since increase or decrease of temperature can lead to lower system function capability (increase resistance of system as the heat increases thus lowering the flux, affecting the accuracy of the result)

v. Membrane unit: filtering the solution, please refer to figure 13 for the breakdown of the unit

vi. Feed solution: originally contain DI water only, but depending on the experiment type this is where the different salt (NaCl + $CaCl_2$) and polysaccharide are injected into feed solution

vii. Draw solution: a saturated NaCl solution is in the tank to constantly enforce the gradient of osmotic pressure, note that the draw solution will be kept saturated throughout the experiment

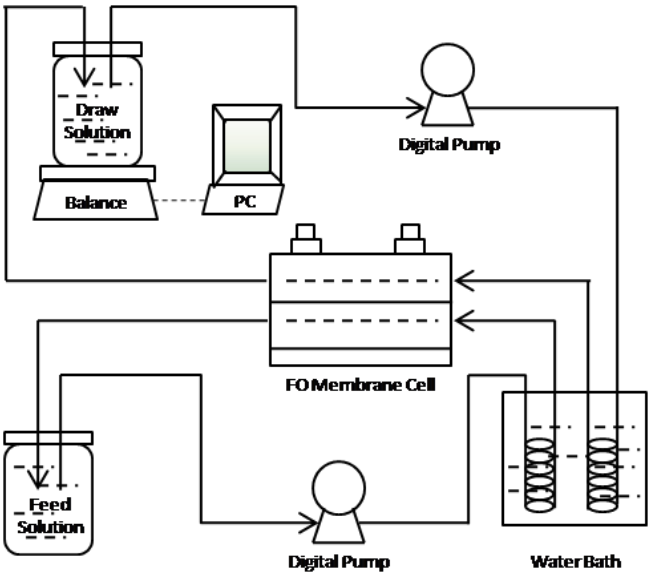

Figure 10: A diagram showing the setup of the forward osmosis bench-scale system that was designed for the experiments (Courtesy of Zhangwang Xie)

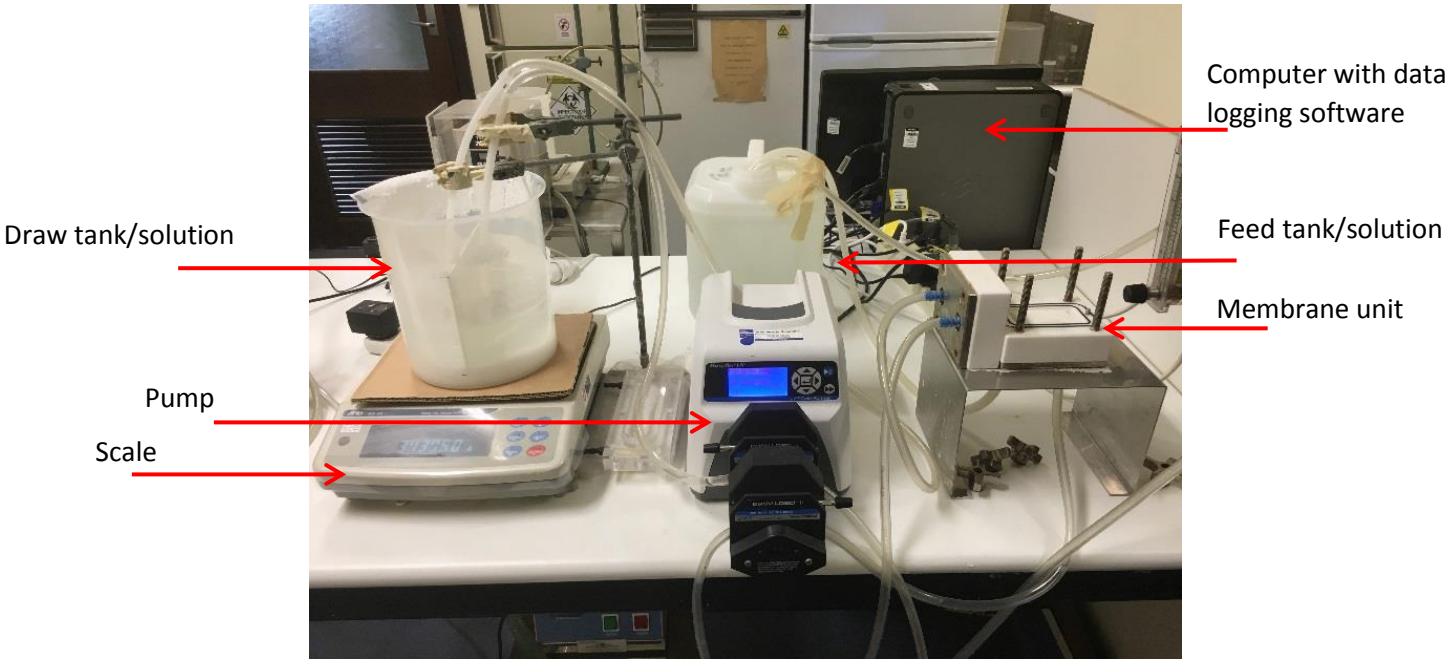

Figure 11: Photo of the forward osmosis setup in the lab.

a) b)

c)

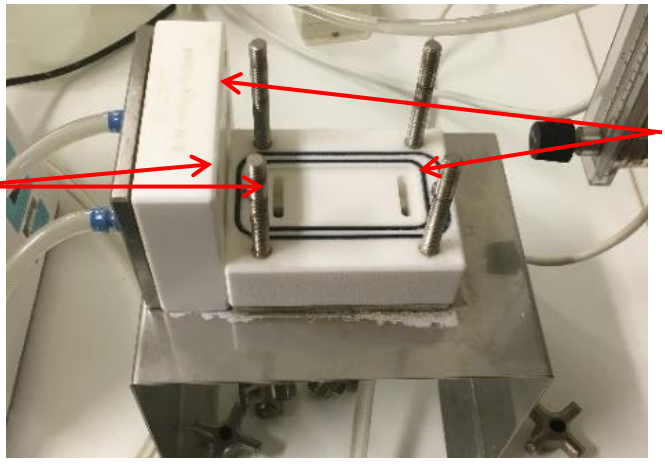

Figure 12: Front (a), top (b) and inside (c) view of the membrane unit

Figure 13, shows the close-up of the membrane unit where the two solutions from draw side and feed side interact between the membranes (please refer to appendix H for membrane specifications). The draw side has a much higher concentration (that is NaCl saturated solution) than feed solution. The difference in concentration leads to a different in osmotic pressure which causes a phenomenon that induces a flux to flow from the lower concentration (feed) to the higher concentration (draw). While the flux permeates into the draw side, the pollutants are retained in the feed solution with an addition of salt permeating from the saturated NaCl solution. This is called back diffusion.

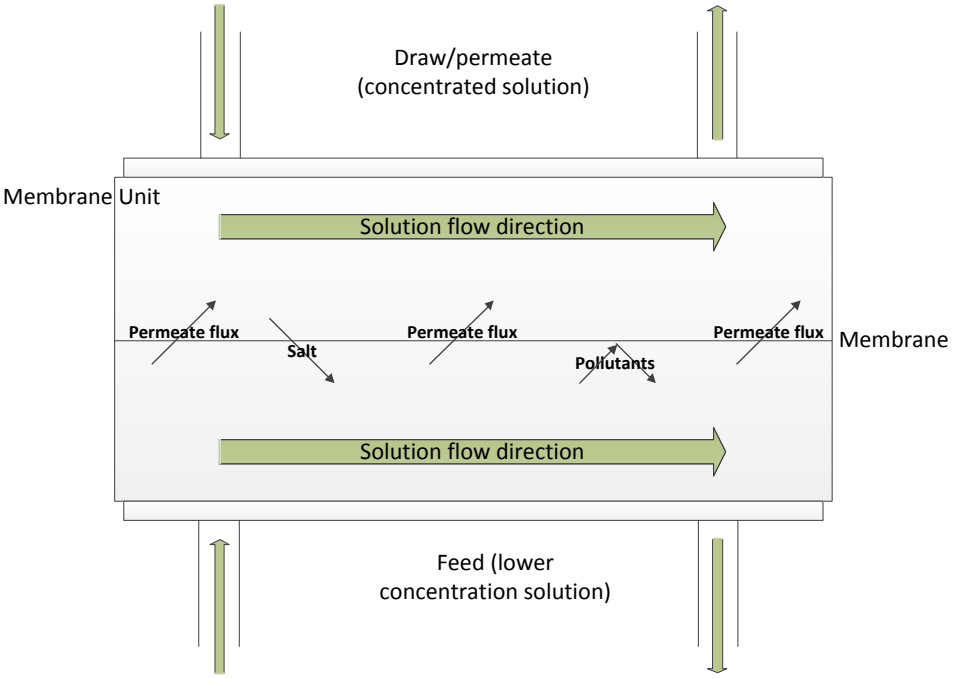

Figure 13: A broken down diagram of the membrane unit as well as the expected movement of flux, salt, and pollutants.

Generally, different chemicals will have a variation of method but are still similar in general design. Each experiment is required to be repeated at least once to ensure that data is within an acceptable range of error. In a case where the two data standard deviation is greater than 10%, another repetition is required until at least two set of data are under an acceptable range of error. Eventually, an average will be calculated from the two or three chosen sets of data in order to increase its accuracy. In addition, normalising the data was done for further comparison of data between different experiments (Borgatti 2015).

There is 5 type of experiment required to be conducted, 2 repetitions of each type thus a total of at least 10 experiments to be completed assuming all experiments are done properly and their data are within an acceptable margin of error. For each experiment one of attempt is required to be tested for resistance due to blockage while the second replicate, the membrane is kept in a petri dish for further analysis.

3.2.Experiment with salt only (NaCl + $CaCl_2$), baseline

At t = 0 hours to t = 2 hours, the experiment is conducted with just DI water running through the FO system. The reason that this process is required is so the membrane layers are compact causing the flowing pressure and cross velocity to reach a point where it stabilises, hence this stage is called compaction (Chung *et al* 2010). Before commencing the second stage, the conductivity in the feed tank is measured and recorded. At t = 2 hours, the chosen type and amount of salt, which was premixed in approximate 175ml of DI water, is injected into the feed tank and mixed within the tank thoroughly. The stabilisation stage (generally last for 2 hours) starts at t = 2 hours. Once a total of 26 hours has lapsed, the conductivity of the feed tank is measured and recorded once again. Finally, the experiment ceases and the data is collected from the logging software.

Conductivity is to be measured at hour 2, 4 and 26 while noting the appropriate unit.

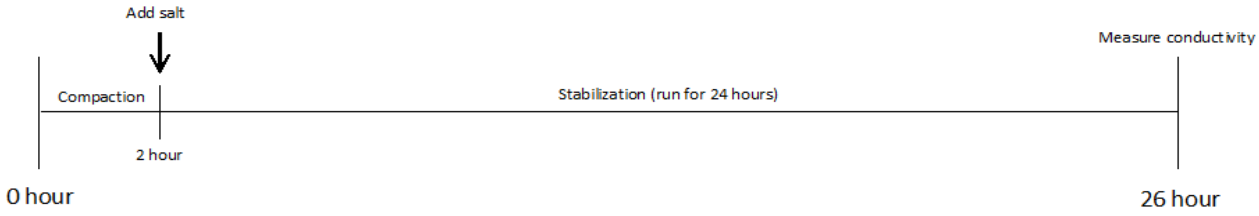

Figure 14: Timeline of experiment for NaCl and $CaCl_2$ only.

3.3.Experiment with foulant only (Alginate or Xanthan Gum)

This experiment follows the similar procedures as the baseline experiment, however instead of injecting salt water into the feed tank, a premixed of the chosen foulant of 2 grams in 300ml of DI water is used instead. This specific volume is due to the desired concentration of 0.2g/L or 2g/10L. This process is now called fouling and is to be continued over 24 hours as per experiment 1.

Conductivity is to be measured at hour 2, 4 and 26 while noting the appropriate unit.

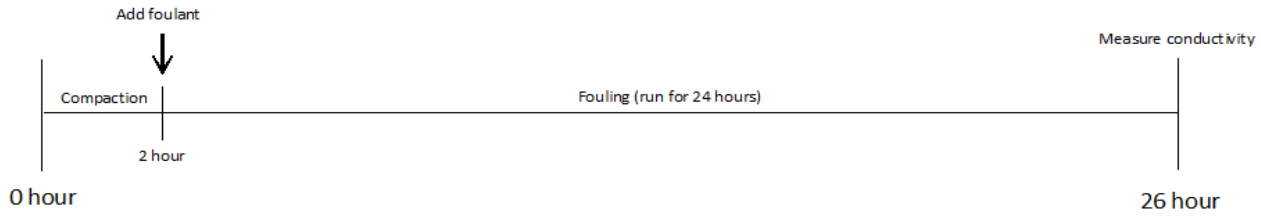

Figure 15: Timeline of that includes only the foulant agent.

3.4.Experiment with salt and foulant (NaCl + $CaCl_2$ + Alginate or NaCl + $CaCl_2$ Xanthan)

At t = 0 hours to t = 2 hours, the experiment is conducted with just DI water running through the membrane system. Before commencing the second stage, the conductivity in the feed tank is measured and recorded. When t = 2 hours, the chosen type and amount of salt is that was premixed in approximately 175ml of DI water is injected into the feed tank and mixed within the tank thoroughly. The stabilisation stage begins and is continued for 2 hours. When t = 4 hours, the conductivity is measured and recorded again, then the chosen foulant is added. The foulant is premixed in 300ml of DI water and stirred thoroughly, this enters the third stage, fouling. The fouling is continued for over 24 hours, thus, when t = 28 hours, the conductivity of the feed tank is measured and recorded once again. Finally, the process can be ceased and the data can be collected from the logging software.

Conductivity is to be measured at hour 2, 4 and 28 while noting down the appropriate unit.

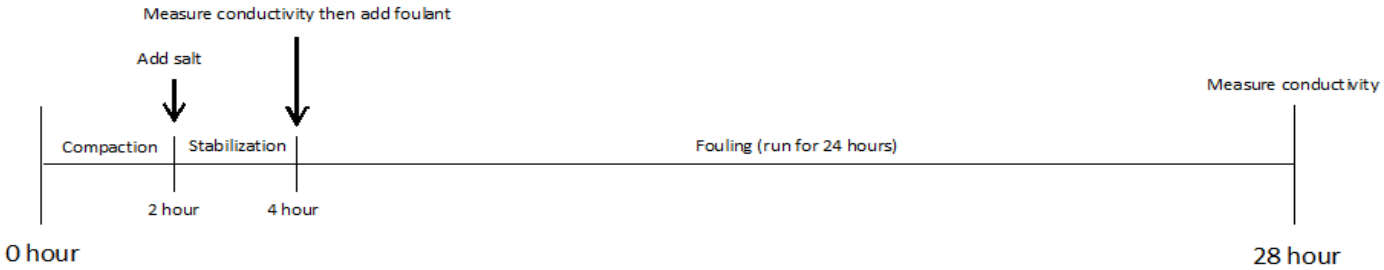

Figure 16: Timeline of experiment 4 and 5 which includes both salt and foulant in the same experiment.

3.5.Experiment Parameters

Crossflow rate = 0.5363 L/min → cross-flow velocity = 8.5 cm/s (maintained by the pumping system)

Pressure = 400 psi (this was assumed since the drawing tank will always be saturated with NaCl during the entire experiment)

Temperature = 25 ± 0.5 °C (temperature was controlled by a chiller bath) provided by Perth Scientific PTY LTD.

One sample of the used membrane from each experiment will be kept for further inspection on the CLSM. The membrane is stored in a petri dish with a cover and a few drops of DI water to maintain moisture and finally, the sample is kept in a refrigerator. The experiment is required to be conducted again where the experiment is carried on for four additional hours for cleaning and testing after the fouling tests. The extension hours are split into two sections: the first section is after the membrane has been cleaned with DI water and the feed consists only of DI water; the second section is after the membrane has been taken out of the unit and DI water is sprayed. The foulant gel is then physically removed from the membrane. This is done to test for a blockage that may contribute to the membrane hence causing a reduction in flux.

The four main chemical component that will be used in this experiment are Sodium Chloride (NaCl), Calcium Chloride ($CaCl_2$), [Sodium] Alginate (fouling agent) and Xanthan gum (fouling agent). Magnesium which is also another possible salt to be used was not involved with this experiment due to the lack of time. The following is a table containing some background information regarding the aforementioned four chemicals.

Table 1: Chemical used in the experiment with their providers.

Chemical	**Provider**
Sodium Chloride (NaCl)	CHEM-SUPPLY [Australia]
Calcium Chloride ($CaCl_2$)	CHEM-SUPPLY [Australia]
[Sodium]	SAFC [USA]

Alginate	
Xanthan gum	SIGMA [Germany]

3.6.Membrane sample storage

The procedure for storing membrane are as follows; once the experiment has ceased of its operation period; the membranes were are carefully taken of the unit and placed onto a petri dish with approximately 5 drops of DI water to maintain the humidity of the membrane for further analysis. The humidity will prevent the membrane from curling up and causing problems for confocal microscopy investigation. From here onwards, the membrane that is kept for analysis shall be called 'membrane sample'. Membrane sample is to be kept in a refrigerator where the temperature is controlled to be just above 0 degrees Celsius. The naming of membrane sample was marked on the petri dish to keep track of different sample. The stored membrane sample will be used for membrane weighting analysis to identify the layer formed on the membrane surface while a small section can be used for confocal laser scanning microscopy (CLSM) analysis.

3.6.1. Membrane weighting analysis

The membranes that were kept from each experiment were perfectly cut to the size of a 22mm x 22mm microscope glass slide. Each glass slide was weighted (noted as W_1) and noted accordingly to the sample used as different glass slide will have small variation was weight. Prepared sample was then stored in an incubator for 24 hours while controlling the temperature to be at 55°C, this is done to remove the excess water and moisture. A similar process is also done for a fresh membrane, to be used as a control (noted as W_2). The dried sample is then placed on a scale (noted as W_3). The following equations are used:

$W_2 - W_1 \rightarrow$ weight of fresh membrane without glass

$W_3 - W_1 \rightarrow$ weight of sample membrane without glass

$(W_3 - W_1) - (W_2 - W_1) \rightarrow$ weight of fouling layers and salt particles

This allows the study of fouling agents and their effect on the membrane, fouling layers and salt deposition on the membrane. Refer to appendix D for a table of results regarding membrane weight.

3.6.2. Confocal Laser Scanning Microscopy (CLSM) analysis

The objective of this analysis is to identify the thickness and concentration of fouling layers as well as the distribution of the layers.

The membranes that were stored in the fridge will be analysed further by confocal microscope, which will kindly be done by Murdoch staff, Dr. Lucy Skillman (technical staff specialised in biofouling). The staff mentioned that she was using a paper written by Mehboob Ahmed, Lucas J. Stal and Shahida Hasnain named "DTAF: an efficient probe to study cyanobacterial-plant interaction using confocal laser scanning microscopy (CLSM) as guidance.

The process to prepare the membrane for CLSM is as follows. Membrane sample is cut out to approximately 10mm x 10mm and placed on a glass slide for ease of transporting purpose. A staining solution called DTAF (pH 9), will highlight the fouling layer under the CLSM. DTAF are carefully stain on the membrane sample, using 75 mL for each sample to avoid excessive staining. A microscope cover glass is then cautiously placed on top of the DTAF solution then stored out of light for at least 18 hours. The stained sample was then analysed by the Nikon C2 Confocal Microscope System.

Microscope used for CLSM: Nikon C2 Confocal Microscope System (figure 17)

Figure 17: Pictures of the Nikon C2 Confocal Microscope System.

A series of images was captured and collected at a uniformed depth interval. The images were then collated by the Nikon software to create one 3D image, which can be found in 'CLSM image' chapter.

3.7.Liquid sample storage

The objective of collecting a liquid sample from the draw solution is for total organic carbon (TOC) analysis. According to LAR Process Analysers, a German company specialising in measuring water parameters, they stated that TOC is one of the most important composite parameters in the assessment of the organic pollution of water (LAR Process Analysers 2016). In the case of the TOC measurement from the liquid, this refers to the amount of polysaccharide contain in the draw solution at a particular point in time. With this analysis combining with the membrane weight study, a better understanding of deposition of polysaccharide on membrane surface can be obtained.

An approximate of 200mL of liquid samples were collected from one duplicate of each type of experiment after 4 hours (for salt or polysaccharide only) or 6 hours (when both salt and polysaccharide are used) and this is required to be stored in a refrigerator where temperature is controlled to be just above 0 degrees Celsius. Another liquid sample was taken at the end of each

experiment, after 24 from the start of conducting the experiment (at time 26 hours for salt or polysaccharide; at time 28 hours when a combination of salt and polysaccharide are used).

3.7.1. Total Organic Carbon (TOC) analysis

TOC measurement is conducted by a team of professional staff in Marine and Freshwater Research Laboratory (MAFRL) located in Murdoch University, South street campus, physical science building in room 3.026. The MAFRL will require approximately 200mL of liquid sample that was stored by the previous chapter from each experiment for the TOC testing. Please refer to appendix D for the table of the result.

3.7.2. Standard Curve

The objective of a standard curve is to draw a correlation between concentration and conductivity.

A standard curve for NaCl and $CaCl_2$ at 50mM was determined using dilution method. In the actual experiment, 27.5g of NaCl and 1.47g of $CaCl_2$ was used in 10 litres (10000mL) of DI water. However, to determine the standard curve, it is not required to use as much as 10000mL, thus, the mixture can be scale down (while keeping the same ratio and concentration). Therefore, the new requirements are; 0.275g of NaCl and 0.0147g of $CaCl_2$ mixed in 100mL. The following are steps for dilution to identify the standard curve:

1. Mix 0.275g of NaCl and 0.0147g of $CaCl_2$ into 100mL of DI water in a 100mL volumetric flask. Place lid on and shake vigorously. Mark that this is 50mM in concentration.
2. Carefully and accurately, using a funnel, pour the solution made in step 1 into a 50mL volumetric flask. When precisely 50mL of saline solution has been transferred, pour it again into an empty 100mL volumetric flask. Using roughly 10 mL of DI water, wash the 50mL volumetric flask that was just used and pour it into the 100mL volumetric flask that is currently half empty. Repeat 3 times. Fill the 100mL volumetric flask up to the mark and shake vigorously. Mark that this is 25mM in concentration.
3. Repeat the second step with the 25mM solution. This now become 12.5mM in concentration.

4. For the 5mM saline solution, 10mL is to be pipetted out of the 25mM saline solution and placed into an empty 50mL volumetric flask. Fill the solution up to the mark with DI water. Now this becomes a 5mM saline solution.
5. Pipette 25mL out of the 5mM saline solution and place it into a 50mL volumetric flask. Fill the latter volumetric flask to 50mL mark with DI water. This now becomes a 2.5mM saline solution.
6. Measure each solution conductivity while noting down the respective concentration. Keep all the unit consistent throughout the entire experiment.
7. Plot a graph of conductivity vs. concentration.

A correlation can now be drawn between the conductivity and concentration for a NaCl with $CaCl_2$ solution. Please refer to result chapter for more information.

3.8.Conductivity vs Time baseline (DI water only)

The objective of this is to identify the back diffusion rate of salt from the draw side to the feed side.

This is done by conducting an experiment over 26 hours with the first 2 hours for compaction. After the first 2 hours of compaction has finished, the conductivity of the draw solution was measured at an hourly rate while noting the time it was taken at. A plot of conductivity vs time will present the change of conductivity over time and with the use of standard curve, a conductivity over time graph can be drawn.

4. Modelling

In order to understand the concept of biofouling effects, different equation and data manipulations are devised and used.

4.1.Flux

Darcy's Law illustrates the relationship between flux with pressure and resistance. This will allow this paper to model the interaction of flux with the total resistance (Zhao and Zou 2011, Zankel 2016)

$$Flux, J = \frac{\Delta P}{\mu \cdot R_t} \quad \text{(Eq. 1)}$$

Where:

- ΔP is the pressure that was applied onto the membrane (in Pa, Pascal)
- μ is the viscosity of permeate through a medium (in Pa·S, Pascal-second)
- R_t is the total hydraulic resistance (in m^{-1}, per meter)

However, in the case of the forward osmosis system, the ΔP is split into

$$\Delta P = \pi_{d,m} - \pi_{f,m} \quad \text{(Eq. 2)}$$

Where:

- $\Pi_{d,m}$ is the osmotic pressure on the draw side of the membrane (in Pa, Pascal)
- $\Pi_{f,m}$ is the osmotic pressure on the feed side of the membrane (in Pa, Pascal)

Therefore, Eq. 1 becomes:

$$J = \frac{\pi_{d,m} - \pi_{f,m}}{\mu \cdot R_t} \quad \text{(Eq. 3)}$$

Further manipulation of the equation can be done to identify resistance of membrane (R_m), cake resistance (R_c) and concentration polarisation (R_{cp}) all in the unit of m^{-1}. This can be found by breaking the total hydraulic resistance down as per the following equations.

$$R_t = R_m + R_c + R_b \quad \text{(Eq. 4)}$$

OR

$$R_t = R_m + R_{cp} + R_b \text{ (Eq. 5)}$$

Where:

- R_b is the resistance caused by blockage (in m^{-1}, per meter)

Note that in all of the calculation the R_b will be assumed as 0 m^{-1}. This was confirmed by multiple experiments conducted to test for blockage resistance which was not found or were too small hence neglecting it was reasonable to do so.

4.2.Resistance

Total resistance can be found by rearranging Eq. 3 to be the following:

$$R_t = \frac{\pi_{d,m} - \pi_{f,m}}{\mu \cdot J} \text{ (Eq. 6)}$$

4.2.1. Concentration Polarisation

Concentration polarisation can only be used in a case where salt and DI water is in the feed. With the adaptation of Eq. 5 and Eq. 6, the following equation can be made:

$$R_{cp} = R_t - R_m - R_b = \frac{\pi_{d,m} - \pi_{f,m}}{\mu \cdot J} - R_m - R_b \text{ (Eq. 7)}$$

4.2.2. Cake resistance

Cake resistance is caused by the involvement of polysaccharide only. With the adaptation of Eq. 4 and Eq. 6, the following equation can be made:

$$R_c = R_t - R_m - R_b = \frac{\pi_{d,m} - \pi_{f,m}}{\mu \cdot J} - R_m - R_b \text{ (Eq. 8)}$$

4.2.3. Cake enhanced layer (Cake resistance + Concentration polarisation)

Cake enhanced layer is the product of the cake layer and concentration polarisation process occurring together in one experiment. Therefore, this equation is used when both salt and polysaccharide are used in the system. With the adaptation of Eq. 4, Eq. 5 and Eq. 6, the following equation can be made:

$$R_{cp} + R_c = R_t - R_m - R_b = \frac{\pi_{d,m} - \pi_{f,m}}{\mu \cdot J} - R_m - R_b \quad \text{(Eq. 9)}$$

4.3.External Concentration Polarisation on draw side

External concentration polarisation on draw side (ECP_d) or also known as dilutive external concentration polarisation (DECP) is the difference between the two adjacent osmotic pressures. Henceforth, the following equation can be derived to find the ECP of the draw side:

$$ECP_d = \pi_{d,b} - \pi_{d,m} \quad \text{(Eq. 10)}$$

Where:

- ECP_d is the external concentration polarisation on draw side (in Pa, Pascal)
- $\Pi_{d,b}$ is the osmotic pressure on the draw side of the bulk solution (in Pa, Pascal)
- $\Pi_{d,m}$ is the osmotic pressure on the draw side of the membrane (in Pa, Pascal)

4.4.External Concentration Polarisation on feed side

External concentration polarisation on feed side (ECP_f) or also known as concentrative external concentration polarisation (CECP) is the difference between the two adjacent osmotic pressures. Henceforth, the following equation can be derived to find the ECP_f of feed side:

$$ECP_f = \pi_{f,b} - \pi_{f,m} \quad \text{(Eq. 11)}$$

Where:

- ECP_f is the external concentration polarisation on feed side (in Pa, Pascal)
- $\Pi_{f,b}$ is the osmotic pressure on the feed side of the bulk solution (in Pa, Pascal)
- $\Pi_{f,m}$ is the osmotic pressure on the feed side of the membrane (in Pa, Pascal)

4.5.Internal Concentration Polarisation

For the system to be constantly operating, the osmotic pressure of the draw side on membrane has to match the osmotic pressure of the feed on membrane side, 400psi of pressure (2.758 x 10^6 pa) and ICP. Therefore, an equation can be made to put ICP as the final answer:

$$\pi_{d,m} - 400psi\ (2.758x10^6pa) - \pi_{f,m} = ICP \quad \text{(Eq. 12)}$$

Where:

- ICP is the internal concentration polarisation (in Pa, Pascal)

4.6.Osmotic pressure of a solution

By utilising De Van't Hoff's equation (equation 13), the osmotic pressure of NaCl saturated solution was able to be identified and were assumed to be correct hence was used in other calculations.

$$\pi = i \cdot M \cdot R \cdot T \text{ (Eq. 13)}$$

Where:

- Π is the osmotic pressure (pa.s)
- i is the van 't Hoff's factor
- M is the concentration of the solution (mol/L)
- R is the gas constant which is 0.08206 L·atm/mol·K
- T is temperature in Kelvin

4.7.Osmotic pressure of salt on membrane surface

The osmotic pressure can be found by understanding that:

$$\Delta P = P - P_0 - \pi_{cp} = \pi_{f,m} - \pi_{d,m} - \pi_{cp} \quad \text{(Eq. 14)}$$

Applying this (Eq.14) to Eq. 1 and Eq. 5 (with the assumption of R_b is zero), another equation can be made:

$$J = \frac{P - P_0 - \pi_{cp}}{\mu \cdot (R_{cp} + R_m)} \quad \text{(Eq. 15)}$$

Therefore:

$$\pi_{cp} - \pi_{f,m} = \mu \cdot J \cdot R_{cp} \quad \text{(Eq. 16)}$$

4.8.Concentration of salt on membrane surface

The equation to find a concentration of salt on membrane surface is given by the following equation (de Van't Hoff's equation).

$$C_{cp} = \frac{\pi_{cp}}{i \cdot R \cdot T} \quad \text{(Eq. 17)}$$

Where:

- C_{cp} is the concentration of salt on the membrane surface (mol/L)
- Π_{cp} is the osmotic pressure (pa.s)
- i is the van 't Hoff's factor
- R is the gas constant which is 0.08206 L·atm/mol·K
- T is temperature in Kelvin

4.9.Fick's Law

Based on Fick's law, the rate of diffusion was able to be identified using the following Fick's Law equation (http://america.pink/fick-laws-diffusion_1545735.html):

$$\mathrm{R} = \mathrm{D} \cdot \frac{\mathrm{A} \cdot \Delta \mathrm{C}}{\mathrm{h}} \quad \text{(Eq. 18)}$$

Where:

- R is the rate of diffusion (in m^2/s or cm^2/s)
- D is the diffusion coefficient
- A is the effective area of the membrane (in m^2, meter square)
- h is the thickness of the biofilm (in m^2, meter square)

5. Results & Discussion

5.1.Standard Curve of Conductivity vs Salt Concentration

Dilution experiment was conducted multiple times to achieve a set of data where the R^2 value is greater than 0.995. From the chosen set of data, a concentration vs conductivity graph can be constructed with an equation. Note that the graph has the y-axis intercept set to zero so it matches the theoretical conductivity of DI water which is 0μS. A relationship between the two is given by the equation:

$$y = 0.0168x$$

Where y is the concentration of NaCl and $CaCl_2$ solution in millimol and x is the conductivity of that solution in micro Siemens.

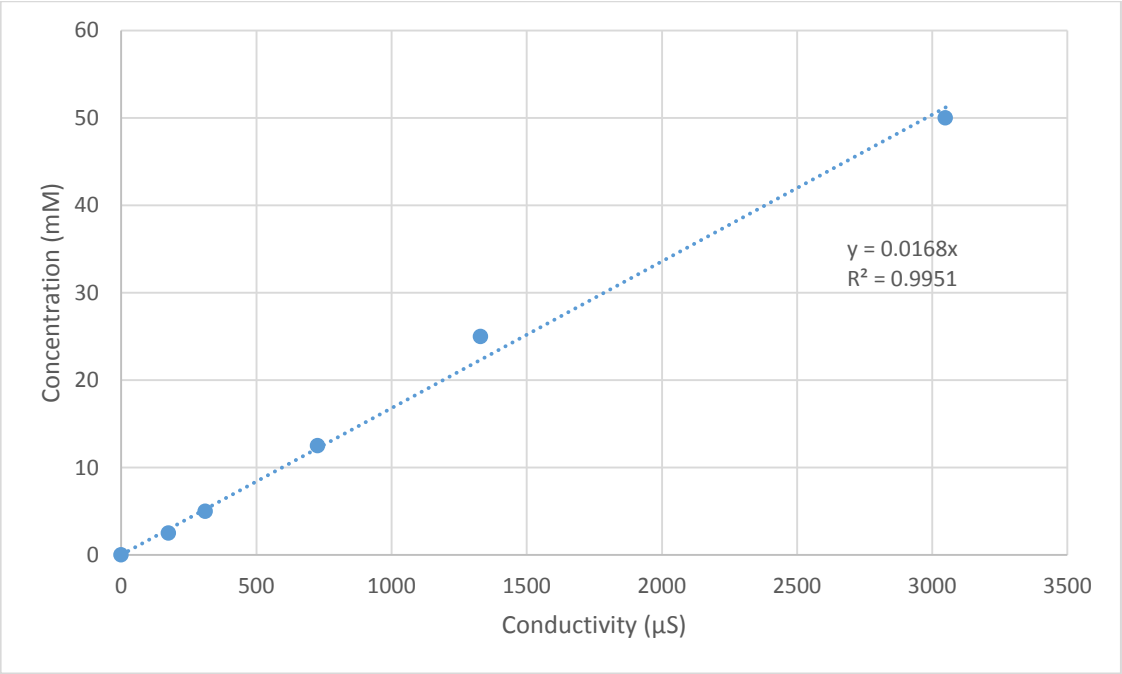

Figure 18: Graphical representation of the data collected for standard curve, concentration vs conductivity.

5.2.Conductivity vs time baseline (DI water only)

The graph (figure 19) represents the conductivity of an FO system where the draw solution is a saturated NaCl solution and feed solution is DI water.

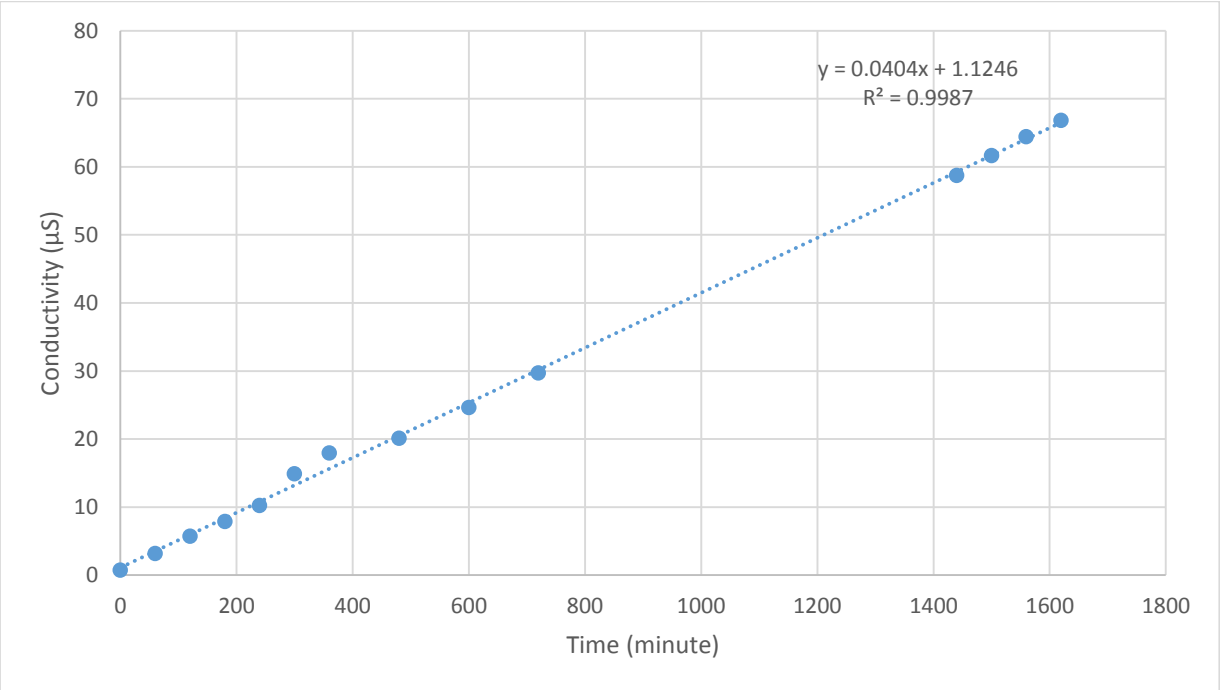

Figure 19: Graphical representation of the data collected for the dilution of NaCl and $CaCl_2$ at 50 mM, conductivity vs time.

The conductivity was measured at an hourly rate where possible. There is in total 14 data points. A line of best fit is drawn based on the data point along with its equation and R^2 value. For this experiment R^2 value of 0.9987 is acceptable (greater than 99.5 % is acceptable) hence, the data is useable. By utilising the equation:

$$y = 0.0404x + 1.1246$$

Where y is the conductivity in micro Siemens and x is the time in minutes. This will allow the understanding of back diffusion rate of NaCl saturated solution via the membrane. Refer to appendix B for a table of the result.

5.3.Forward Osmosis results

The data that was collected from each experiment was analysed and modelled (using formula stated in the modelling section) to obtain flux, resistance, concentration polarisation, cake layer resistance, cake enhanced layer resistance and normalised data which are separated into small chapters. Please refer to appendix E for a summary of flux & resistance and appendix F for a summary of conductivity for each experiment. Appendix G is the schedule for each experiment that was conducted and some comments as to whether each experiment was successful.

5.3.1. Average flux

In each experiment, the weight of the draw solution was measured at one-minute intervals. The flux was calculated using this weight difference per ten minutes (10-minute average), consider to the following equation:

$$J = \frac{(m_2 - m_1)}{10} \cdot \frac{1kg}{1000g} \cdot \frac{60\ minutes}{1hour} \cdot \frac{A}{100 \cdot 100} \text{(Eq. 19)}$$

Where:

- J is the average flux per 10 minutes (in LMH, litre per hour per meter square)
- m_2 is the weight measured at t = 10 (in g, gram)
- m_1 is the weight measured at t = 1 (in g, gram)

- A is the effective area of the membrane (in cm^2, centimetre square)

The flux that was calculated from eq. 19 was then plotted against its respective time (over 24 or 26 hours depending on the experiment). A line graph was chosen to emphasize the flux trend whether it's decreasing or increasing as well as determining any fluctuation or outlying points that should not occur. In addition, multiple chosen types of experiments were plotted on one graph for better comparison viewing. The modelled data of the flux is presented over next 4 figures.

In the case of averaged flux (figure 20), the result shows that it has the lowest flux (by an average of 2.2 LMH) as it does not pose as a great resistance on the membrane which is why the trend of the flux was low compared to alginate and xanthan. However, the initial flux of the three experiments when compared are relatively far apart and this could be because of the different membrane (section that was cut out) having different membrane resistance (R_m) values. Unfortunately, for FO system, the membrane resistance cannot be identified so instead an assumed membrane resistance value was calculated in the RO system and used with FO system for all of the experiments conducted (even though this may not be the true resistance).

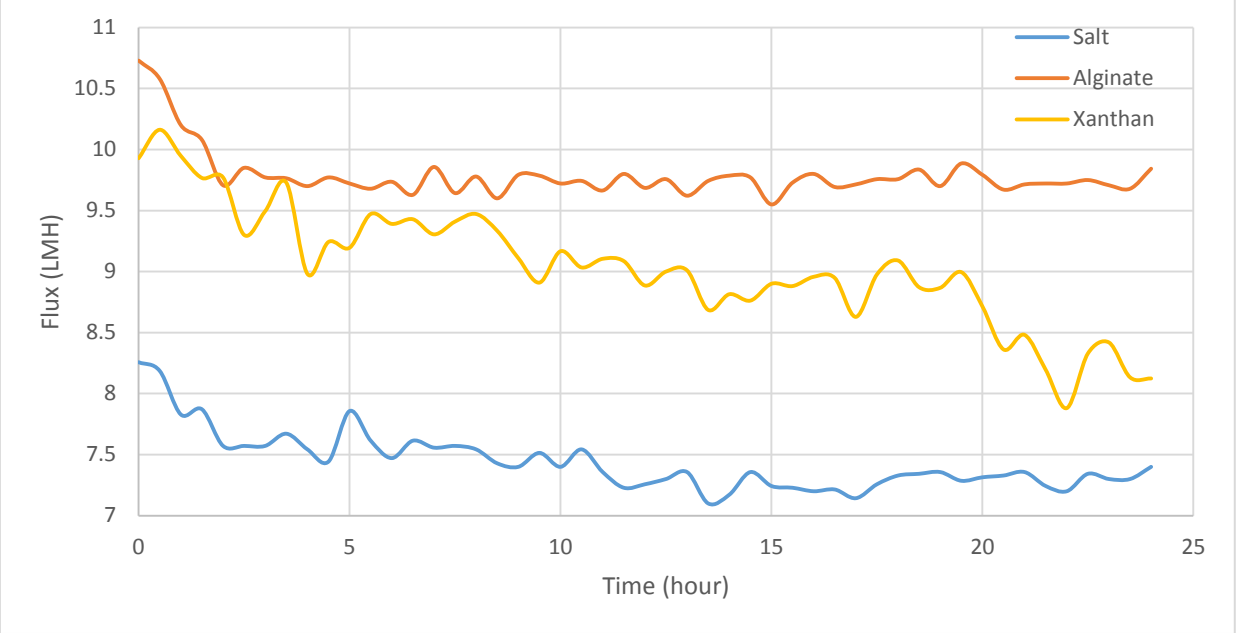

Figure 20: Graph of flux from 3 different experiment (salt, alginate, and xanthan).

Figure 20 demonstrates that salt and alginate resulted in similar trend regarding the flux where they start out with a big decline (about 1.5 LMH over 4 hours) in flux but stabilise soon after

whereas the xanthan and salt (figure 21) shows a slow declining trend that actually does not stabilise within the 24 hours.

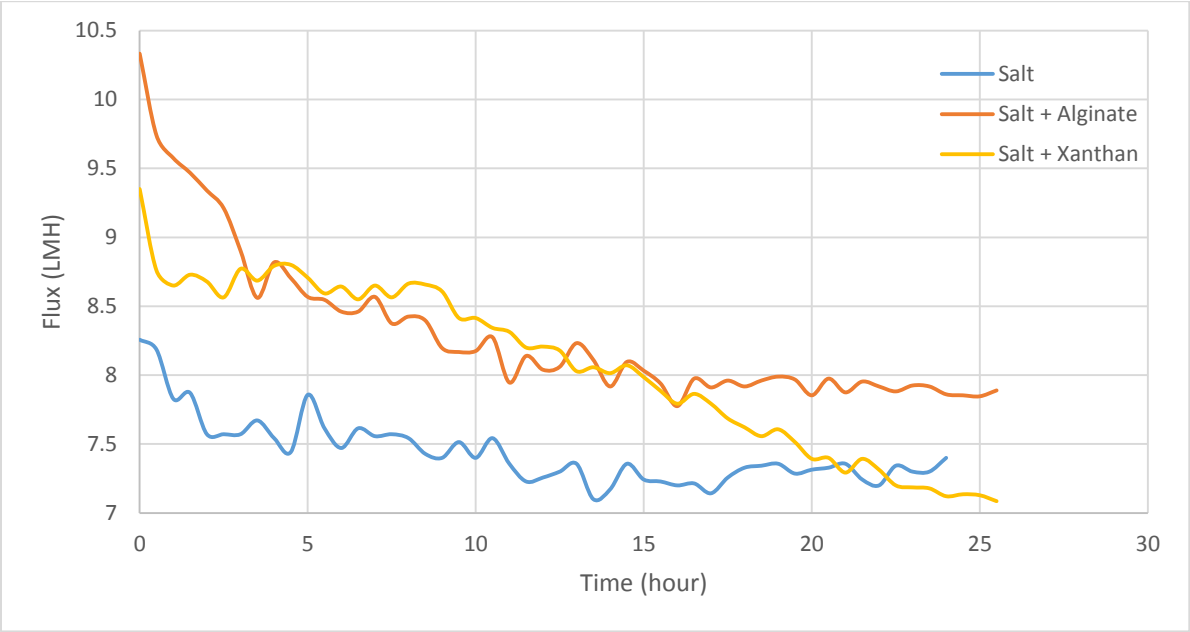

Figure 21: Graph of flux from 3 different experiment (salt, salt + alginate and salt + xanthan).

Figure 20 and 21 demonstrates that regardless of the inclusion of salt with alginate the flux will maintain the same trend (that is a large decline followed by a gradual stabilisation). However, in the case of with salt alginate had a much larger initial decline and also took longer to stabilise. Moreover, the xanthan and salt flux doesn't decrease until hour 9 but there is a gradual decline.

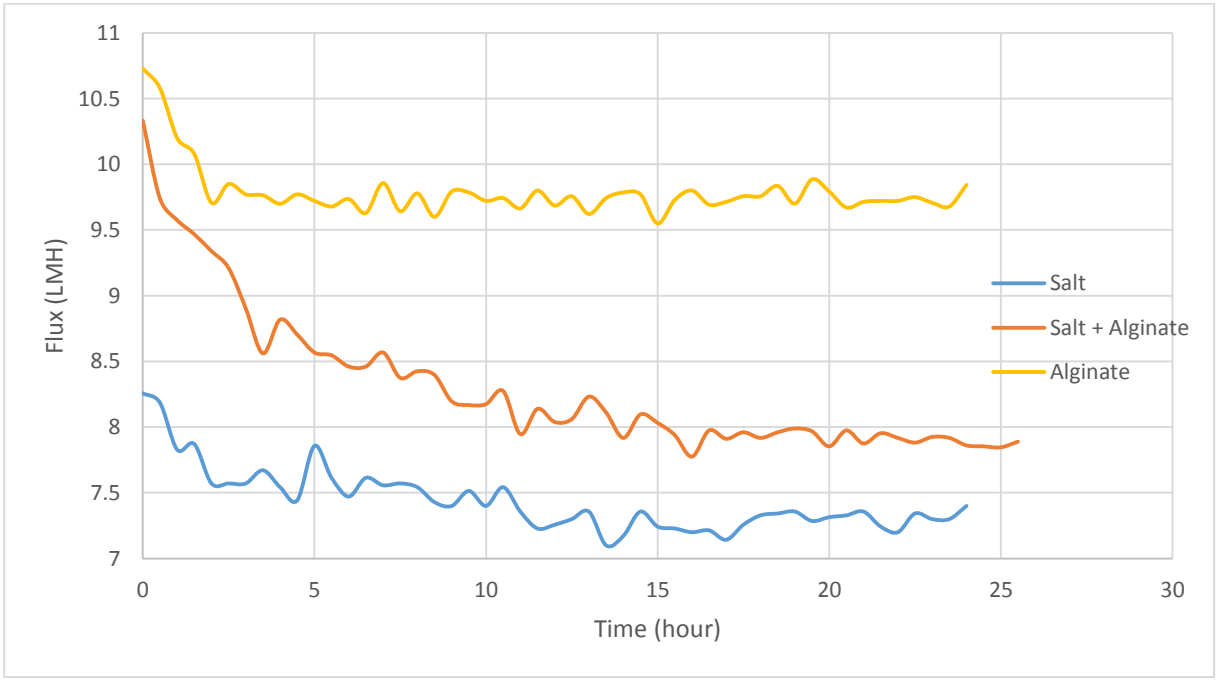

Figure 22: Graph of flux from 3 different experiment (salt, salt + alginate and alginate).

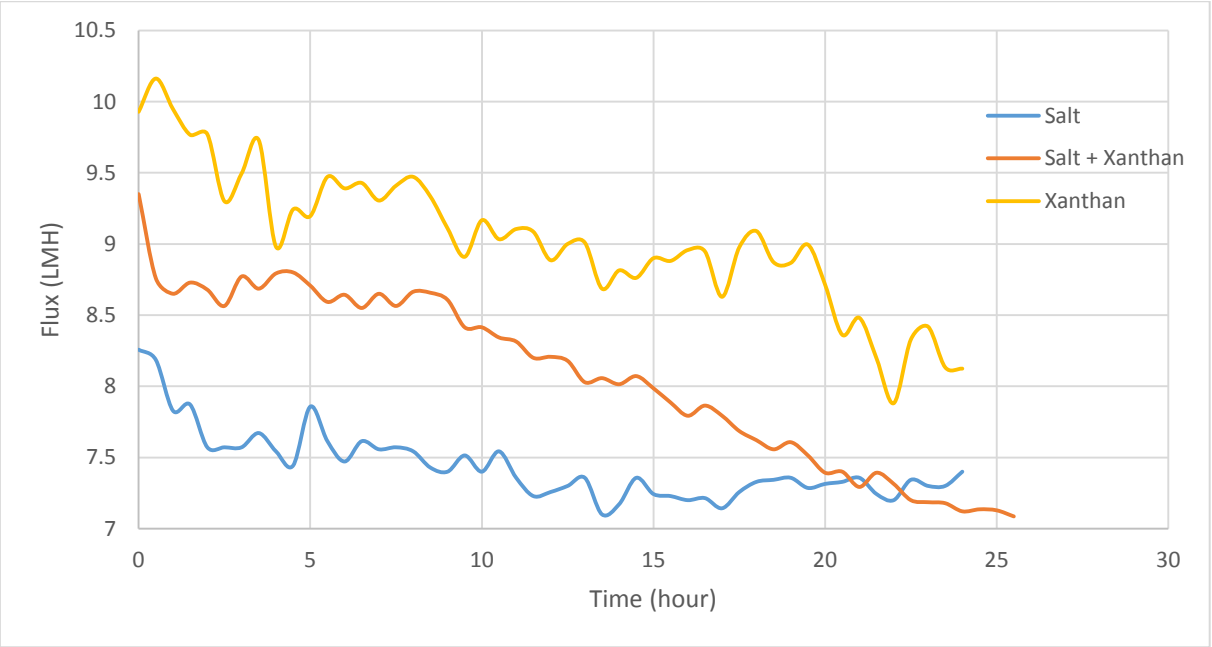

Figure 23: Graph of flux from 3 different experiment (salt, salt + xanthan and xanthan).

Figure 22 and 23 highlight the fact that once salt is added to the polysaccharide whether its alginate or xanthan, the flux will be lower. In addition, for the xanthan and salt experiment, the flux actually has less fluctuation between the hours (smoother line).

A more thorough comparison will be made in the next section where the data is normalised.

5.3.2. Normalised flux

When data between experiments have a different base flux, normalising the data is necessary so the comparison is more meaningful. In order to normalise the flux, the following equation was used:

$$J_N = \frac{J}{J_0} \quad \text{(Eq. 20)}$$

Where:

- J_N is the normalised flux
- J is the flux (in LMH or m/s)
- J_0 is the initial flux, that is flux at the first minute (in LMH, m/s)

Normalised data will remove the unit of measurement while reorganising the data to bring all the variables into proportion with one and another (Abdi 2010). This will allow the data to be reflected on relativity between each data point and different experiments while outlining a clear trend of the data (Etzkorn 2011).

A more accurate comparison of flux between each experiment can be drawn with normalised data as they are now normalised to the same base value. It is clearer now that the experiment with salt even though in figure 20 it has the lowest flux, the normalised data actually shows that salt isn't the lowest flux (figure 24). In the case of figure 24, the salt flux compared to the other experiments was not as low, in fact, it is higher than xanthan by 0.07. Moreover, in figure 25, when it's being compared with the salt + alginate and salt + xanthan, it has the highest flux.

The xanthan data in figure 24 shows that it flucuates more than the other two experiment and also has the lowest final flux, reaching as low as 0.8 while the other two experiments finish around 0.9 to 0.92. In addition, xanthan also causes the most fluctuation, bouncing up and down.

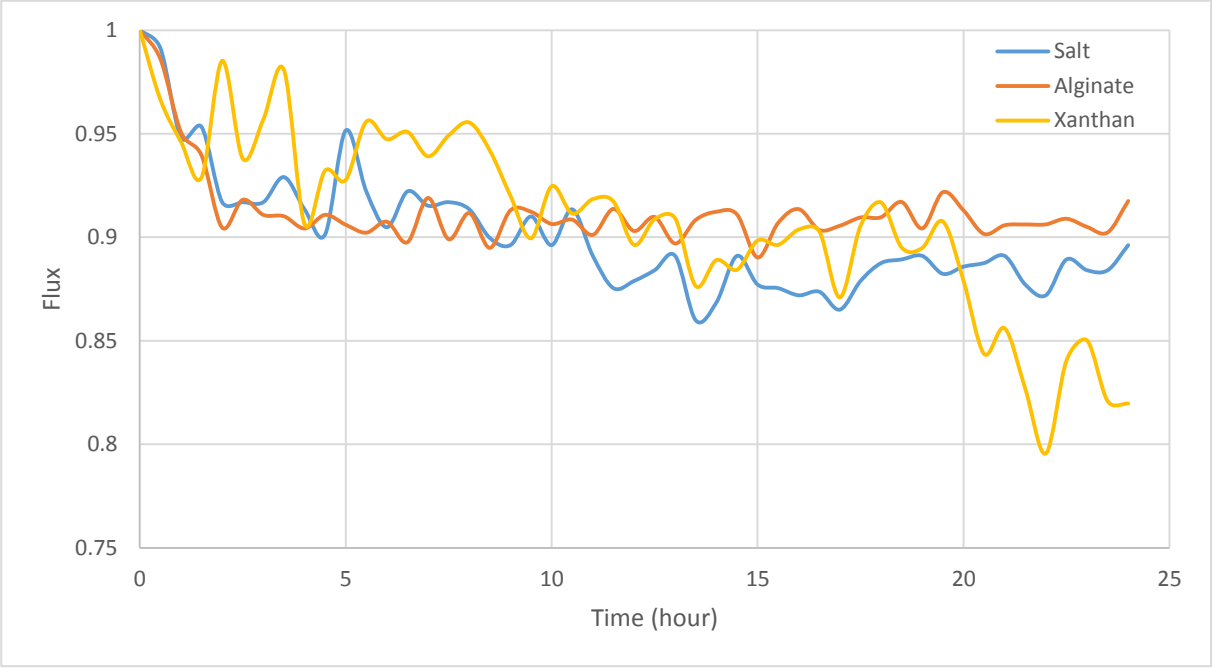

Figure 24: Graph of normalised flux from 3 different experiment (salt, alginate, and xanthan).

Between salt + alginate and salt + xanthan in figure 25 both show a different trend where the salt + alginate has a larger decrease (dropping from 1 to 0.78 in 15 hours) and the salt + xanthan has slow decrease (dropping from 1 to 0.85 in 15 hours). However, both cases finish at 0.76. This

means that salt combination with both types of polysaccharide causes a similar decline in flux intensity. However, the slope and gradient are different and this is potentially due to how fast the gel is formed on the membrane. For example, in the case of salt and xanthan, the gel formation is more casual and constant over the 26 hours of the experiment. On the other hand, the salt and alginate have a sharper decline which possibly means that the gel forms at a faster pace and reaches its maximum gel formation potential causing the flux to stabilise around the 15th hour.

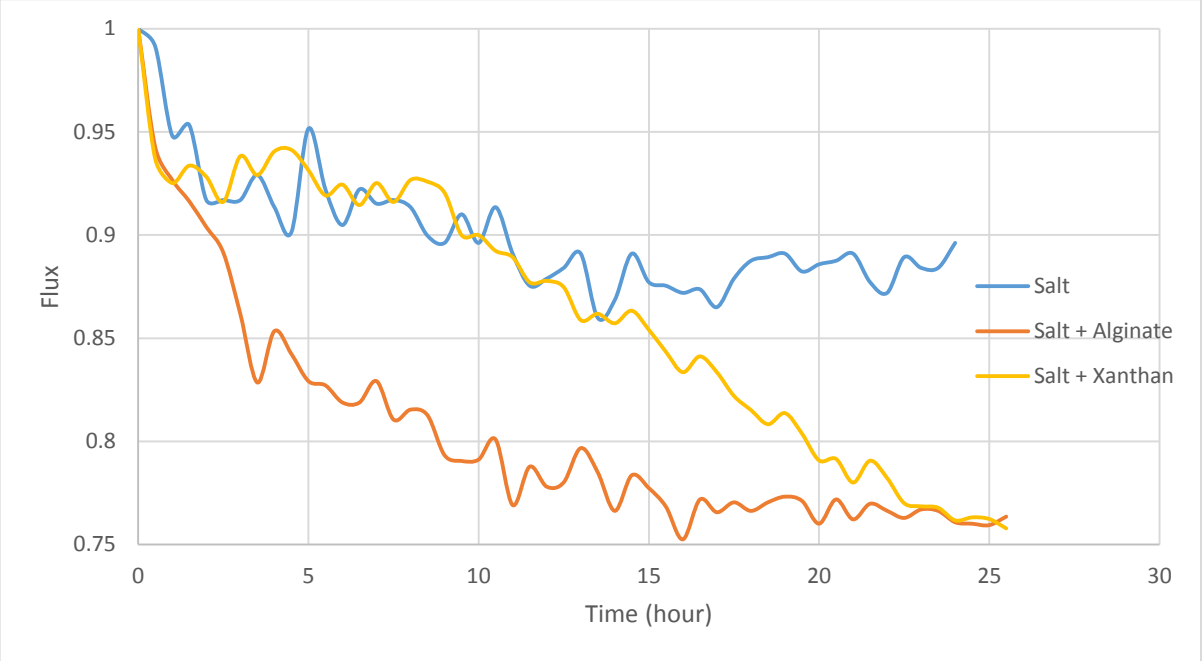

Figure 25: Graph of normalised flux from 3 different experiment (salt, salt + alginate and salt + xanthan).

In figure 26 and 27, they both highlight the effect of having a mixture of polysaccharide and salt. It is clear that polysaccharide combining with salt, the flux greatly reduces to 0.76 in both alginate and xanthan's case. For alginate, the reduction of flux when compared to alginate alone, it reduces by 0.15 while in the case of xanthan it is less evident, the reduction was by 0.08. This reduction demonstrates that when the salt combines with the polysaccharide, it triggers some sort of resistance on the membrane that causes the flux changes as revealed in figure 26 and 27. As for the trend of reduction, it seems that the salt + alginate has a stronger decreasing rate and stabilises at the 15th hour or so while the salt + xanthan case has a gradual constant decreasing rate. This could possibly be because the gel formation process is much earlier in the alginate case whereas the xanthan has a slow gradual build-up of the gel development.

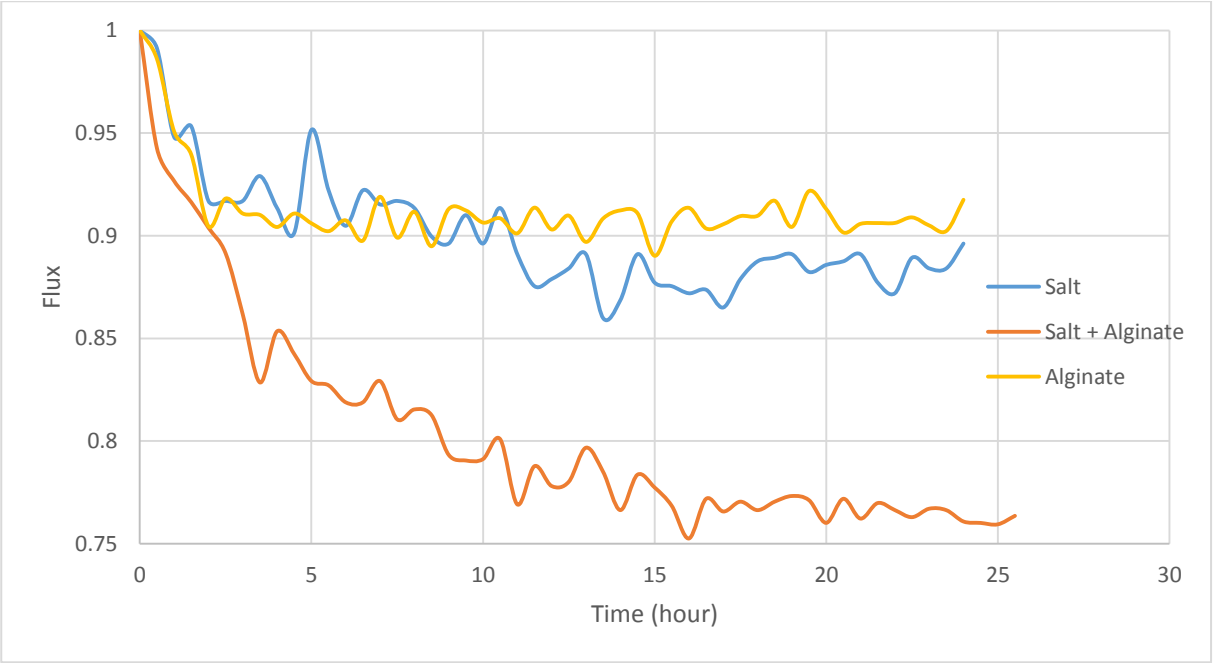

Figure 26: Graph of normalised flux from 3 different experiment (salt, salt + alginate, and alginate).

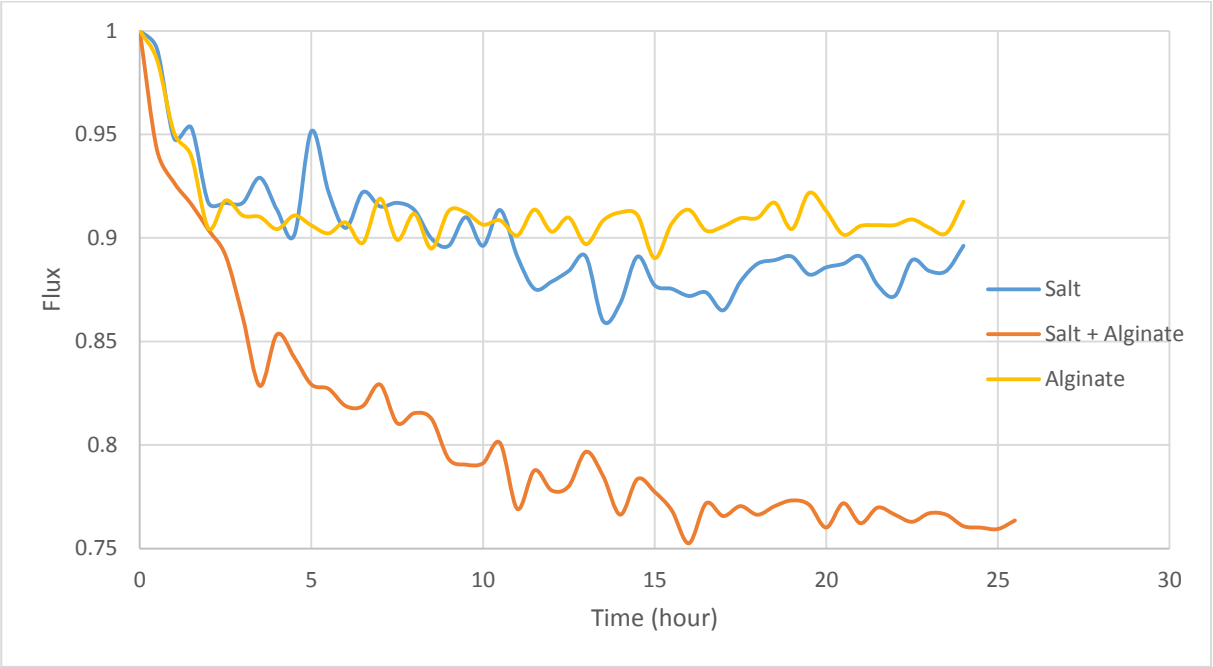

Figure 27: Graph of normalised flux from 3 different experiment (salt, salt + xanthan and xanthan).

5.3.3. Normalised total resistance

After eq. 6 has been applied to the flux calculated in the previous chapter, the resistance is then plotted with the same combination of experiments for a more effective comparison. The flux is then normalised using the following equation.

$$R_N = \frac{R}{R_0} \quad \text{(Eq. 21)}$$

Where:

- R_N is the normalised resistance
- R is the resistance (in x 10^{16} m^{-1})
- R_0 is the initial resistance, that is resistance at the first minute (in x 10^{16} m^{-1})

It was assumed that membrane resistance is to be constant over all of the experiments conducted. In addition, R_m can be found by inspecting the total resistance of the first experiment (DI water only) since R_{cp} and R_c does not exist yet. Therefore, the first point of normalised resistance in this section for every experiment will be removed as it does not flow with the trend. However, the other data points will still be normalised in the same manner as eq. 21.

The resistance of the baseline is unreasonably high compared to the other experiments and this is due to the assumption of membrane resistance to be consistent for all experiments. Unless the membrane resistance can be calculated for each individual experiment, an accurate total resistance will have minor error in them. It seems that the baseline experiment's membrane resistance was higher than the other, causing its initial resistance to be this high. In addition, salt compared to other cases does not trigger any formation of biofilm hence the resistance being that high is only caused by the actual high R_m value (this can be illustrated by eq. 4 and eq. 5).

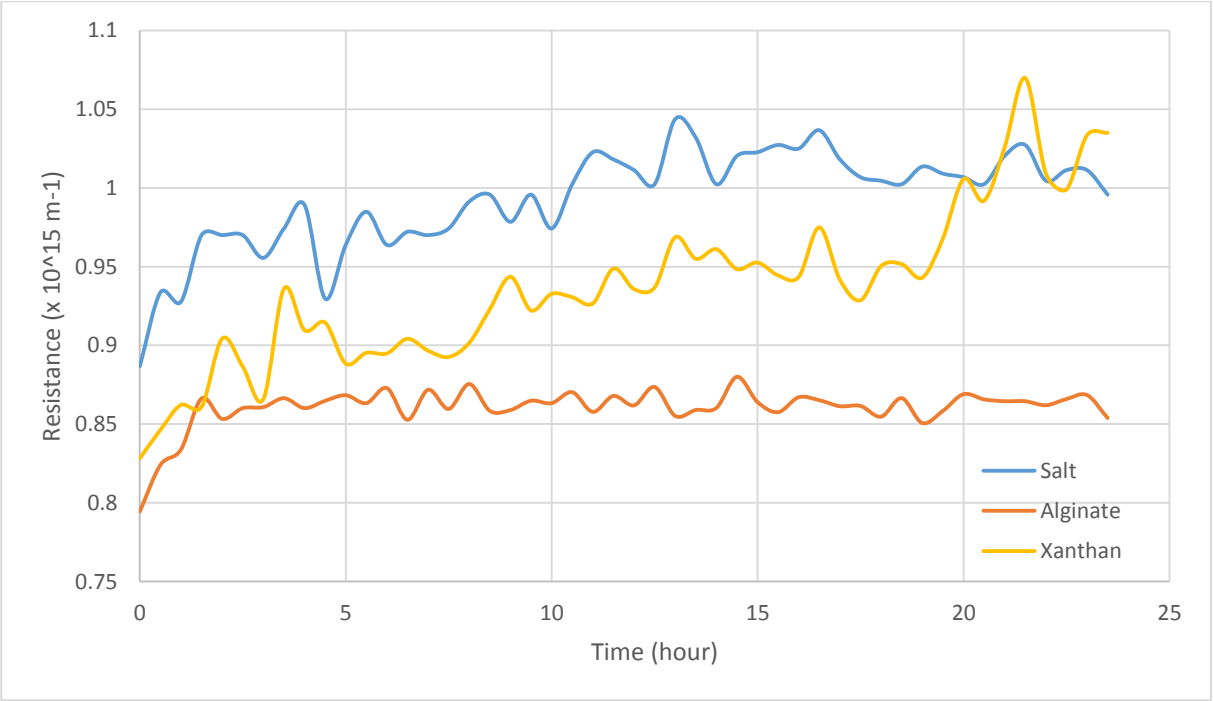

Figure 28: Graph of normalised resistance from 3 different experiment (salt, alginate, and xanthan).

As it was expected from the flux in figure 21 with the lowest resistance being salt coupled with xanthan, therefore, the highest resistance in this case (figure 29) was the salt and xanthan as well. The difference between the two polysaccharides with salt was 0.9, considered to be a relatively large difference thus showing that alginate reduces less flux between the two cases.

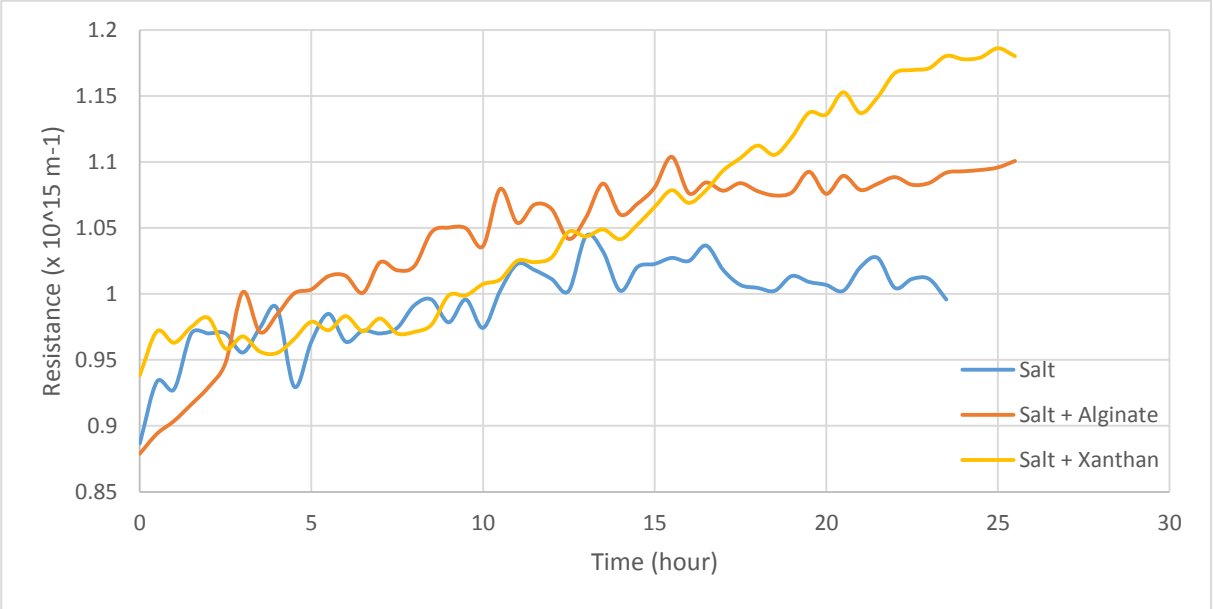

Figure 29: Graph of normalised resistance from 3 different experiment (salt, salt + alginate and salt + xanthan).

Figure 30 and 31 highlight the resistance differences when salt is mixed with the chosen polysaccharide. The resistance increases as expected from the decrease of flux in figure 22 and

23. As shown once again, the coupling calcium ions (from $CaCl_2$) causes the dramatic increase in resistance due to the formation of the gel. Inspecting figure 30 and 31 and using the resistance scale, it can, once again, validate that xanthan with salt mixture, having a resistance of 1.2, will result in a higher resistance than alginate salt mixture, having a resistance of 1.12.

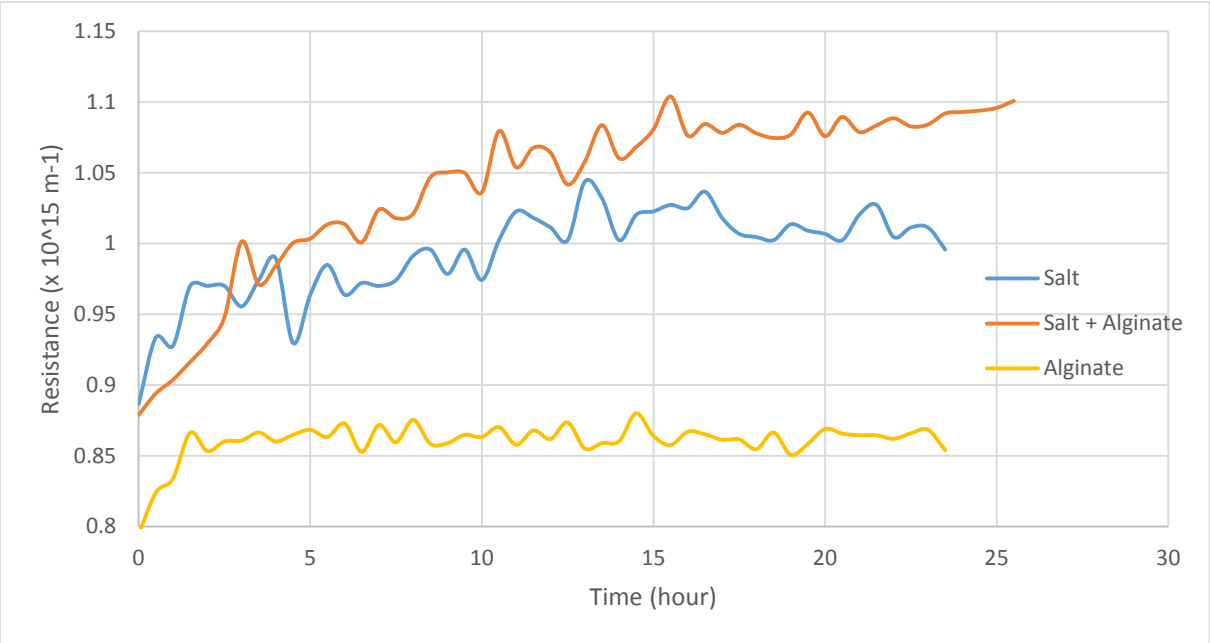

Figure 30: Graph of normalised resistance from 3 different experiment (salt, salt + alginate and alginate).

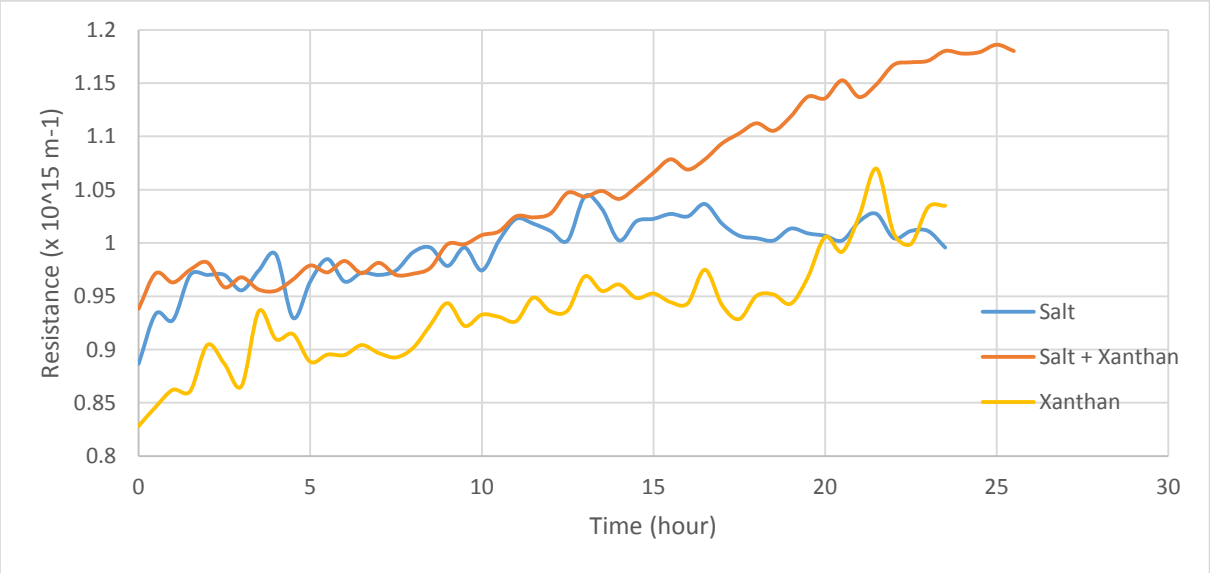

Figure 31: Graph of normalised resistance from 3 different experiment (salt, salt + xanthan and xanthan).

5.3.4. Cake layer resistance

R_c or also known as cake layer resistance occurs only when polysaccharides are used in the experiment. In this case, xanthan and alginate R_c were plotted on the same graph to differentiate its behaviour.

In figure 32, alginate shows a greater resistance over xanthan for the first 8.5 hours where then the xanthan matches the same resistance as alginate and overtakes it thereafter. The final resistance than xanthan has 2.5 times higher resistance than alginate, this fact represents that xanthan causes biofouling at a higher level than alginate does but at a slower pace. In addition, FO system seems to have a better handle of alginate compared to xanthan since the alginate trend does not fluctuate as much as xanthan.

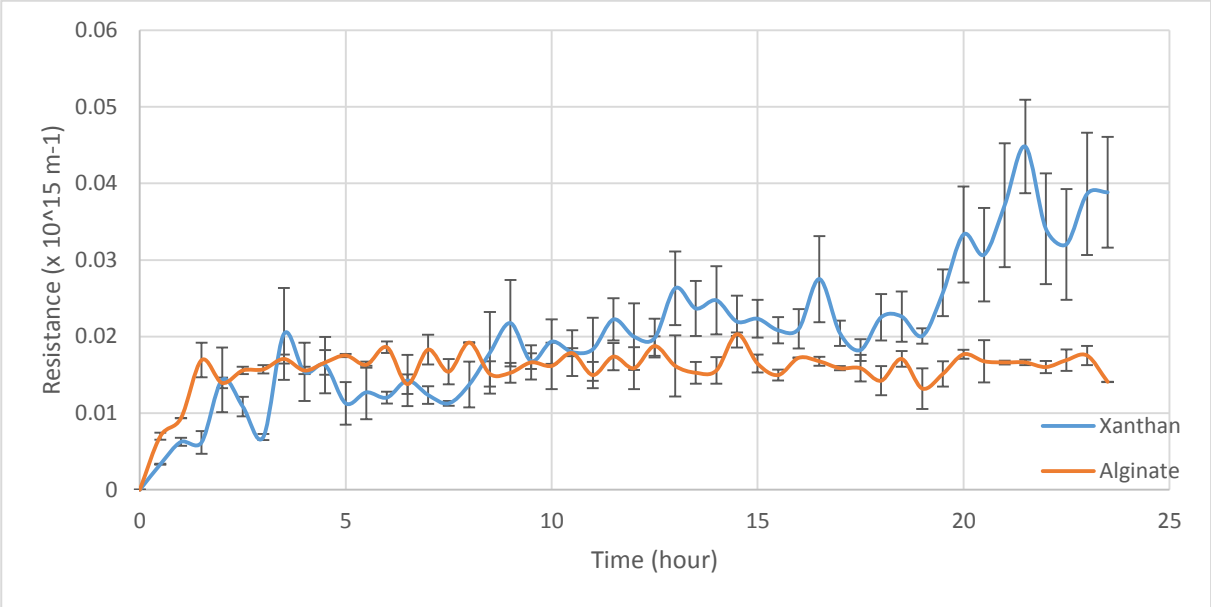

Figure 32: Resistance due to cake layer generated by alginate and xanthan experiments.

5.3.5. Concentration polarisation resistance

R_{cp} (resistance due to concentration polarisation) occurs only when salt (NaCl and $CaCl_2$) is used. The resistance caused by this is relatively low compared to R_c value.

In figure 33 when put into comparison with the cake and cake enhanced resistance, it demonstrates to have the lowest flux. Since salt does not trigger any form of major physical matter to increase the resistance, therefore the resistance is presented to be minimal as seen in

figure 33. Refer to the CLSM image in figure 48 the confocal image of this baseline experiment is found to be at only 50µm (the least among all the experiments) where most of that thickness is salt particles deposited on the membrane surface. The only reason that there is an increase in resistance is due to the increase concentration of salt at the membrane surface and therefore the osmotic pressure at the membrane as well (Kim *et al.* 2006).

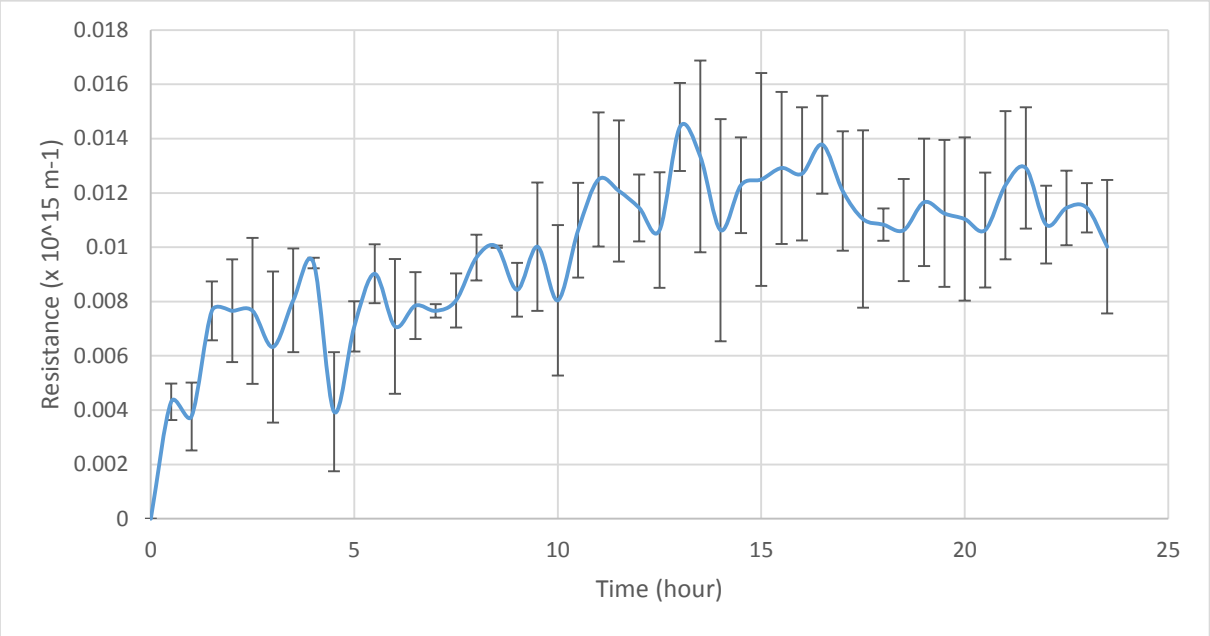

Figure 33: Resistance due to concentration polarisation caused by baseline experiment.

5.3.6. Cake-enhanced layer resistance

R_c + R_{cp} is known as cake-enhanced layer resistance which occurs when both salt and polysaccharides are used in a membrane system.

As per figure 34 and figure 35 compared with figure 32, the resistance is much greater (figure 34 and 35) and this is due the divalent cation in calcium chloride. What it does is the cation creates non-permanent bonds between the monosaccharide (single saccharide) causing a chain of connections. This connection will trigger the gel formation on the membrane. In addition, calcium chloride also affects the alginate and xanthan by strengthening the adhesiveness to the membrane surface. (Lee and Elimelech 2006; Paul *et al.* 2012). Therefore, with the addition of salt (calcium chloride in particular), it will increase the resistance of membrane and empower the stickiness of the triggered gel. And for these reasons, the permeate flux will decrease when the calcium chloride (cations) and polysaccharide mixture is found in any membrane system.

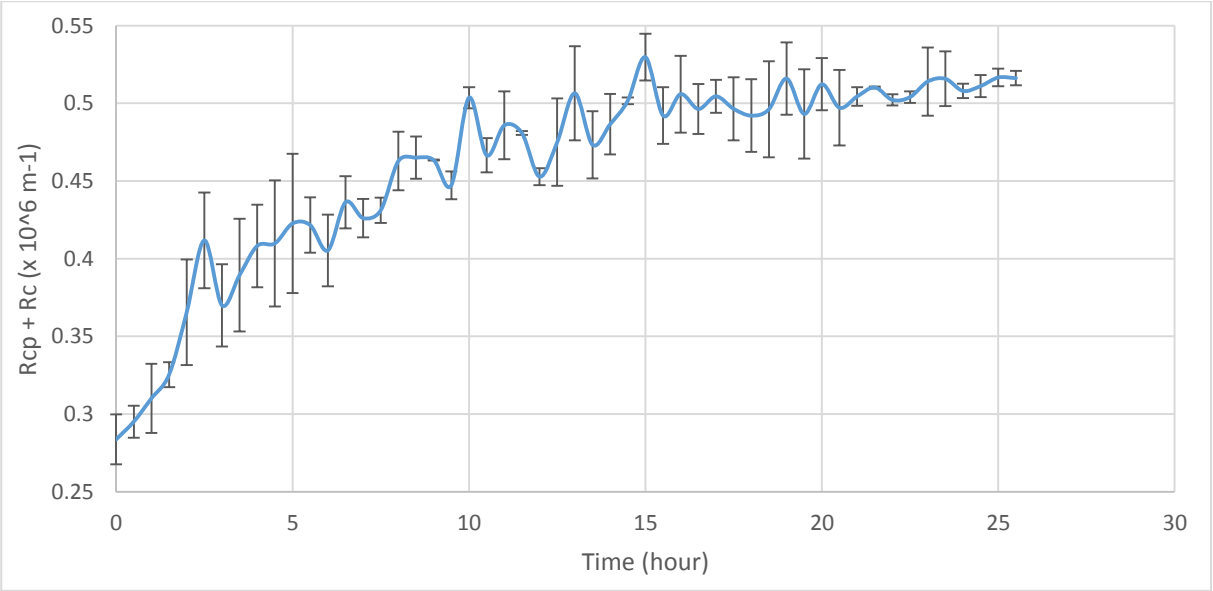

Figure 34: Resistance due to cake-enhanced layer caused by NaCl and $CaCl_2$ mixed with alginate.

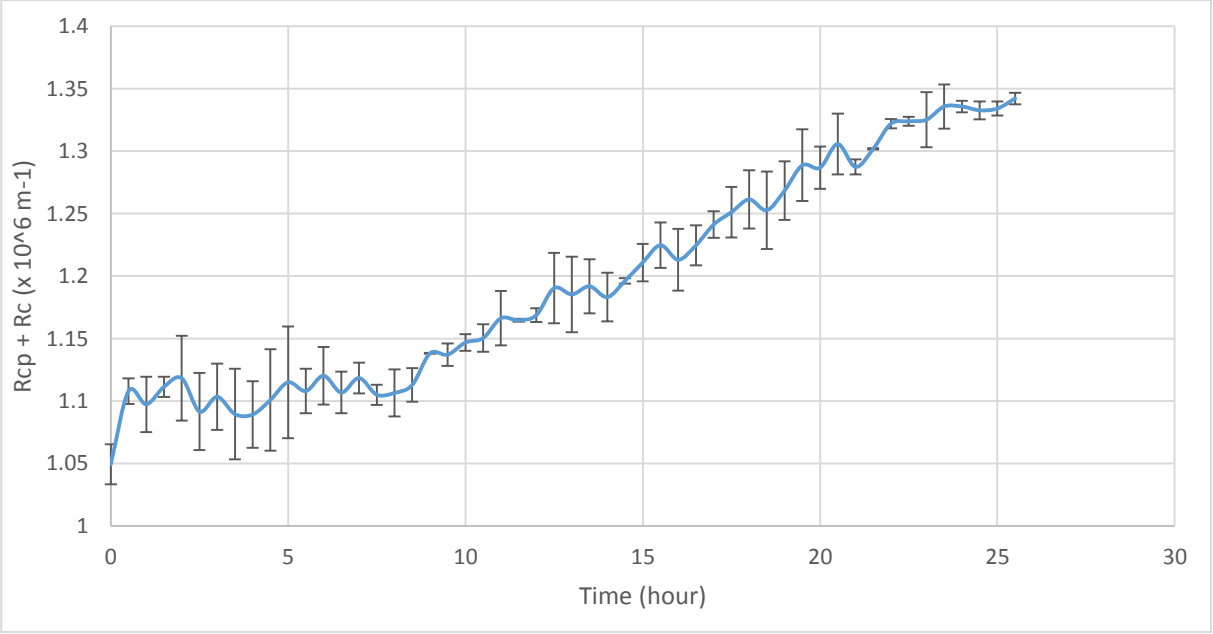

Figure 35: resistance due to cake-enhanced layer caused by NaCl and $CaCl_2$ mixed with xanthan.

5.4.Internal and External Concentration Polarisation

McCutheon and Elimelech referred external concentration polarisation effects as it inhibits permeate flow due to an increase of osmotic pressure at the membrane active layer surface (McCutheon and Elimelech 2006). In addition, ECP (external concentration polarisation) can occur on both sides of the membrane that is an active layer which is facing the feed solution and support layer which is facing the draw solution. The side that is in contact with feed solution which is concentrated hence naming it as concentrative ECP whereas the side that is facing the

draw solution having a lower concentration thus able to call it as dilutive ECP. Even though ECP poses a threat to the FO system efficiency, it is less problematic compared to ICP (internal concentration polarisation) (Suh and Lee 2013, McCutcheon, McGinnis and Elimelech 2006, McCutheon and Elimelech 2006). In this study, the dilutive ECP (draw side) was assumed to be constant as the concentration of the draw solution will always be saturated NaCl solution hence applying the same pressure to the support layer (may have a short delay of pressure where the concentration polarisation is building up onto the membrane surface) therefore the DECP (dilutive ECP) graphs will not be shown.

Figure 36 demonstrates one line from the experiment which involves salt only. The external concentration polarisation was intentionally marked at zero in the zeroth hour as assumed that there are no ECP when the system is inactive. The reason for this is because ECP does not exist at the start of the experiment but once the system starts operating, the ECP starts to build up to reach a level where it stabilises or at least does not increase as much as the first 2 hours. Moreover, even though the experiment started out prior to the 24 hours plotted on the graph (having 2 hours of stabilisation, DI water only), the ECP was still zero. This can be supported by Suh and Lee's statement in one of their papers saying that 'concentrative ECP on the surface of the active layer is relatively insignificant when the feed solution is pure water, but it is not negligible in a feed solution with a high solute concentration' (Suh and Lee 2013). The rest of the trend represents how much resistance each component causes via external concentration polarisation which was established earlier that salt demonstrates a relatively small amount of resistance.

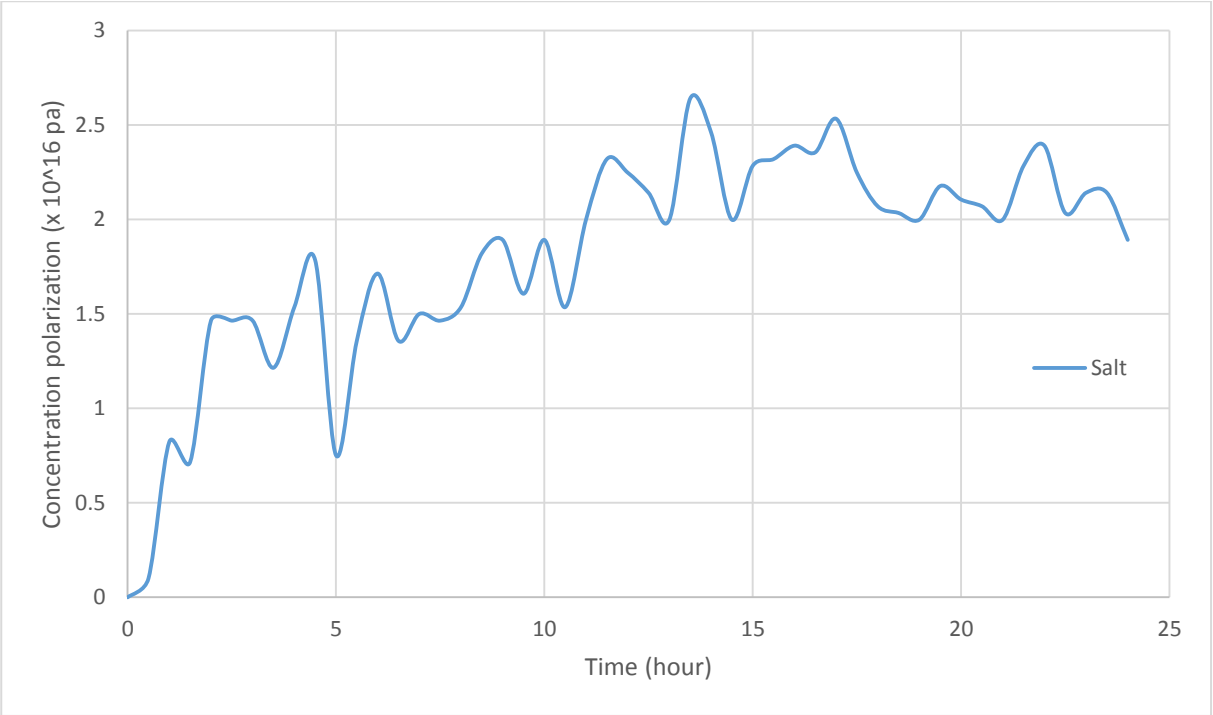

Figure 36: Graph of external concentration polarisation of baseline, alginate and xanthan experiments. Note that it a started at 0 due to the fact that at zero hour the concentration polarisation did not exist and was only build-up afterwards.

Salt and xanthan data in figure 37 shows a surprisingly low ECP, this was unexpected as xanthan should have had the greatest ECP among the three data. However, the alginate with salt when compared with figure 36, alginate only, the salt influenced the ECP to have a larger resistance. The difference between the two was 1.4 x10^{16} pa (increased by 21%), concluding that the salt enhanced the ECP.

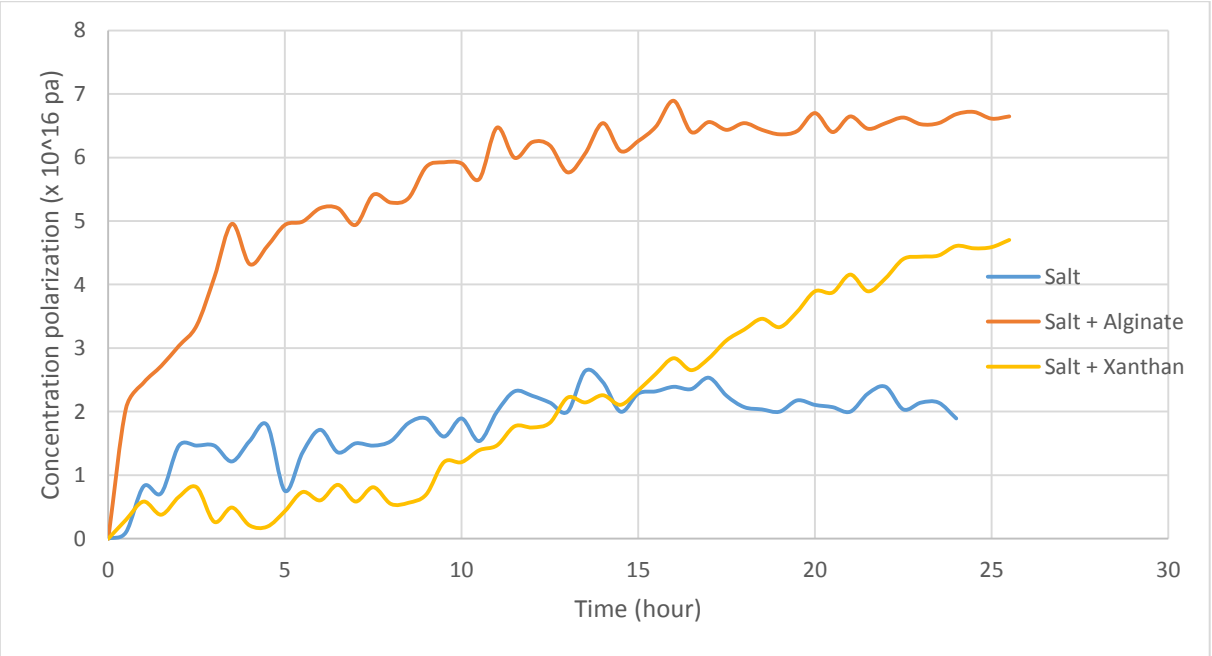

Figure 37: Graph of external concentration polarisation of baseline, alginate with salt and xanthan with salt experiments.

ICP was described by Suh and Lee as when the support layer is oriented towards the draw solution (concentrated solution), the solute from the draw side diffuses into the support layer causing a decrease in osmotic pressure gradient across the active layer (Suh and Lee 2012).

The general trend where it starts at a higher ICP and gradual decline and stabilises can be explained by the fact that support layer is porous hence allowing for the salt and polysaccharide to deposit within the support layer quickly and easily. As the experiment progresses, the ICP decline due to cross-flow velocity dragging the particle in the support layer hence diluting the ICP. After the deposition and diluting continues, the ICP will eventually reach a stable level causing the ICP as seen in figure 38 and 39 to stabilise after a period of time.

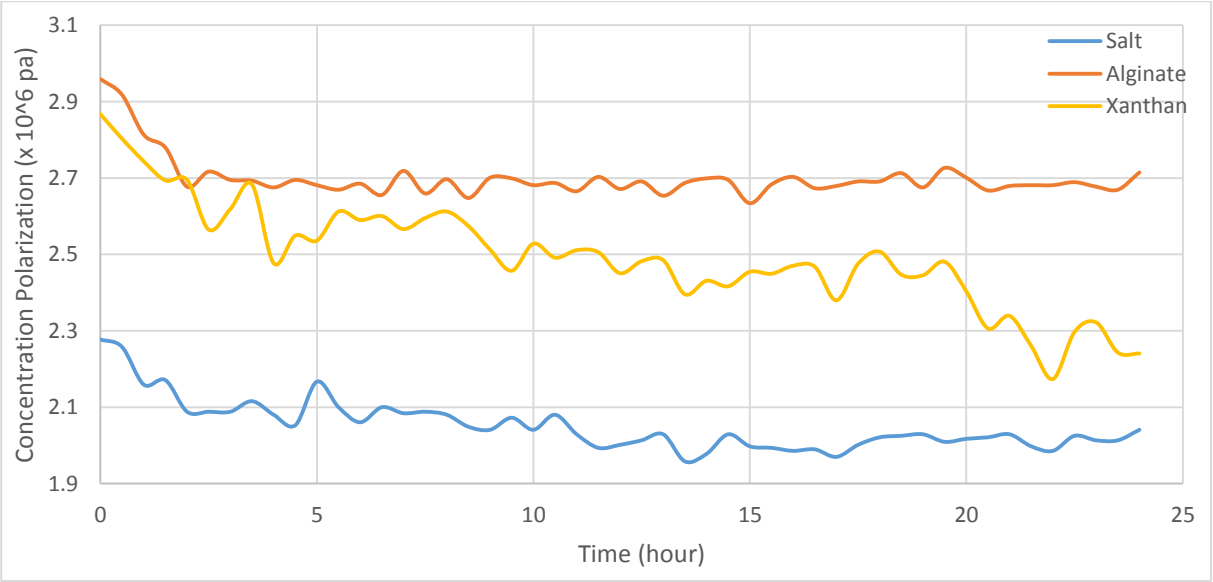

Figure 38: Graph of internal concentration polarisation of baseline, alginate and xanthan experiments.

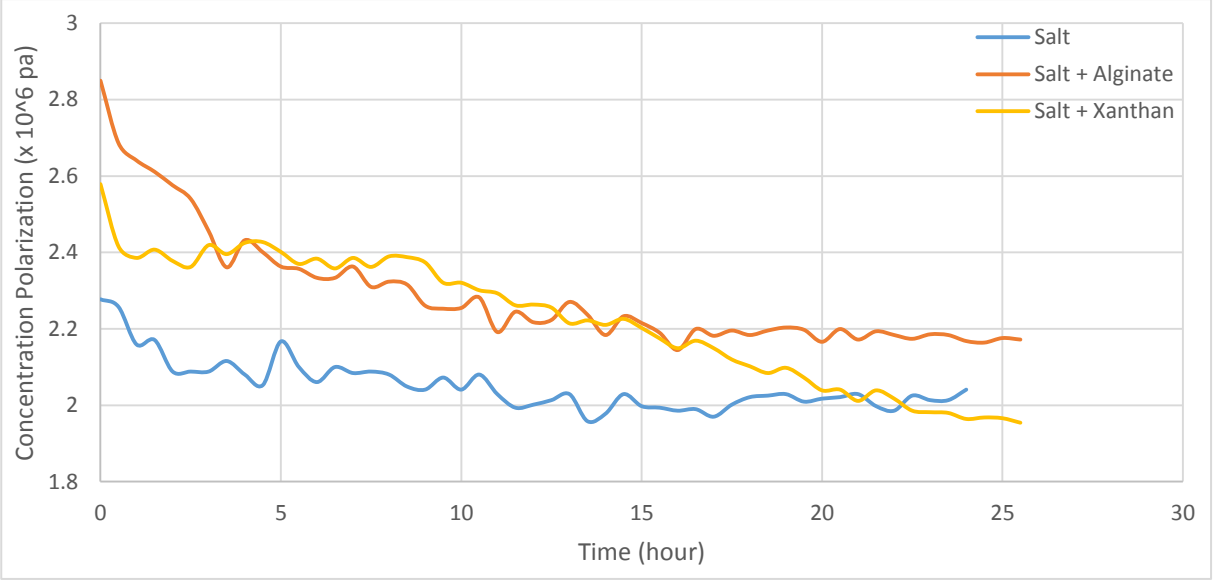

Figure 39: Graph of internal concentration polarisation of baseline, alginate with salt and xanthan with salt experiments.

Between figure 38 and 39, the ICP when salt is added with polysaccharide demonstrates to have a lower ICP level for both alginate and xanthan. This is due to the gel formation on the active side causing the osmotic pressure on the membrane to increase hence the ICP whereas in a case that there is no gel formation (such as baseline experiment) or gel formation is not enhanced with salt, the osmotic pressure will be lower and hence the ICP will follow.

5.5.Concentration of salt on membrane vs Osmotic pressure on feed side

With the application of Eq. 3 and 17, $\pi_{feed,\ membrane}$ and C_{cp} can be found. By plotting the two data together (figure 40), it shows that the concentration of salt on the membrane strongly influences the osmotic pressure on the membrane surface. This means that the more salt deposited on the surface, the higher the osmotic pressure of the feed side of the membrane will be.

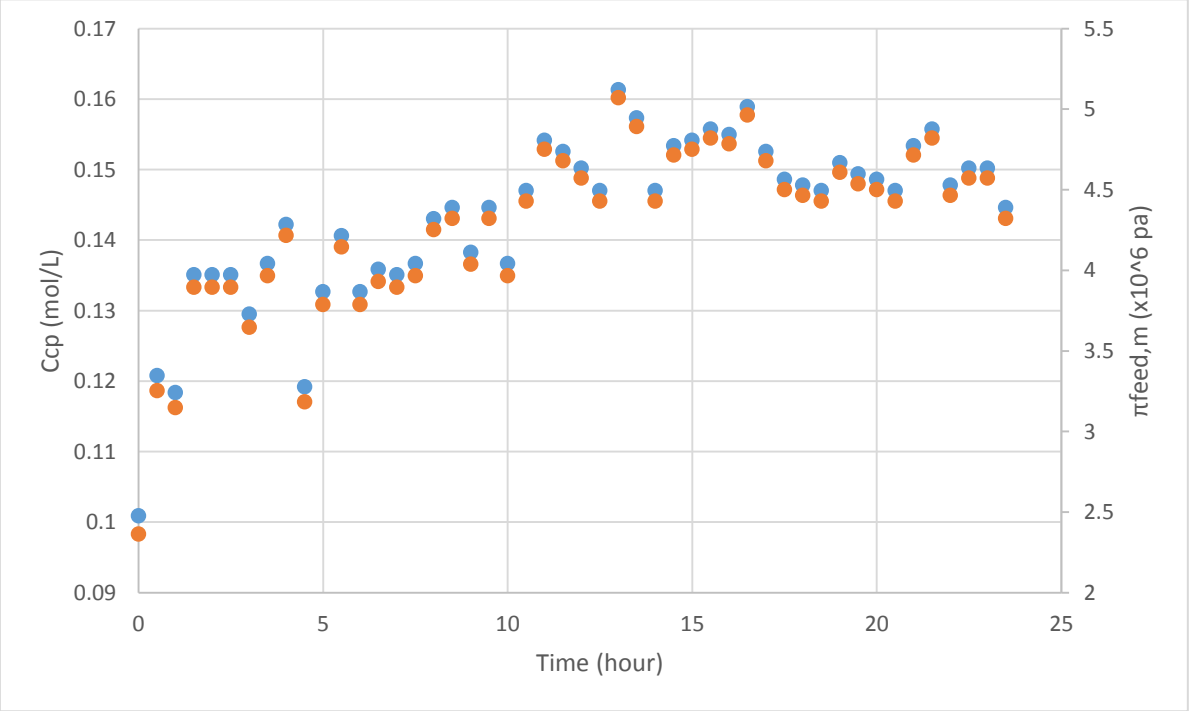

Figure 40: Graph of concentration of salt on membrane surface vs osmotic pressure on the feed side of the membrane.

5.6.Comparison of Result between FO and RO system

In the previous year, another thesis student, Damien K. Arnaud, including John, (Ph.D. student, lab supervisor) had conducted similar experiments with the same chemical component and experimental parameters hence, the FO data that was obtained from this experiment can be compared. With this comparing and contrasting of results, similarities and differences can be drawn upon the behaviour of fouling effect between RO (given by Damien and John) and FO system.

5.6.1. Baseline Experiment

This experiment which involves only NaCl and $CaCl_2$ with DI water, the flux of FO is lower for the majority of the 24 hours of conducting the experiment. In the raw (not normalised) flux graph (figure 41), the decline of flux for FO system seems to be minimal compared to the RO system, however, finishes at a higher flux of 0.2 LMH compared to RO. On the other hand, in the normalised graph (figure 42), both cases of FO and RO system have a similar trend, being that both of them have a gradual decline and stabilise after the 18th hour. At the final hour, the flux of FO system was lower than the RO which was unlike the raw flux.

The lower flux over time of FO system shows that the RO has a better production volume over time when only salt is in the feed. Nevertheless, the RO has a greater gradient of declination in flux (of LMH unit) which possibly is representing the fact that RO is more prone to salt particles acting as a resistance on the system.

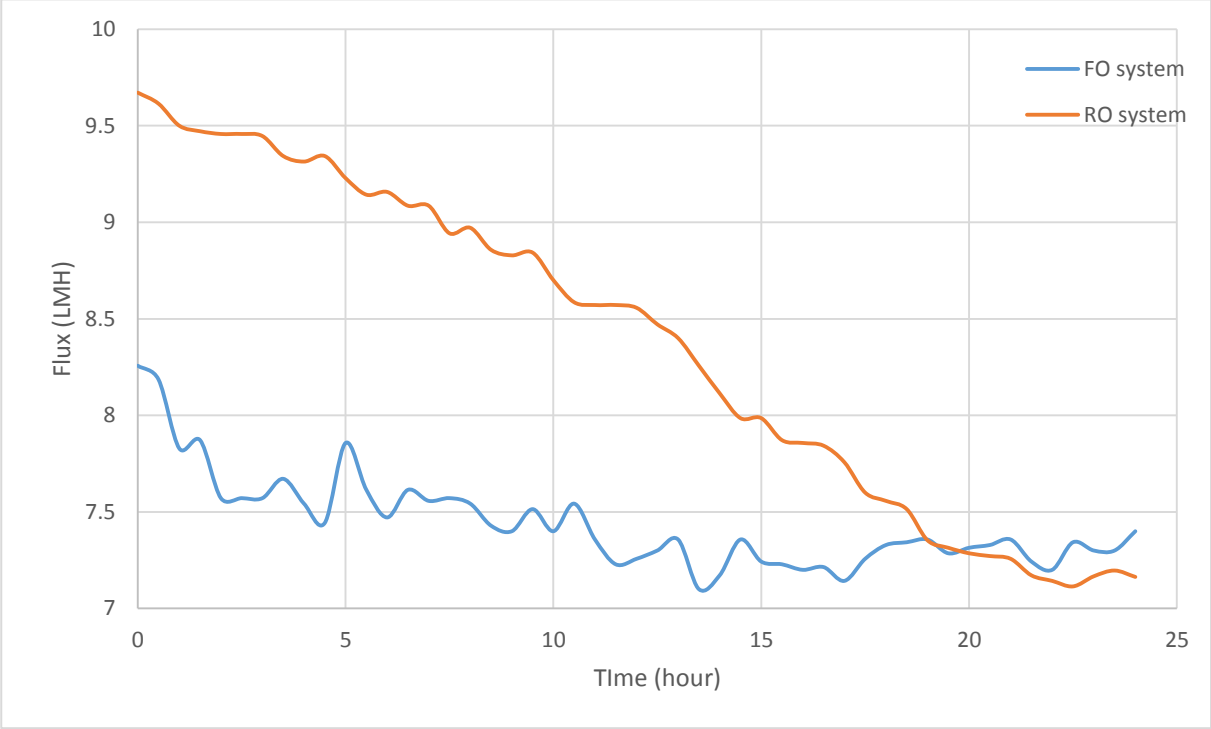

Figure 41: Flux in LMH of RO and FO system for baseline experiment.

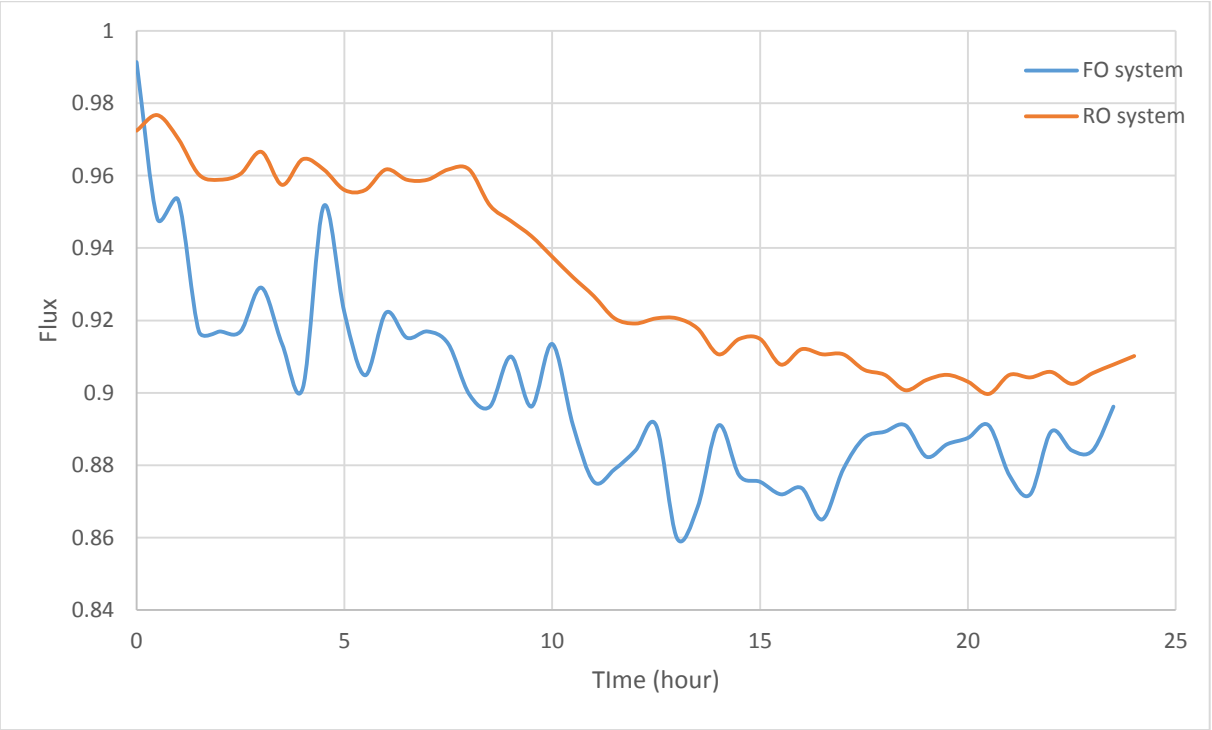

Figure 42: Normalised flux of RO and FO system for baseline experiment.

5.6.2. Alginate Experiment

In RO system, the flux has a decreasing trend while FO stabilises just after 5 hours after the alginate has been injected into the system. Furthermore, after the alginate has stabilised, the flux does not change much when compared to the last point of data which is 9.679 LMH. On the other hand, RO system had a dip between hour 18 and 20 where the flux dropped to 8.114 LMH which does not follow the trend, hence this might have been caused by the surrounding environment or the control parameters. The final flux for RO system is at 8.714 LMH, having a difference to FO system by 0.965 LMH.

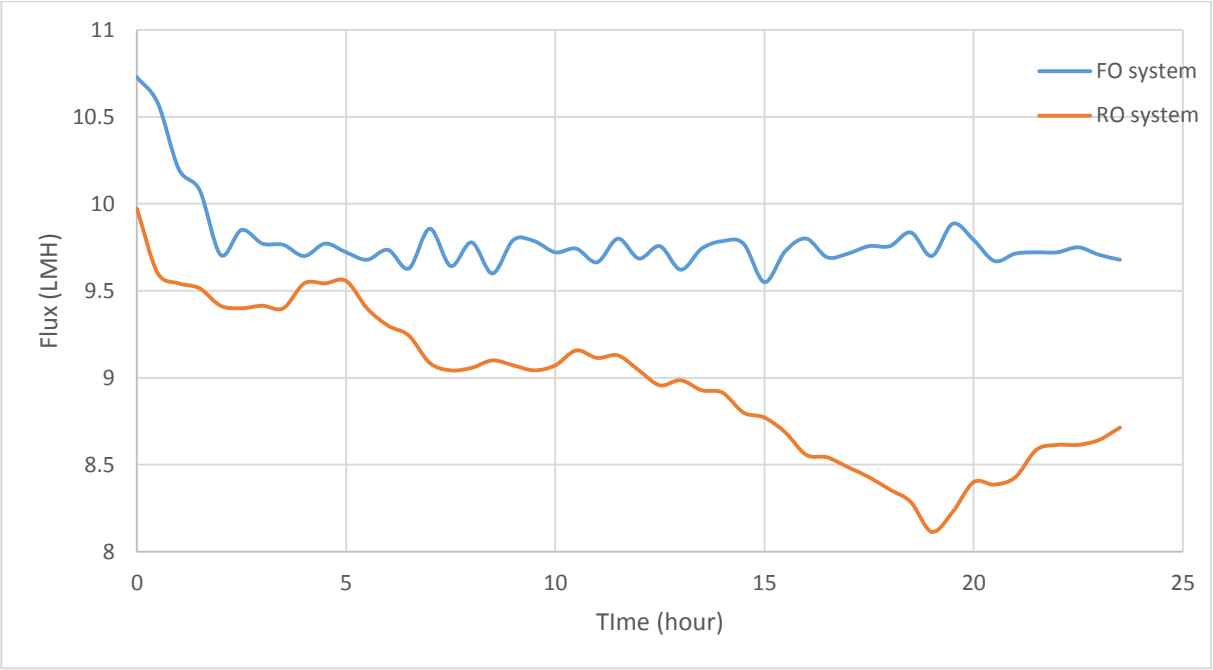

Figure 43: Flux in LMH of RO and FO system for alginate experiment.

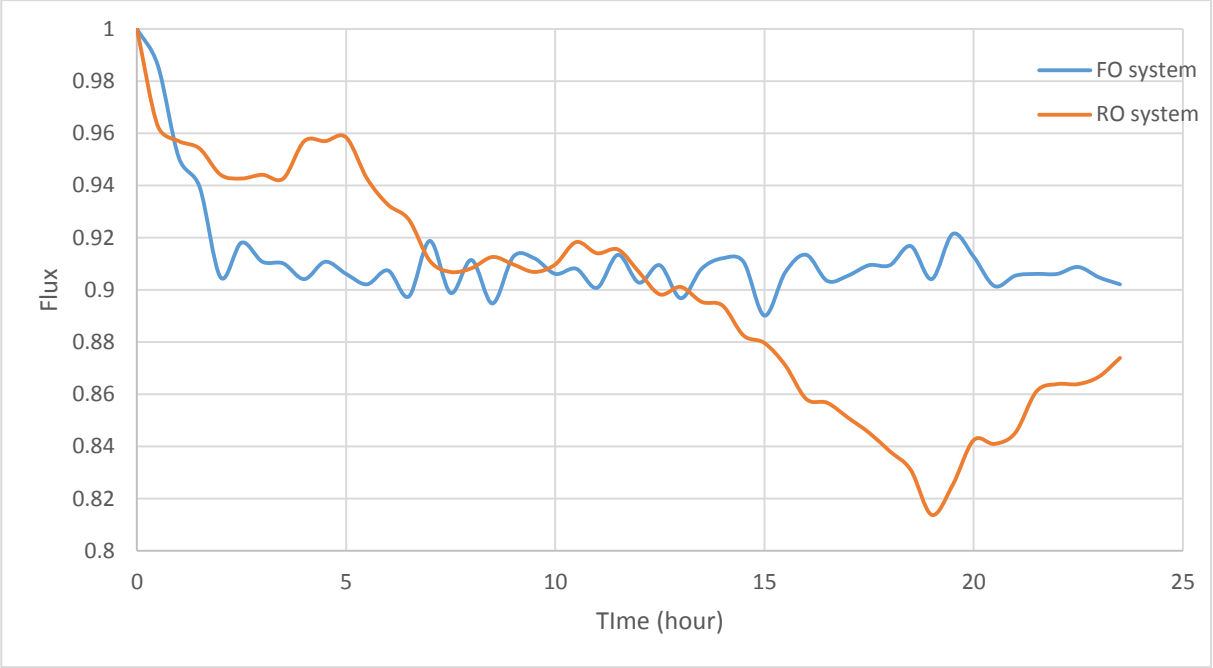

Figure 44: Normalised flux of RO and FO system for alginate experiment.

In the raw flux graph (figure 43), the RO demonstrates to be at a lower flux throughout the entire duration including the first and last hour by 0.7 and 0.9 LMH respectively. While the FO system has a dramatic decline during the first three hours, and even out for the rest of the conducting period, maintaining a flux of roughly 9.8 LMH. On the other hand, RO system has a slower and steadier decline that stops at the 19th hour and jumps up with a similar increasing gradient as the decrease. In the normalised graph (figure 44), the trend of both systems remains

the same as the raw flux graph. The only difference is the interaction between them, the RO system appears to be at a higher flux for the first 12 hours of the experiment but still finishes at a lower flux towards the end period.

Both figure 43 and 44 demonstrates that when the polysaccharide in the form of alginate is involved in both systems, FO shows to have a higher flux thus operating at a higher production volume. This is possibly caused by the alginate when forming the gel layer on the membrane, the RO system has a greater fouling effect by the layer than the FO system thus causing the resistance to be higher and ultimately resulting in a lower flux.

5.6.3. NaCl + $CaCl_2$ and Alginate Experiment

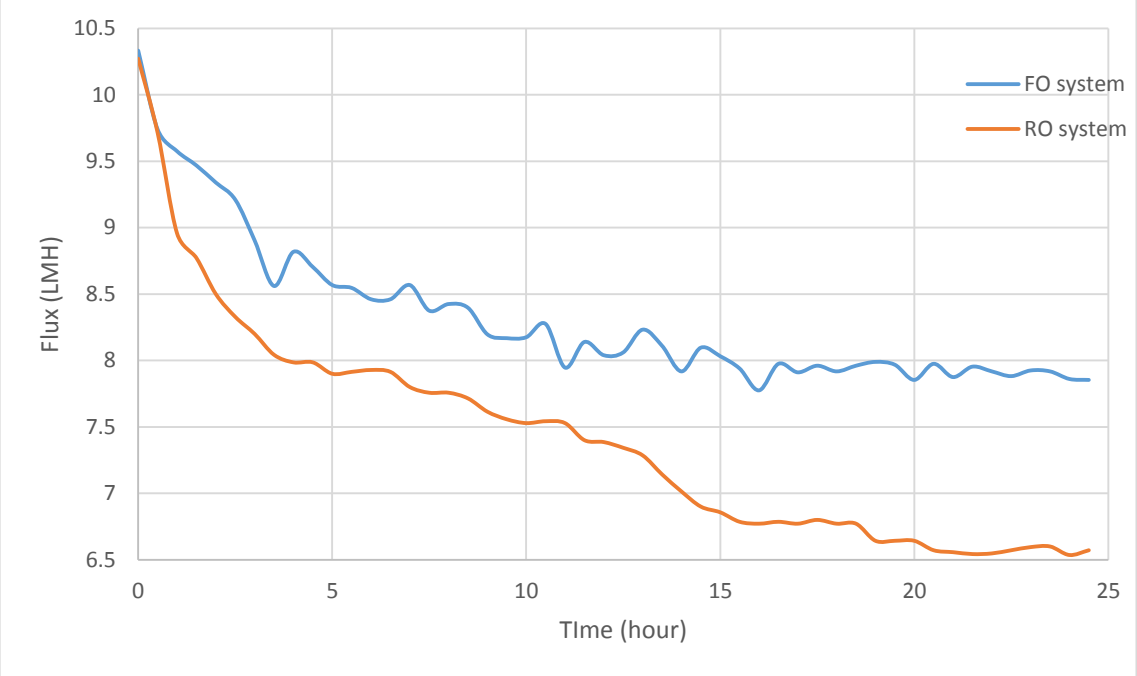

Figure 45: Flux in LMH of RO and FO system for salt with alginate experiment.

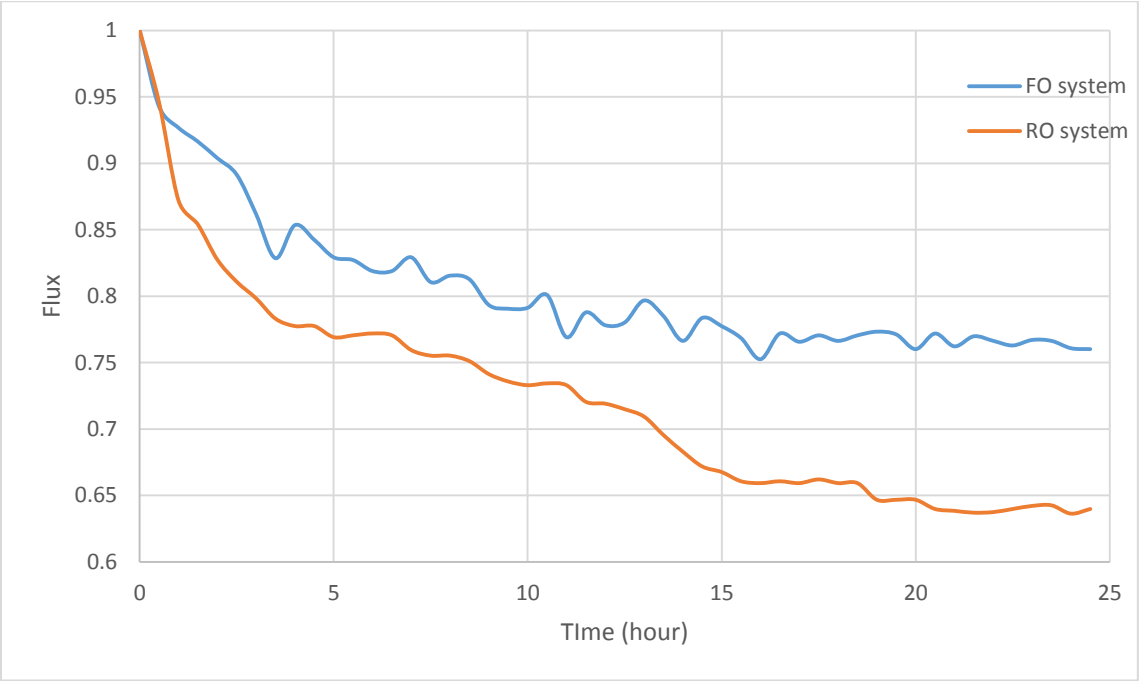

Figure 46: Normalised flux of RO and FO system for salt with alginate experiment.

Both of the graphs in figure 45 and 46 demonstrates the same trend as the raw flux for both systems are closely related. RO and FO both has a gradual decreasing flux where it stabilises around the 17th hour onwards. For FO it stabilises at 7.9 LMH and for RO at 6.55 LMH hence with a difference of 1.35 LMH. Even though both of the systems follow the same trend, the FO system shows to be the superior as it stabilises at the higher flux meaning that the salt and alginate combination have less flux declining effect on the system compared to the RO system.

Moreover, if this was compared with the alginate only experiment, the flux in this experiment has approximately double the declining of flux. One of the reasons for this is the salt solution that was mixed with the alginate triggers biofilm formation creating some resistance causing it to have a greater flux decrease than the alginate only case. This goes for both FO and RO system.

5.6.4. NaCl + $CaCl_2$ and Xanthan Experiment

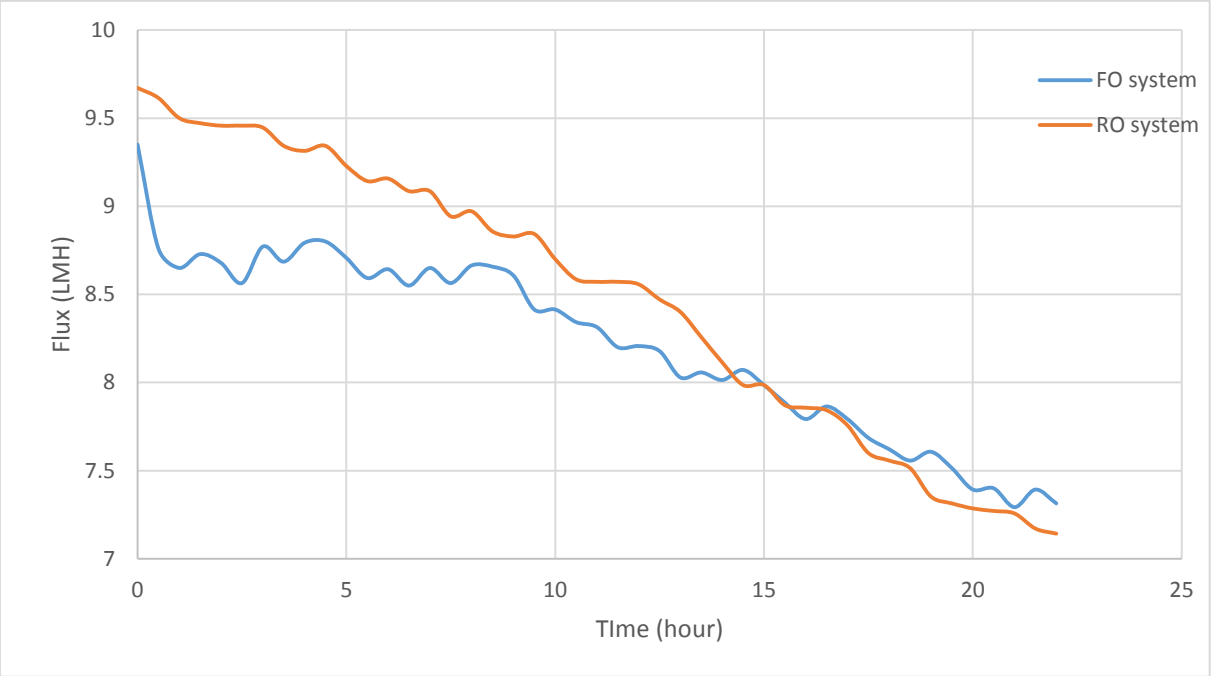

Figure 47: Flux in LMH of RO and FO system for salt with xanthan experiment.

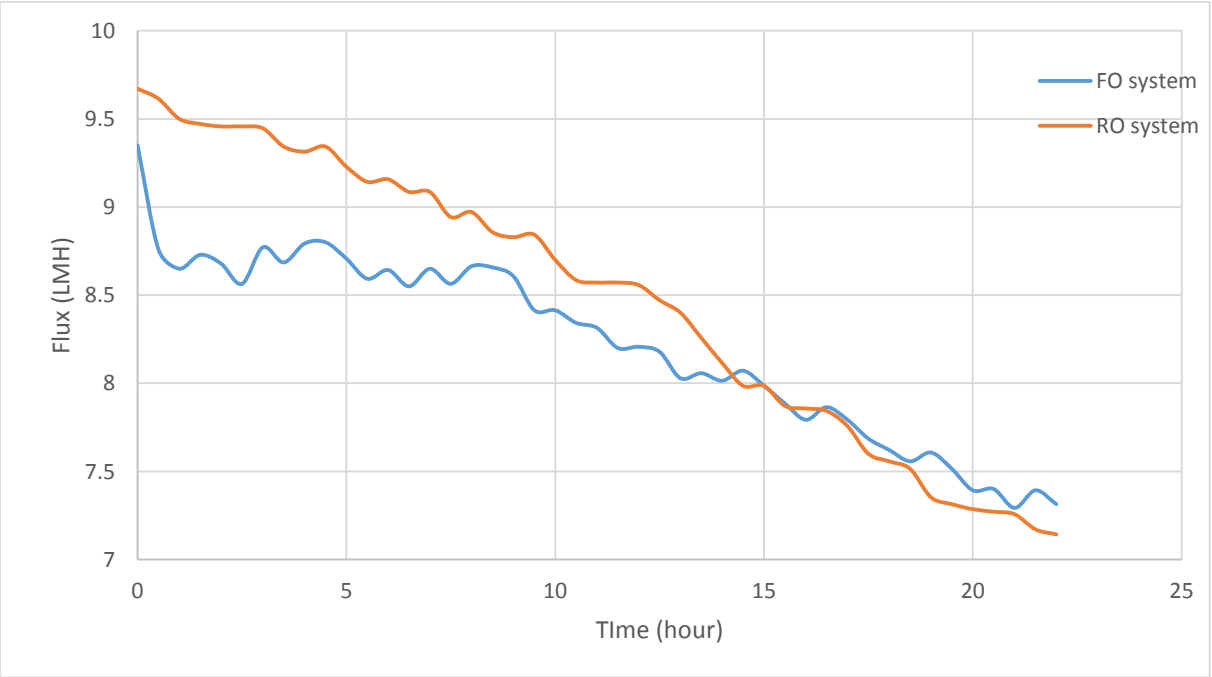

Figure 48: Normalised flux of RO and FO system for salt with xanthan experiment.

Between the two graphs (figure 47 and 48), the general trends are the same, however, the few final hours the FO system has a higher flux than the RO system which was clear in the normalised graph. From the two system, when salt and xanthan is part of the feed, the system both has the same flux declining trend which both had the same final flux at 7.1 LMH. However,

the normalised data (figure 48) states otherwise as the FO finishes higher. This is due to the fact that the starting flux was not the same in the raw data causing an inconsistent starting condition. Therefore, in this experiment, the FO system demonstrates to be doing better as the higher flux was reached at the final hour in the normalised graph.

5.6.5. General Discussion

As a general trend, FO system demonstrates a relatively large fluctuation between hours whereas the RO system has a rather smooth trend. This is the nature of the FO system to have such an up-and-down fluctuation. The fluctuation can be further illustrated by the appendix I, J, K, L, M which is a graph of frequency distribution of flux for each experiment. The graphs demonstrate that xanthan has a spread out (not bell shape) frequency distribution more than alginate and this effect was enhanced when salt was mixed with the polysaccharide. In conclusion, in most cases except the baseline, FO system was able to maintain the flux at a higher level after 24 hours of operating period. A clear example can be illustrated by the alginate cases, with and without salt in the mixture, hence, it can be stated that with these experimental parameter and alginate combinations, FO system will have a superior outcome in term of permeate flux. In addition, from the graph, it seems that FO system is able to deal with the chemical at a faster pace, meaning that the system requires less time for the flux to stabilise compared to the RO system.

In the case where cake enhanced layer exists causing an increase in osmotic pressure. This was known as an important mechanism to have an impact that will decline the flux on NF (nano-filtration) and RO system (Lee *et al*. 2010, Hoek, Kim and Elimelech 2002, Hoek and Elimelech 2003, Lee, Cho and Elimelech 2004, Herberg and Elimelech 2007). Therefore, having that CEOP (cake enhanced osmotic pressure) phenomenon causes the RO flux to be at an inferior level compared to FO as seen in figure 45 and 47 or in a normalised data in figure 45 and 47.

A paper was written by Lee *et al*. which experimented similar experiments with different cross-flow velocity ranging from 8.54 to 25.6 cm/s on both RO and FO system and found that fouling on FO system is strongly affected by the flux. They concluded that FO system with highest cross-

flow velocity (34.2 cm/s) had almost no flux decline while RO system was not able to observe the same trend as the aforementioned (Lee *et al*. 2010).

Out of the four comparisons made with RO data, the experiment that resulted in the greatest flux decline was the RO system with salt and alginate where it decreased to just below 0.65. On the other hand, the least flux decrease was also the RO system but in the baseline experiment where it decreased by only 0.91. This proves that RO system is easily influenced by other external factors such as chemicals since it shows that the baseline had such a small decrease but when salt or polysaccharide is introduced the flux trend decreases. In the case of polysaccharide and salt mixture acting as part of the feed, the flux dropped by at least 200% of baseline. This goes to show that the RO's flux is prone to chemical changes. Please refer to table 2 for a summary of flux decline percentage between the two systems.

Table 2: Summary table of flux decline for FO and RO system

	Flux decline (%)	
Experiment	FO	RO
Baseline	3.93	6.40
Alginate	6.95	11.60
Salt + alginate	14.85	32.35
Xanthan	15.01	N/A
Salt + xanthan	16.85	25.89

5.7.Weight of Fouling Layers on Membrane

After the analysis of fouling layer by using weight, differences have been conducted, a summary table of data was constructed as per table 3. Please refer to appendix C for a screenshot from excel spreadsheet.

Table 3: Summary of result from the weighting analysis of the experiments.

Experiment type	Deposit on membrane (g)	Density of deposit (g/cm^3)
Baseline	0.1128	0.5372
Alginate	0.1128	0.1414
Salt + alginate	0.1736	0.1271

Xanthan	0.1996	0.1105
Salt + xanthan	0.3384	0.1874

With this data and the confocal images, the density of each experiment can be defined). This is done by using the thickness from confocal image analysis with the effective area of the membrane cell and the weight in table 3 along with the following equation.

$$Density\ (\frac{g}{cm^3}) = \frac{mass\ (g)}{area\ (cm^2) \cdot thickness\ (cm)}$$

5.8.Confocal Laser Scanning Microscopy

A confocal image that was analysed by Nikon C2 will be presented as a 3D image with 3 axis, namely x axis (length), y axis (height) and z axis (depth). For these images, the most interesting aspect to analyse is the thickness of the gel formed, distribution of gel, compactness and density while correlating with the flux and resistance in each case.

5.8.1. Baseline/control CLSM image

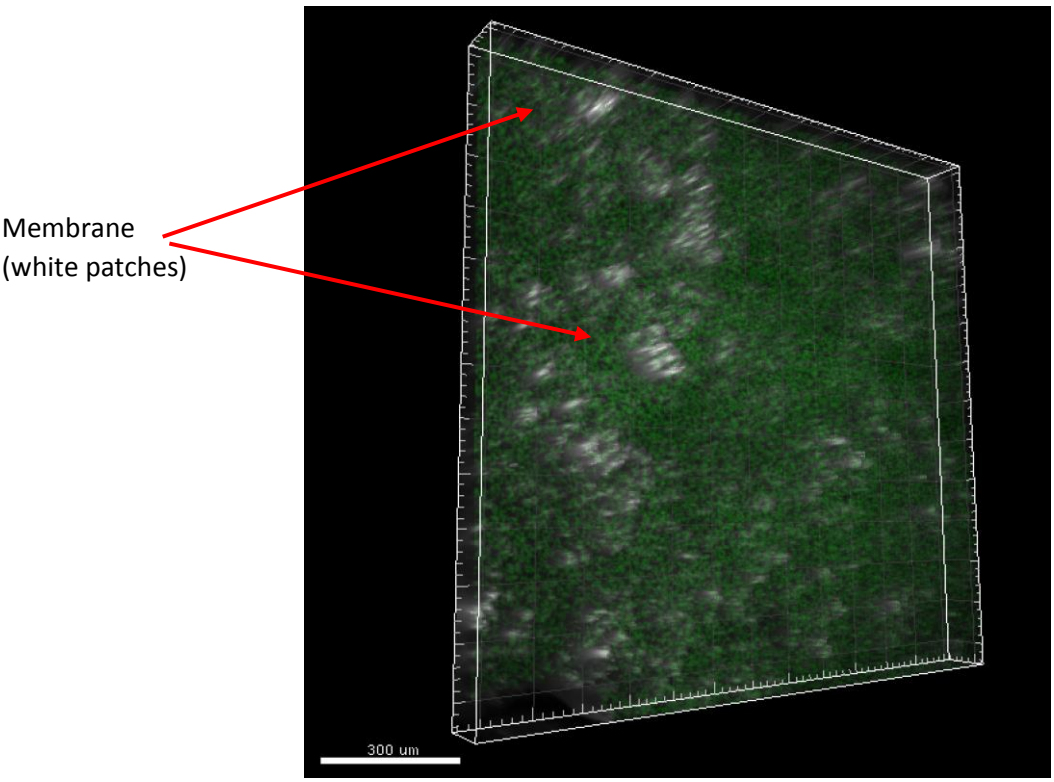

Figure 49: Confocal image of the baseline experiment (NaCl + CaCl2).

Thickness: 50µm

Flux decrease: 1.46%

Salt deposited on membrane: 0.1128g

Density of polysaccharide: 0.5372g/cm^3

Average resistance: 0.961 x 10^{15} m^{-1}

Comments: The salt particles are shown to be compressed and remain intact to the membrane, this is shown by the appearance of white patches between clear green dots. This image has the lowest thickness and smallest flux decrease percentage as expected since the feed contains only 50mM of NaCl and $CaCl_2$.

5.8.2. Alginate CLSM image

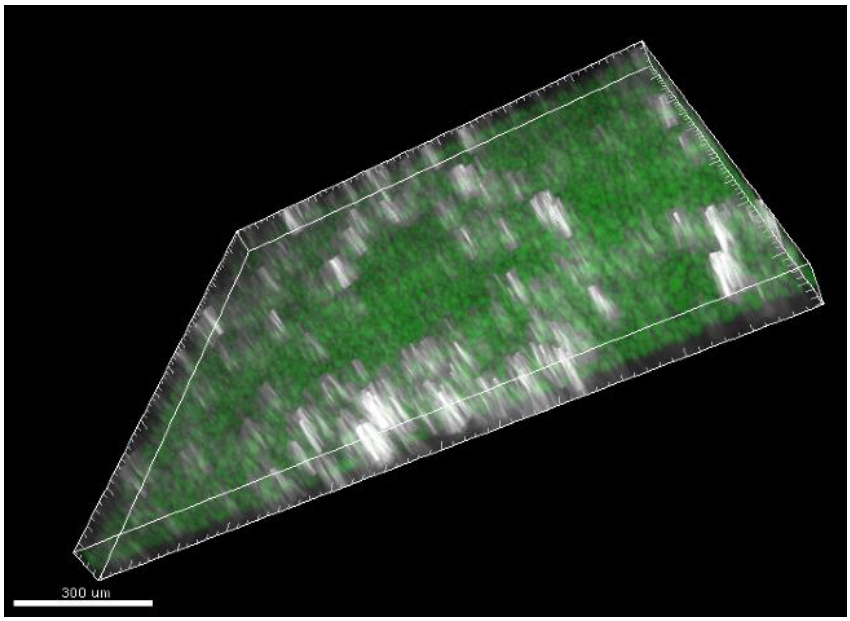

Figure 50: Confocal image of the alginate experiment (alginate only).

Thickness: 190µm

Flux decrease: 6.95%

Polysaccharide deposited on membrane: 0.1128g

Density of polysaccharide: 0.1414g/cm^3

Average resistance: 0.863 x 1015 m-1

Comments: Image shows that the alginate layer is quite compacted while being attached to the layer tightly as shown by the high ratio of white to green colour on the image.

5.8.3. Alginate, NaCl and $CaCl_2$ CLSM image

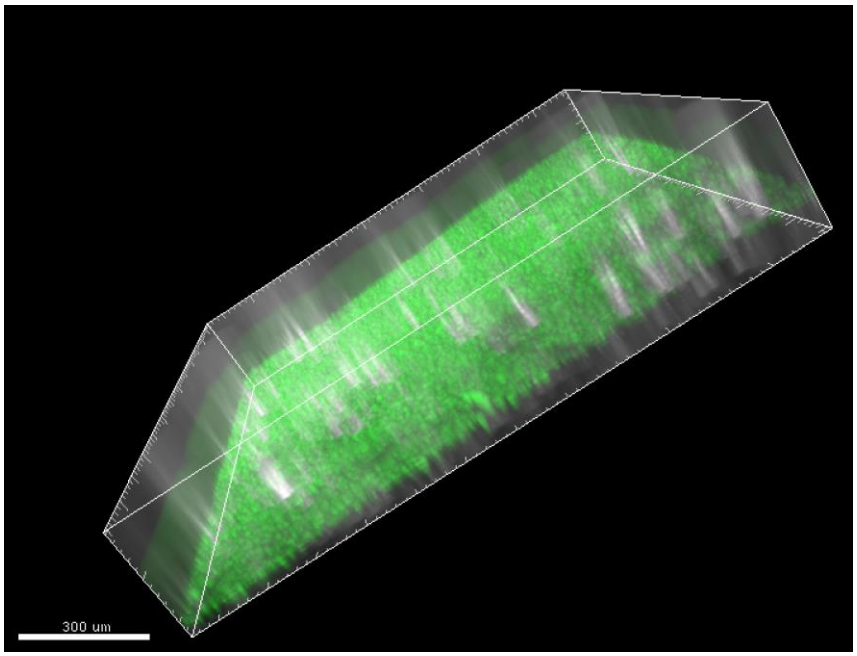

Figure 51: Confocal image of the salt and alginate experiment (NaCl + CaCl2 + alginate).

Thickness: 325µm

Flux decrease: 19.5%

Polysaccharide and salt deposited on membrane: 0.1736g

Density of polysaccharide: 0.1271g/cm^3

Average resistance: 1.043 x 10^{15} m^{-1}

Comments: The clear dotted greens represent the alginate being unevenly distributed but compacted on the membrane surface. Note that this experiment has the greatest flux decline percentage.

5.8.4. Xanthan CLSM image

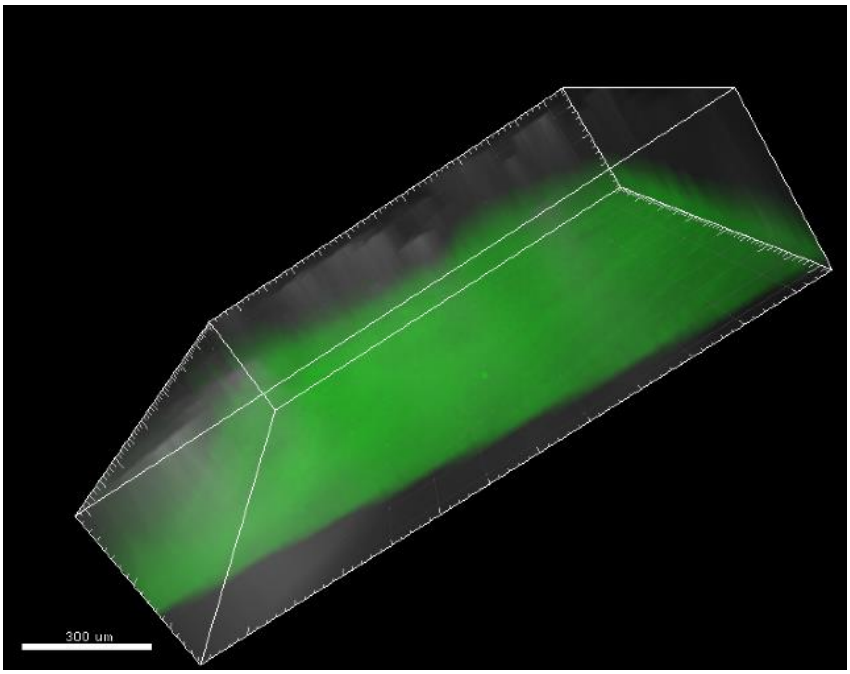

Figure 52: Confocal image of the xanthan experiment (xanthan).

Thickness: 430µm

Flux decrease: 18.3%

Polysaccharide deposited on membrane: 0.1996g

Density of polysaccharide: 0.1105g/cm^3

Average resistance: 0.938 x 10^{15} m^{-1}

Comments: Image shows that the xanthan layer to be sparsely spread out as shown by the cloud-like greens. By this fact, the xanthan layer is not compact hence the polysaccharide layer is assumed to be uniformly distributed on the surface of the membrane.

5.8.5. Xanthan, NaCl and $CaCl_2$ CLSM image

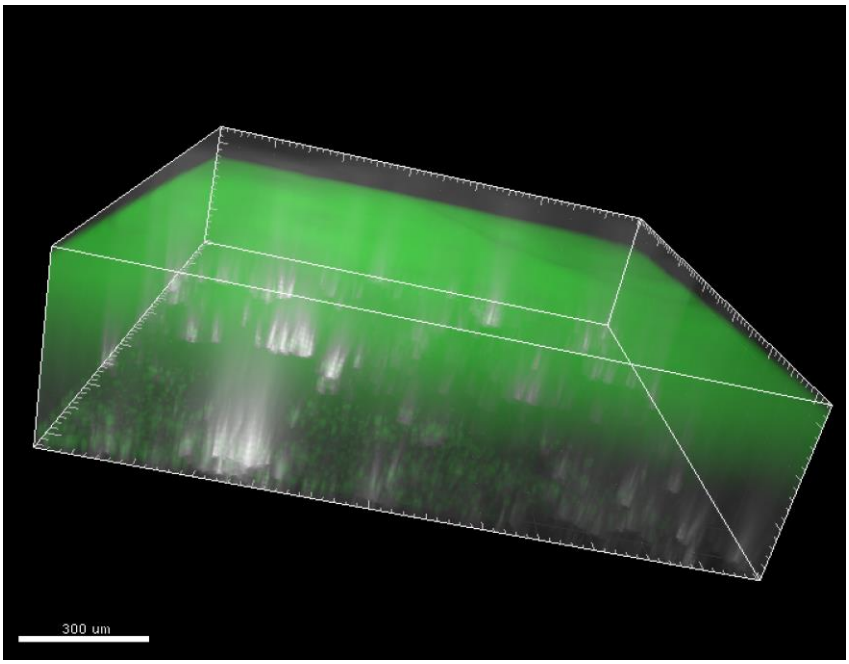

Figure 53: Confocal image of the salt and xanthan experiment (NaCl + CaCl2 + xanthan).

Thickness: 430µm

Flux decrease: 18.7%

Polysaccharide and salt deposited on membrane: 0.3384g

Density of polysaccharide: 0.1874g/cm^3

Average resistance: 1.050 x 10^{15} m^{-1}

Comments: The xanthan layer on top is shown as a cloudy green (not compact) however, towards the bottom of the image where the membrane (white colour) is, the xanthan becomes more compacted hence this is a case where the polysaccharide layer is semi-compact. It is not evenly distributed throughout the layer. The polysaccharide layer is attached quite strongly to the membrane as there is a presence of white colour towards the bottom of the image.

5.8.6. Comparison between CLSM images

Baseline experiment where the only salt was involved has the highest density among all the experiment, however, the flux decreased percentage was only by 1.46% the least out of all. The reason for this is that salt does not cause any gel formation on the membrane surface. Salt only causes concentration polarisation which is considered to be relatively small resistance

compared to cake and cake-enhanced resistance. Therefore, thickness and density of deposit are not comparable with another experiment unless the chemical component is the same or at least similar.

Between xanthan and xanthan with salt, both has the same thickness but the xanthan with salt is heavier causing the density to be higher. By comparing the flux decline, the case where salt is also involved, it is noticed to be higher and the reason for this is the density in the salt case is higher. When the layer is denser and compacted than the other, it will force the feed solution to move through a more rigged and blocked layer of deposit.

On the other hand, when alginate and alginate with salt are compared, the flux decline percentage was 12% higher than the case without the salt. In this case, the clear difference between the two cases is the thickness, where comparing alginate with alginate with salt, the thickness increased by 235μm as well as increasing the deposit weight by 0.14g thus ultimately elevating the density as well. Therefore, this case (alginate with salt) where all the factors that will decrease the flux were occurring (large thickness, high density, and heavy deposit) resulting in such a large flux decline compared to the case without salt.

6. Conclusion

The objective that was set for this project thesis was to identify and compare the fouling behaviour of polysaccharide, particularly alginate and xanthan, with and without the mixture of sodium chloride and calcium chloride to see the changes in their fouling behaviours.

By analysing the results that was obtained from a series of designed experiments and modelling Darcy's law, it can be seen that when hydraulic resistance increases the flux decreases and thus reducing the efficiency of the system, which means less product with the same power input. The hydraulic resistance was seen to be caused by gel formation which is triggered by polysaccharide but even more when salt (NaCl and $CaCl_2$) is mixed with the polysaccharide. This is due to the cation from calcium chloride in the salt mixture binding the polysaccharide hence enhancing the gel formation causing it to be thicker and denser, as shown in the confocal images.

By putting the alginate and xanthan side by side, it was shown within the result and discussion section that xanthan is the polysaccharide that causes more flux decline due to its chemical property that forms a thicker gel because of its chemical structure. Hence, xanthan, if used in FO system, will reduce the flux at a greater level than alginate thus reducing the efficiency of the system. In addition, the bonding between calcium chloride and xanthan is shown to be stronger as well due to the increase in resistance between alginate and xanthan. This is because the biofilm that was generated on the membrane surface potentially shows more hydrophobic effects (repel water permeation) compared to the salt and alginate mixture. In addition, these can also be correlated to the thickness shown in the CLSM section where the thicker and denser the polysaccharides layer, the higher the flux decline will be. The CLSM images also demonstrate that the distribution of the xanthan biofilm is more even compared to alginate with or without salt mixture. Moreover, these results were also proven by the flux decline percentage between the experiments since the xanthan regardless of whether there is salt or not, always has a higher flux decline.

For the comparison of RO and FO system, it was concluded that the FO system in most cases had the lower flux decline (as shown in table 2) as well as having a more stable flux over time. Nevertheless, the permeate quality comparison is still unknown because the FO rejection rate was unable to be conducted.

With these conclusions, membrane fouling problems are clearly identified thus encouraging further study, research, and adjustment to be made with the aim of increasing system efficiency by reducing hydraulic resistance caused by membrane fouling.

7. Future Work

During the study of this project, the behaviour of fouling on FO system using alginate and xanthan with and without the combination of sodium chloride and calcium chloride mixture. However, there are other aspects that would be useful and interesting to see their outcome thus the following are some key areas that are worth conducting a project on:

i. By using the same set of system and experimental parameters, changing variables such as membrane specifications or brand, using different cross-flow velocity and pressure and different draw solution as well as recording power consumption of the system. The effect of each variable can be modelled to locate the highest efficiency of the system and by adjusting each variable, a low power consuming system can produce the highest amount of product (perfect adjustments to find a balance between the two factors).

ii. Rather than using saturated Sodium chloride as draw solution, some other papers (Cath and Elimelich 2006, Wang *et al*. 2007) use glucose instead and this would be interesting to see the difference between the two draw solutions with the same experimental parameters. The differences could possibly provide some findings on how the polysaccharide interact with glucose which could potentially increase or decrease the resistance as glucose may act as a resource for the polysaccharide.

iii. In this experiment, calcium chloride was used acting as part of the Ca^{2+} ions which form the non-permanent bonds between the polysaccharide. However, there are other chemicals such as Magnesium that would also enhance this effect. Therefore, attempting FO experiment with another chemical that can provide the ions for the polysaccharide to trigger the gel formation could be a great finding as well.

iv. Finally, research methods to reduce the membrane fouling, whether it is to do with a chemical used in the experiments or even system design or anything at all that can potentially minimize the fouling phenomenon. Some research has been conducted (but not enough) on something called 'ionized membrane'. Just like the name, the membrane

is ionized to reduce its concentration polarisation by using the polarity to repel the attraction of ions that create fouling.

8. Reference

Ahmed, Mehboob, Lucas J. Stal, and Shahida Hasnain. 2010. "DTAF: An Efficient Probe To Study Cyanobacterial-Plant Interaction Using Confocal Laser Scanning Microscopy (CLSM)". Journal Of Industrial Microbiology & Biotechnology 38 (1): 249-255. doi:10.1007/s10295-010-0820-8.

Alsvik, Inger and May-Britt Hägg. 2013. "Pressure Retarded Osmosis And Forward Osmosis Membranes: Materials And Methods". *Polymers* 5 (1): 303-327. doi:10.3390/polym5010303.

Armstrong, M. W., S. Gallego, and S. P. Chesters. "Removing biofilm from membranes–a practical approach." CDA Qingdao, June (2011): 26-29.

Batiot, Christelle, Cristina Liñán, Bartolomé Andreo, Christophe Emblanch, Francisco Carrasco, and Bernard Blavoux. 2003. "Use Of Total Organic Carbon (TOC) As Tracer Of Diffuse Infiltration In A Dolomitic Karstic System: The Nerja Cave (Andalusia, Southern Spain)". *Geophys. Res. Lett.* 30 (22). doi:10.1029/2003gl018546.

Bisutti, Isabella, Ines Hilke, and Michael Raessler. 2004. "Determination Of Total Organic Carbon – An Overview Of Current Methods". *Trac Trends In Analytical Chemistry* 23 (10-11): 716-726. doi:10.1016/j.trac.2004.09.003.

Bisutti, Isabella, Ines Hilke, and Michael Raessler. 2004. "Determination Of Total Organic Carbon – An Overview Of Current Methods". *Trac Trends In Analytical Chemistry* 23 (10-11): 716-726. doi:10.1016/j.trac.2004.09.003.

Boo, Chanhee, Sangyoup Lee, Menachem Elimelech, Zhiyong Meng, and Seungkwan Hong. 2012. "Colloidal Fouling In Forward Osmosis: Role Of Reverse Salt Diffusion". *Journal Of Membrane Science* 390-391: 277-284. doi:10.1016/j.memsci.2011.12.001.

Borkovec, Michal. 2016. "Laboratory Of Colloid And Surface Chemistry (LCSC)". *Colloid.Ch*. http://www.colloid.ch/index.php?name=membranes.

Boulanger, A., C. Zischek, M. Lautier, S. Jamet, P. Rival, S. Carrere, M. Arlat, and E. Lauber. 2014. "The Plant Pathogen Xanthomonas Campestris Pv. Campestris Exploits N-Acetylglucosamine During Infection". *Mbio* 5 (5): e01527-14-e01527-14. doi:10.1128/mbio.01527-14.

"Calcium Chloride: Uses And Markets". 2016. Calciumchloride.Com. http://www.calciumchloride.com/market.shtml.

Cath, T, A Childress, and M Elimelich. 2006. "Forward Osmosis: Principles, Applications, And Recent Developments". *Journal Of Membrane Science* 281 (1-2): 70-87. doi:10.1016/j.memsci.2006.05.048.

Chaplin, martin. 2016. "Xanthan Gum". *Www1.Lsbu.Ac.Uk*. http://www1.lsbu.ac.uk/water/xanthan_gum.html.

Chung, Tai-Shung, Sui Zhang, Kai Yu Wang, Jincai Su, and Ming Ming Ling. 2012. "Forward Osmosis Processes: Yesterday, Today And Tomorrow". Desalination 287: 78-81. doi:10.1016/j.desal.2010.12.019.

Deneff, Jacob I., Jeffrey R. McCutcheon, and Leslie M. Shor. "Method for direct observation of biofilm formation during operation on forward osmosis membranes." In *Bioengineering Conference (NEBEC), 2014 40th Annual Northeast*, pp. 1-2. IEEE, 2014.

"Desalination". 2016. *Environment.Gov.Au*. https://www.environment.gov.au/topics/science-and-research/state-environment-reporting/soe-2006-desalination#what.

Dixon B., P.J. Abbott, P. Verger, G. Pascal, and M. Di Novi. nd. Pullulan. Food Standards Australia New Zealand, Canberra, Australia; Institut National de la Recherche Agronomique, Paris, France; and US Food and Drug Administration, College Park, Maryland, USA. URL: http://www.inchem.org/documents/jecfa/jecmono/v56je05.pdf.

Dumitriu, Severian. 2016. "Polysaccharides: Structural Diversity And Functional Versatility, Second Edition". *CRC Press*. https://www.crcpress.com/Polysaccharides-Structural-Diversity-and-Functional-Versatility-Second/Dumitriu/p/book/9780824754808.

E.M.V. Hoek, A.S. Kim, M. 2002. Elimelech, Influence of crossflow membrane filtergeometry and shear rate on colloidal fouling in reverse osmosis and nanofiltration separations, Environ. Eng. Sci. (19) 357–372.

E.M.V. Hoek, M. Elimelech. 2003. Cake-enhanced concentration polarisation: a newfouling mechanism for salt-rejecting membranes, Environ. Sci. Technol. (37) 5581–5588.

"Forward Osmosis Technology | HTI Water". 2016. *Htiwater.Com*. http://www.htiwater.com/technology/forward_osmosis/.

Gray, Gordon T., Jeffrey R. McCutcheon, and Menachem Elimelech. 2006. "Internal Concentration Polarisation In Forward Osmosis: Role Of Membrane Orientation". Desalination 197 (1-3): 1-8. doi:10.1016/j.desal.2006.02.003.

Group, Edward. 2016. "Understanding Your Nutrition: What Are Polysaccharides?". Dr. Group's Natural Health & Organic Living Blog. http://www.globalhealingcenter.com/natural-health/understanding-nutrition-polysaccharides/.

Hervé, Abdi. 2010. Normalizing Data. Encyclopaedias of Research Design, Thousand Oaks.

Imeson, A. 2010. Food Stabilisers, Thickeners, And Gelling Agents. Ames, Iowa: Blackwell Pub.

Imeson, A. 2010. *Food Stabilisers, Thickeners, And Gelling Agents*. Ames, Iowa: Blackwell Pub.

Katzbauer, Barbara. 1998. "Properties And Applications Of Xanthan Gum". *Polymer Degradation And Stability* 59 (1-3): 81-84. doi:10.1016/s0141-3910(97)00180-8.

Lee, Sangyoup, Chanhee Boo, Menachem Elimelech, and Seungkwan Hong. 2010. "Comparison Of Fouling Behavior In Forward Osmosis (FO) And Reverse Osmosis (RO)". Journal Of Membrane Science 365 (1-2): 34-39. doi:10.1016/j.memsci.2010.08.036.

M. Herzberg, M. ElimelecH. 2016. Biofouling of reverse osmosis membranes:"Espwaterproducts.Com". Espwaterproducts.Com. https://www.espwaterproducts.com/about-reverse-osmosis/.

Marie Helmenstine, Anne. 2016. "Can You Define Diffusion?". *About.Com Education*. http://chemistry.about.com/od/chemistryglossary/a/diffusiondef.htm.

McCutcheon, Jeffrey R. and Menachem Elimelech. 2006. "Influence Of Concentrative And Dilutive Internal Concentration Polarisation On Flux Behavior In Forward Osmosis". Journal Of Membrane Science 284 (1-2): 237-247. doi:10.1016/j.memsci.2006.07.049.

McCutcheon, Jeffrey R., Robert L. McGinnis, and Menachem Elimelech. 2006. "Desalination By Ammonia–Carbon Dioxide Forward Osmosis: Influence Of Draw And Feed Solution Concentrations On Process Performance". Journal Of Membrane Science 278 (1-2): 114-123. doi:10.1016/j.memsci.2005.10.048.

Mitchell, John. 2016. "Non-Food Uses Of Polysaccharide". Presentation.

Meng, Fangang, So-Ryong Chae, Anja Drews, Matthias Kraume, Hang-Sik Shin, and Fenglin Yang. 2009. "Recent Advances In Membrane Bioreactors (Mbrs): Membrane Fouling And Membrane Material". *Water Research* 43 (6): 1489-1512. doi:10.1016/j.watres.2008.12.044.

Nguyen, Thang, Felicity Roddick, and Linhua Fan. 2012. "Biofouling Of Water Treatment Membranes: A Review Of The Underlying Causes, Monitoring Techniques And Control Measures". *Membranes*2 (4): 804-840. doi:10.3390/membranes2040804.

"Normalization". 2016. *Analytictech.Com*. http://www.analytictech.com/ba762/handouts/normalization.htm.

Park, Minkyu, Ji Jung Lee, Sangho Lee, and Joon Ha Kim. 2011. "Determination Of A Constant Membrane Structure Parameter In Forward Osmosis Processes". Journal Of Membrane Science 375 (1-2): 241-248. doi:10.1016/j.memsci.2011.03.052.

"Particles, Scaling And Biofouling". 2016. *Lenntech.Com*. http://www.lenntech.com/particles-scaling-biofouling.htm.

Perry, Mark. 2013. "Concentration Polarisation In Forward Osmosis Membranes | Forwardosmosistech". *Forwardosmosistech.Com*.

http://www.forwardosmosistech.com/how-forward-osmosis-performance-is-limited-by-concentration-polarisation/.

Polarisation In Forward Osmosis: Role Of Membrane Orientation". Desalination 197 (1-3): 1-8. doi:10.1016/j.desal.2006.02.003.

"Polysaccharide: Definition & Examples - Video & Lesson Transcript | Study.Com". 2016. *Study.Com*. http://study.com/academy/lesson/polysaccharide-definition-examples-quiz.html.

"Polysaccharides Definition, List, Functions, Food Examples". 2014. *Nutrients Review*. http://www.nutrientsreview.com/carbs/polysaccharides.html.

Ryder, Cynthia, Matthew Byrd, and Daniel J Wozniak. 2007. "Role Of Polysaccharides In Pseudomonas Aeruginosa Biofilm Development". *Current Opinion In Microbiology* 10 (6): 644-648. doi:10.1016/j.mib.2007.09.010.

S. Lee, J. Cho,M.Elimelech. 2004. Influence of colloidal fouling and feed water recoveryon salt rejection of RO and NF membranes, Desalination (160) 1–12.

"Seawaterfouling - What Is Biofouling?". 2016. *Seawaterfouling.Wikispaces.Com*. https://seawaterfouling.wikispaces.com/What+is+Biofouling%3F?responseToken=07c35bf91ac36d5eb125d63f6a70df1a3.

"Sodium Alginate (Alginate, Algin)". 2013. *Molecular Recipes*. http://www.molecularrecipes.com/hydrocolloid-guide/sodium-alginate-alginate-algin/.

"Sodium Alginate | Ingredients And Utensils | Gourmet Goldmine". 2016. *Gourmetgoldmine.Com.Au*. http://www.gourmetgoldmine.com.au/products/sodium-alginate.

"Sodium Alginate". 2016. *Fao.Org*. http://www.fao.org/docrep/w6355e/w6355e0x.htm.

"Sodium Alginate". 2016. *Modernistpantry.Com*. http://www.modernistpantry.com/sodium-alginate.html.

Stephen, Alistair M, Glyn O Phillips, and Peter A Williams. 2006. Food Polysaccharides And Their Applications. Boca Raton, FL: CRC/Taylor & Francis.

Suh, Changwon and Seockheon Lee. 2013. "Modeling Reverse Draw Solute Flux In Forward Osmosis With External Concentration Polarisation In Both Sides Of The Draw And Feed Solution". Journal Of Membrane Science 427: 365-374. doi:10.1016/j.memsci.2012.08.033.

Tang, Warling and How Yong Ng. 2008. "Concentration Of Brine By Forward Osmosis: Performance And Influence Of Membrane Structure". Desalination 224 (1-3): 143-153. doi:10.1016/j.desal.2007.04.085.

"The Australian Continent | Australia.Gov.Au". 2016. *Australia.Gov.Au*. http://www.australia.gov.au/about-australia/our-country/the-australian-continent.

"TOC-Total Organic Carbon - LAR Process Analysers". 2016. *Lar.Com*. http://www.lar.com/products/toc-analysis/toc.html.

Vu, Barbara, Miao Chen, Russell J. Crawford, and Elena P. Ivanova. 2009. "Bacterial Extracellular Polysaccharides Involved In Biofilm Formation". *Molecules* 14 (7): 2535-2554. doi:10.3390/molecules14072535.

Wang, L., R.M. Shelton, P.R. Cooper, M. Lawson, J.T. Triffitt, and J.E. Barralet. 2003. "Evaluation Of Sodium Alginate For Bone Marrow Cell Tissue Engineering". *Biomaterials* 24 (20): 3475-3481. doi:10.1016/s0142-9612(03)00167-4.

"Water Filter Systems - Reverse Osmosis Water Filters - Counter Top Water Filters". 2016.*Waterfiltersaustralia.Com.Au*. http://www.waterfiltersaustralia.com.au/.

"What Is Forward Osmosis?". 2016. *International Forward Osmosis Association*. http://forwardosmosis.biz/education/what-is-forward-osmosis/.

"Willpowder - Sodium Alginate". 2016. *Willpowder.Net*. http://www.willpowder.net/sodiumAlginate.html.

"Xanthan Gum". 2014. Molecular Recipes. http://www.molecularrecipes.com/hydrocolloid-guide/xanthan-gum/.

Zankel, Armin. 2016. "3D Characterization Of Asymmetric Microfiltration Membranes".*Slideshare.Net*. http://www.slideshare.net/VSG3D/p03-avizo-eugm2012arminzankelinstituteelectronmicroscopy.

Zhao, Shuaifei and Linda Zou. 2011. "Effects Of Working Temperature On Separation Performance, Membrane Scaling And Cleaning In Forward Osmosis Desalination". *Desalination* 278 (1-3): 157-164. doi:10.1016/j.desal.2011.05.018.

Zhao, Shuaifei and Linda Zou. 2011. "Relating Solution Physicochemical Properties To Internal Concentration Polarisation In Forward Osmosis". Journal Of Membrane Science 379 (1-2): 459-467. doi:10.1016/j.memsci.2011.06.021.

Zhao, Shuaifei, Linda Zou, and Dennis Mulcahy. 2012. "Brackish Water Desalination By A Hybrid Forward Osmosis–Nanofiltration System Using Divalent Draw Solute". Desalination 284: 175-181. doi:10.1016/j.desal.2011.08.053.

Zhao, Shuaifei, Linda Zou, Chuyang Y. Tang, and Dennis Mulcahy. 2012. "Recent Developments In Forward Osmosis: Opportunities And Challenges". Journal Of Membrane Science 396: 1-21. doi:10.1016/j.memsci.2011.12.023.

9. Appendices

Appendix A – Gantt Chart

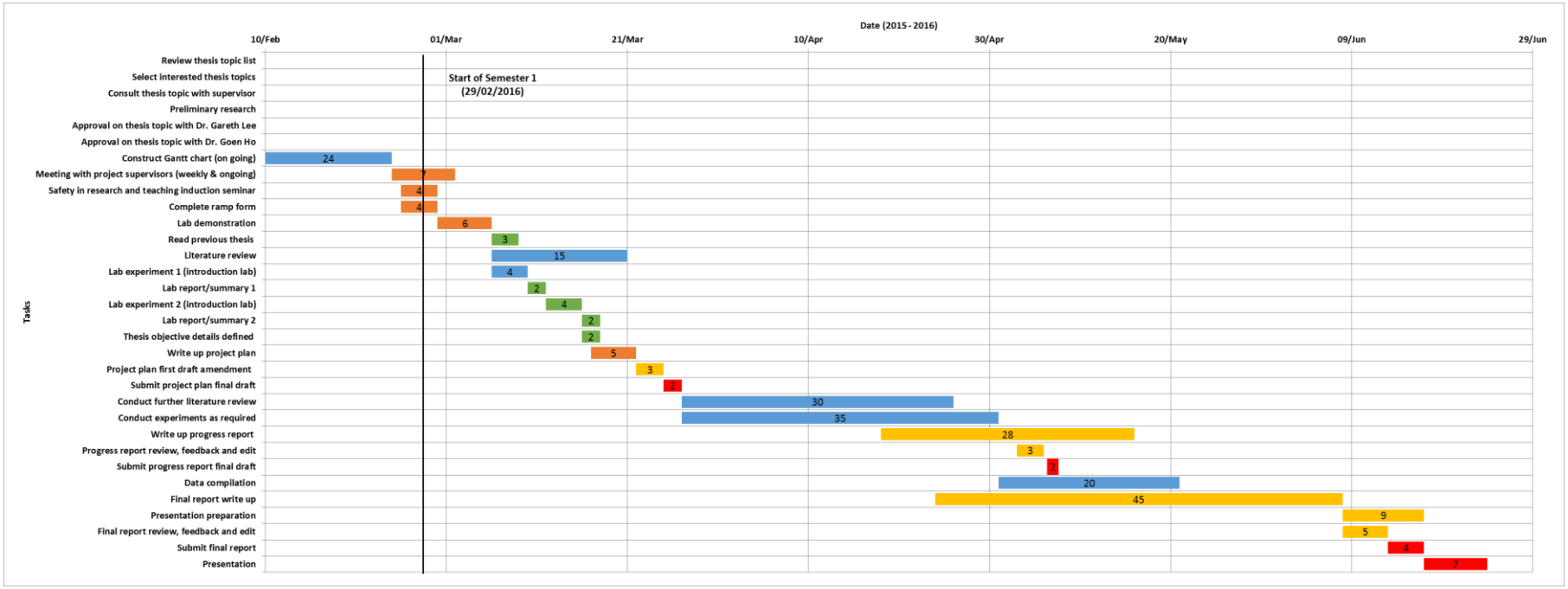

Appendix B – Table of result using the equation, y = 0.404x + 1.1246.

Time	Conductivity (µS)
60	3.5486
120	5.9726
180	8.3966
240	10.8206
300	13.2446
360	15.6686
420	18.0926
480	20.5166
540	22.9406
600	25.3646
660	27.7886
720	30.2126
780	32.6366
840	35.0606
900	37.4846
960	39.9086
1020	42.3326
1080	44.7566
1140	47.1806
1200	49.6046
1260	52.0286
1320	54.4526
1380	56.8766
1440	59.3006
1500	61.7246
1560	64.1486
1620	66.5726
1680	68.9966
1740	71.4206
1800	73.8446
1860	76.2686
1920	78.6926
1980	81.1166
2040	83.5406

Appendix C – Membrane weight of sample calculations

The weighting of membrane sample calculations.

Sample number	FO/RO	Experiment type	Glass weight, W1 (g)	Glass + fresh membrane weight, W2 (g)	Glass + sample, W3 (g)	Fresh membrane weight, W2 - W1	membrane weight, W3 - W1	layer weight, (W3 - W1) - (W2 - W1)	Effective membrane area (cm2)	Salt/polysaccharide deposited on membrane (g)
1	FO	Baseline	0.194	0.248	0.255	0.048	0.061	0.013	42	0.112810
2	FO	Alginate	0.2	0.248	0.261	0.048	0.061	0.013	42	0.112810
3	FO	Salt + alginate	0.196	0.248	0.264	0.048	0.068	0.02	42	0.173554
4	FO	Xanthan	0.198	0.248	0.269	0.048	0.071	0.023	42	0.199587
5	FO	Salt + xanthan	0.196	0.248	0.283	0.048	0.087	0.039	42	0.338430
6	FO	Pullulan	0.197	0.248	0.258	0.048	0.061	0.013	42	0.112810
7	RO	Baseline	0.192	0.248	0.243	0.048	0.051	0.003	42	0.026033
8	RO	Alginate	0.18	0.248	0.232	0.048	0.052	0.004	42	0.034711
9	RO	Pullulan	0.201	0.248	0.252	0.048	0.051	0.003	42	0.026033
10	RO	Salt + alginate	0.2	0.248	0.259	0.048	0.059	0.011	42	0.095455
11	RO	Salt + pullulan	0.195	0.248	0.244	0.048	0.049	0.001	42	0.008678
12	-	Fresh membrane	0.2	0.248	-	0.048	-	-	42	#VALUE!

Polysaccharide originally in feed (g)	Salt originally in feed (g)	Salt/polysaccharide left in feed (g)	NPTOC (g.C/L)	Thickness (microm)	Thickness (cm)	Density (g/cm3)
0	28.97	28.86	0	50	0.005	0.5371901
2	0	1.89	0.57	190	0.019	0.1413658
2	28.97	30.80	0.57	325	0.0325	0.1271456
2	0	1.80	0.445	430	0.043	0.1105132
2	28.97	30.63	0.6	430	0.043	0.1873919
2	0	1.89	0.82	120	0.012	0.2238292
0	28.97	28.94	0	47	0.0047	0.1318797
2	0	1.97	0.59	344	0.0344	0.0240246
2	0	1.97	0.81	180	0.018	0.0344353
2	28.97	30.87	0.57	620	0.062	0.0366569
2	28.97	30.96	0.88	210	0.021	0.0098386
0		#VALUE!			0	#VALUE!

Appendix D – Table of result from TOC analysis

Table 4: Table of NPTOC result obtain from the MAFRL staff.

Experiment type	Time (minute)	NPTOC (mg.C/L)
DI water + Alginate	240	220
DI water + Alginate	1560	57
DI water + Alginate + salt	120	0.7
DI water + Alginate + salt	240	52
DI water + Alginate + salt	1560	57
DI water + Xanthan	1560	44.5
DI water + Xanthan + salt	120	1.1
DI water + Xanthan + salt	240	1.1
DI water + Xanthan + salt	360	57
DI water + Xanthan + salt	1560	60

Appendix E – Summary table of averaged flux, permeate, and resistance

Table 5: This is the table of results from the past fourteen experiments and its averaged data over the conducting period. Note that the sixth experiment (marked in red) data does not fall within the acceptable range.

Experiment	**Average of flux,**	**Average of**	**Averaged**	**$R_b + R_c$**

number	J		permeate	total resistance	percentage over R total
	LMH	x 10^{-6} m/s	mL/minute	x 10^{15} m^{-1}	%
1 ($NaCl + CaCl_2$)	8.635	2.399	0.614	0.974	4.99
2 ($NaCl + CaCl_2$)	8.743	2.429	0.555	0.962	7.60
4 ($NaCl + CaCl_2$)	8.428	2.315	0.585	1.009	2.49
3 (Alginate)	9.836	2.732	0.694	0.855	6.86
5 (Alginate)	9.691	2.692	0.687	0.867	8.60
6 (Xanthan gum)	9.486	2.630	0.892	0.682	8.58
7 (Xanthan gum)	8.646	2.396	0.976	0.606	10.73
8 (Xanthan gum)	8.878	2.466	0.950	0.621	16.08
9 ($NaCl + CaCl_2$ + Alginate)	8.315	2.310	1.015	0.599	17.31
10 ($NaCl + CaCl_2$ + Alginate)	7.917	2.207	1.061	0.554	14.04
12 ($NaCl + CaCl_2$ + Xanthan Gum)	7.969	2.233	1.050	0.563	9.24
13 ($NaCl + CaCl_2$ + Xanthan Gum)	8.097	2.272	1.032	0.572	12.04
15 (Alginate)	8.164	2.266	0.570	1.030	3.063
17 (Xanthan gum)	6.798	1.882	0.476	1.253	15.09

Appendix F – Summary table of conductivity measured at different time

Table 6: This table represents the conductivity measured at each designated time. Note that the conductivity marked in red was reasonably high compared to other attempts and was hence removed from future calculations.

Experiment number	Conductivity at time (µS)		
	Hour 2	Hour 4	Hour 26
1 ($NaCl + CaCl_2$)	11.56		3960
2 ($NaCl + CaCl_2$)	9.6		3830
4 ($NaCl + CaCl_2$)	15.3		3870
3 (Alginate)	16.26		138.5

5 (Alginate)	9.6		102.1
6 (Xanthan)	15.14		223
7 (Xanthan)	5.54		93
8 (Xanthan)	7.0		102.3
9 (NaCl + $CaCl_2$ + Alginate)	5.6	3500	3780
10 (NaCl + $CaCl_2$ + Alginate)	5.7	3530	3840
11 (NaCl + $CaCl_2$ + Xanthan gum)	Failed	Failed	Failed
12 (NaCl + $CaCl_2$ + Xanthan gum)	10.77	3480	3800
13 (NaCl + $CaCl_2$ + Xanthan gum)	5.74	3450	3760
14 (NaCl + $CaCl_2$)	6.92	3460	4010
15 (Alginate)	5.21	40.6	85.6
16 (Xanthan)	Failed	Failed	Failed
17 (Xanthan)	6.44	23.7	67.1

Appendix G – Record of experiments being conducted

Table 7: Schedule of each experiment that was attempted (including failed and successful experiments).

Experiment number	Start date	End date	Experiment descriptions	Remarks
1 Baseline	31 March 2016	01 April 2016	NaCl + $CaCl_2$ First attempt	
2 Baseline	02 April 2016	03 April 2016	NaCl + $CaCl_2$ Second attempt	Membrane was kept for confocal microscopy analysis However, too much DI water was put into the membrane storage thus another experiment was conducted
3 Fouling	05 April 2016	06 April	Alginate First attempt	Blockage testing shows a negative result → no blockage was found

		2016		
4 Baseline	06 April 2016	07 April 2016	NaCl + $CaCl_2$ Third attempt	Membrane was kept for confocal microscopy analysis
5 Fouling	08 April 2016	09 April 2016	Alginate Second attempt	Membrane was kept for confocal microscopy analysis
6 Fouling	10 April 2016	11 April 2016	Xanthan gum First attempt	Blockage testing
7 Fouling	12 April 2016	13 April 2016	Xanthan gum Second attempt	Membrane was kept for confocal microscopy analysis
8 Fouling	14 April 2016	15 April 2016	Xanthan gum Third attempt	Repeat for the first attempt as the Xanthan was not totally dissolved in the solution
9 Salt + fouling	16 April 2016	17 April 2016	NaCl + $CaCl_2$ + Alginate First attempt	Membrane and liquid sample were taken and kept for further analysis
10 Salt + fouling	18 April 2016	19 April 2016	NaCl + $CaCl_2$ + Alginate Second attempt	Blockage testing
11 Salt + fouling	20 April 2016	-	NaCl + $CaCl_2$ + Xanthan First attempt	Failed due to leakage along the tubing
12 Salt + fouling	21 April 2016	22 April 2016	NaCl + $CaCl_2$ + Xanthan Second attempt	Membrane and liquid sample was taken and kept for further analysis
13 Salt + fouling	23 April 2016	24 April 2016	NaCl + $CaCl_2$ + Xanthan Thirds attempt	Blockage testing
14 Baseline	25 April 2016	26 April 2016	NaCl + $CaCl_2$ Fourth attempt	Conductivity measured for the missing values
15 Fouling	27 April 2016	28 April 2016	Alginate Fourth attempt	Conductivity measured for the missing values
16 Fouling	28 April 2016	-	Xanthan Fourth attempt	Failed due to leakage along the tubing
17 Fouling	29 April 2016	30 April 2016	Xanthan Fifth attempt	Conductivity measured for the missing values

Appendix H – HTI OsMEM™ CTA-NW Membrane Specification Sheet

Features:

- The OsMem™ CTA-NW Membrane is HTI's fouling resistant and most chlorine resistant FO membrane cast on a weldable nonwoven support.
- The OsMem™ CTA-NW Membrane is used in all hydration pouches (HydroPack, LifePack, X-Pack, etc.).
- The OsMem™ CTA-NW Membrane is cast on 40'' (1-m) wide rolls and "dried," where vegetable-based glycerine replaces the water.
- The OsMem™ CTA-NW Membrane coupons are shipped "dry," where vegetable-based glycerine replaces the water

Typical FO Performance (Rejection Layer Contacting Feed):

- Water Permeation : 2.4GFD (gallons per square foot each day) (4.0 LMH – litres per square meter each hour)
- Salt Rejection: 99% as defined in Test Conditions

Test Conditions:

- Feed: 1 gpm (4 1 pm) tap water feed at 77F (25C) fed at the bottom into a 4" (100 mm) by 0.2 " (5 mm) open channel with an initial volume of 0.40 gal (1.5

L) and an exit pressure of 5 psi (35 kPa).
- Draw: 7 gph (26 lph) 1 M NaCl (58.5 g/L) at the bottom at 2 psi (15 kPa) feed into a 4" (100 mm) by 0.055" (1.4 mm) channel of two 30-mil (0.76 mm) diamond-type polypropylene feed spacers (strands spaced at 11 strands per inch (25.4 mm)) with an initial volume of 0.13 gal (0.5 L)
- Membrane Area: 0.22 ft^2 (0.020 m^2)

Typical uPRO* Performance (Rejection Layer Contacting Draw Solution):
- Water Permeation: 5.3 GFD (gallons per square foot each day) (9.0 LMH – litres per square meter each hour)
- Salt Rejection: 99% as defined in Test Conditions

Test Conditions:
- Feed: 7 gpm (26 1 pm) tap water at the bottom at 2 psi (15 kPa) feed into a 4" (100 mm) by 0.055" (1.4 mm) channel of two 30-mil (0.76 mm) diamond-type polypropylene feed spacers (strands spaced at 11 strands per inch (25.4 mm)) with an initial volume of 0.26 gal (1.0 L).
- Draw: 7 gph (26 lph) 1 M NaCl (58.5 g/L) at 77F (25C) fed at the bottom into a 4" (100 mm) by 0.2" (5 mm) open channel with an initial volume of 0.2 gal (0.8 L) and an exit pressure of 5 psi (35kPa).
- Membrane Area: 0.22 ft^2 (0.020 m^2)
- Rejection: {1 – [(mol NaCl transferred to feed)/(L water removed)/(1 M]}
- *uPRO: unpressurised Pressure Retarded Osmosis membrane orientation

Operating Limits and Guidelines:
- Membrane Requirements: Membrane coupons are shipped in glycerine. Should be soaked in water for 30 minutes prior to use. After glycerine extraction, the membrane must be kept moist at all times. Do not allow to freeze. Exercise care in handling
- Membrane Type: Cellulose Triacetate (CTA) on heat- or RF-weldable nonwoven support
- Maximum Operation Temperature: 160F (71C)
- Maximum Transmembrane Pressure: 10 psi (70 kPa), if supported
- pH Range: 3 to 8
- Maximum Chlorine: 2ppm
- Cleaning Guidelines: use only cleaning chemicals approved for CA/CTA RO membranes
- Storage Guidelines: Store out of direct sunlight with a couple of mL of water

FO Membrane Notes

The membrane in initially cast on rolls. On a roll, the rejection layer is to the inside of the roll is the shiny side away from the nonwoven backing.

FO membranes behave similarly to RO membranes in that dissolved gases are not rejected well. Their ions are rejected, but the (often small) fraction that exists as a dissolved gas is not rejected. Small polar, water-soluble organics, such as urea, methanol, and ethanol, are also not rejected well.

Brief Start-up Description

If the process is being run with the draw solution contacting the rejection layer (uPRO), make sure that there is water in the cell on the supported side to draw from. Start the pump on the unsupported side. Adjust the flowrate with the inlet valve and the exit pressure to 5 psi (35 kPa) with the exit valve. Start the side with the

membrane support and adjust to the desired inlet pressure of 2 psi (15 kPa). Monitor volume or weight changes, temperature, and concentrations with time.

Brief Shutdown descriptions
Turn off the pumps and drain the high osmotic pressure solution first. Then drain the low osmotic pressure solution. Rising is recommended. The membrane can be stored in the cell – preferably drained.

Source: OsMem™ membrane specification sheet

Appendix I – Graph of frequency distribution for baseline experiment

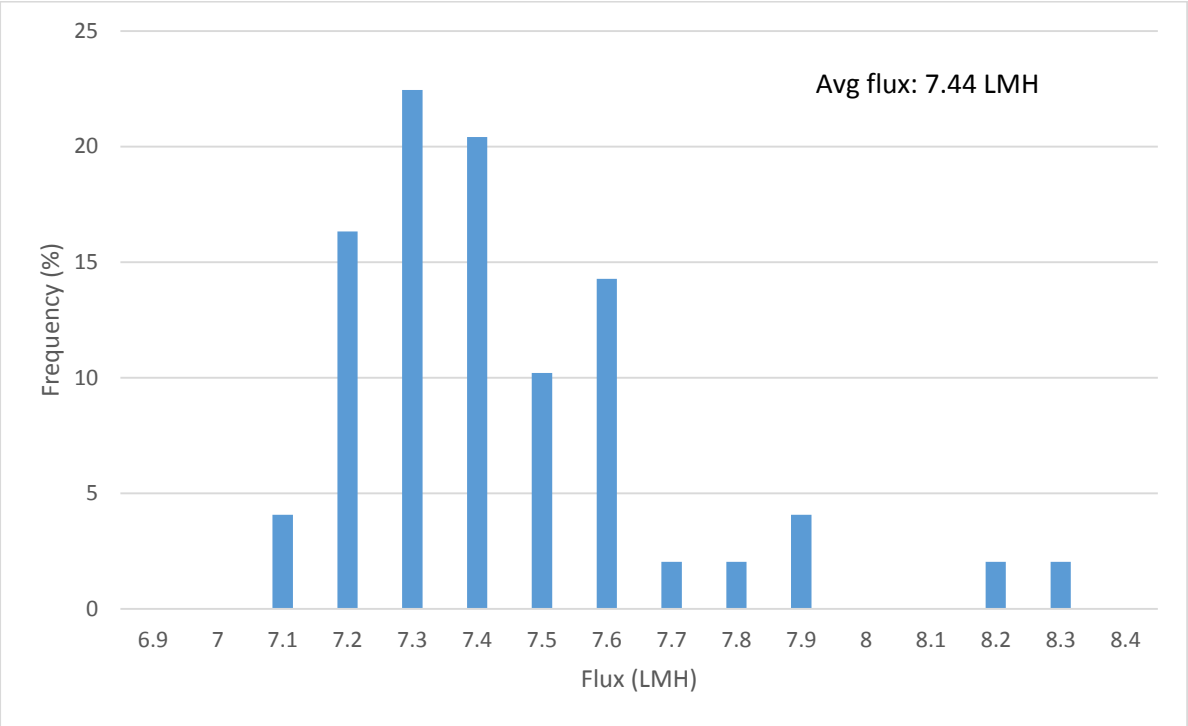

Appendix J – Graph of frequency distribution for salt + alginate experiment

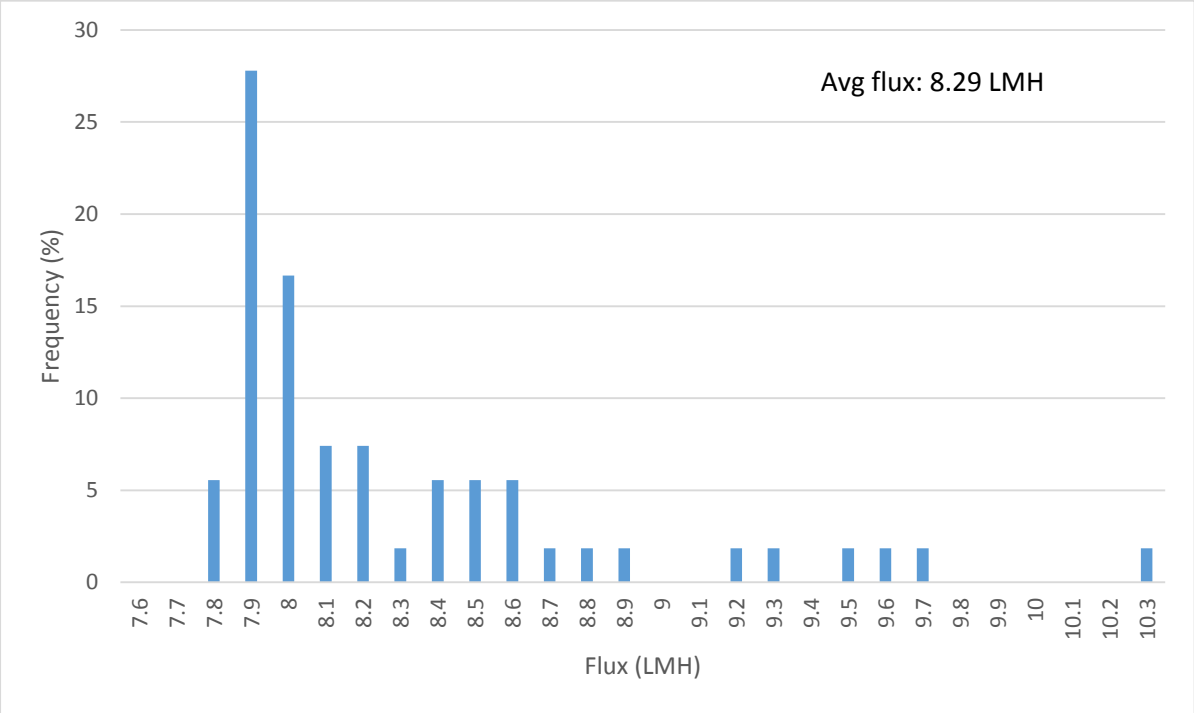

Appendix K – Graph of frequency distribution for alginate experiment

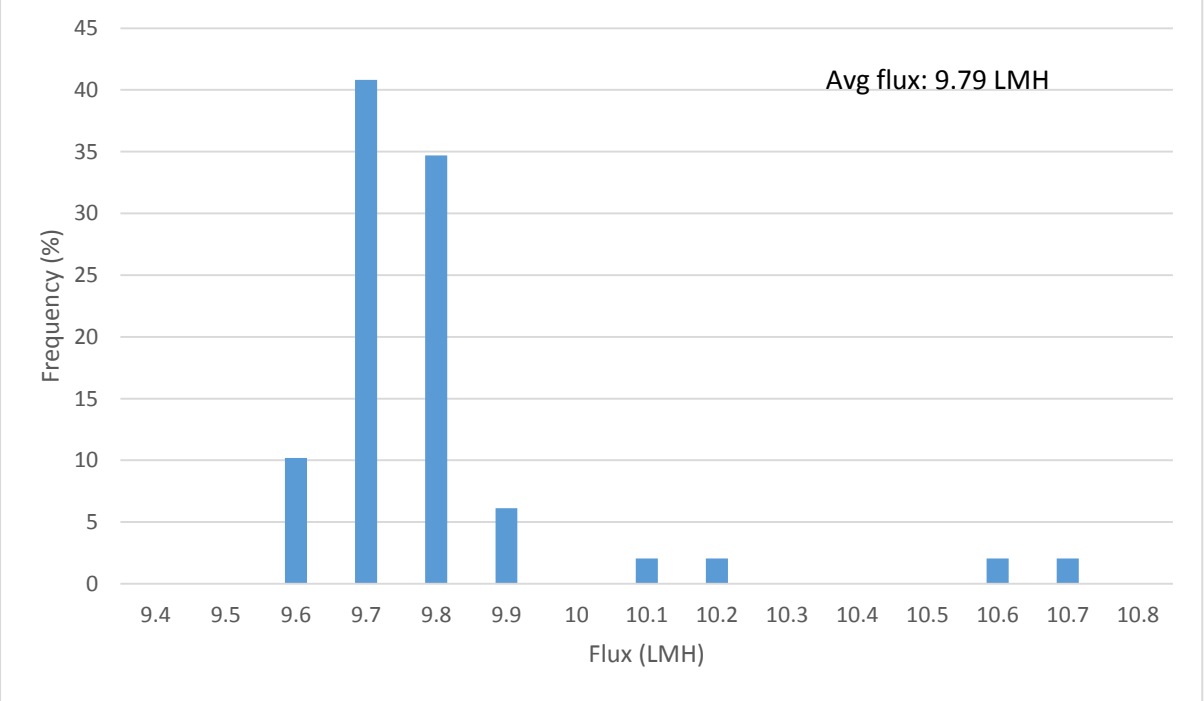

Appendix L – Graph of frequency distribution for salt + xanthan experiment

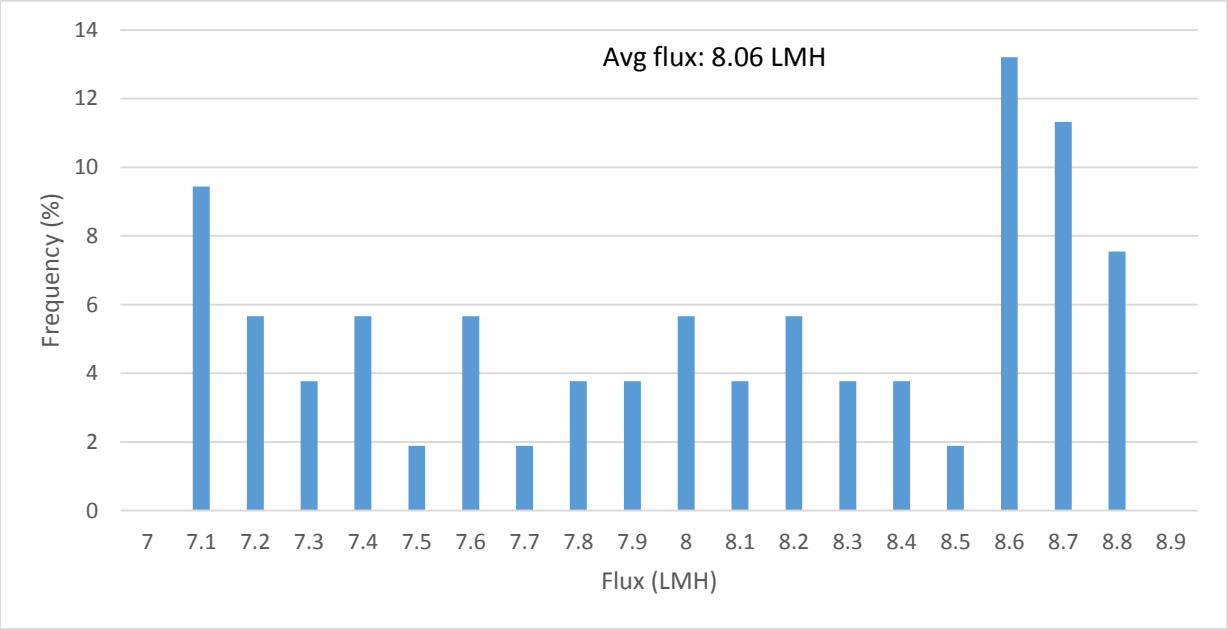

Appendix M – Graph of frequency distribution for xanthan experiment